Dissertation zur Erlangung des Doktorgrades der Fakultät für Chemie und Pharmazie der Ludwig-Maximilians-Universität München

Protein drug molecular environment, mobility, accessibility, and stability in lyophilizates

Ken Lo Presti

aus

Waldshut, Deutschland

2025

Erklärung

Diese Dissertation wurde im Sinne von § 7 der Promotionsordnung vom 28. November 2011 von Herrn Prof. Dr. Wolfgang Frieß betreut.

Eidesstattliche Versicherung

Diese Dissertation wurde eigenständig und ohne unerlaubte Hilfe erarbeitet.

München, den 24.06.2025

_____

Ken Lo Presti

Dissertation eingereicht am 24.06.2025

1. Gutachter: Prof. Dr. Wolfgang Frieß

2. Gutachter: Prof. Dr. Gerhard Winter

Mündliche Prüfung am 28.07.2025

To my family

Acknowledgements

I would like to express my sincere gratitude to everyone who has contributed to the completion of this dissertation. Without their support, guidance, and encouragement, this research would not have been possible. First and foremost, I would like to thank my supervisor, Professor Dr. Wolfgang Frieß, for his steadfast support and guidance throughout the years. I am grateful for all the constructive feedback, encouragement, and trust during my research. His expertise, patience, and creativity shaped my scientific mindset and have been instrumental in writing this dissertation. I would also like to thank you for the possibility of attending eye-opening international scientific conferences and workshops to reach “High Prestige”.

I am thankful for the help and fruitful discussions with the coauthors of the manuscripts. Dr. Nikolay Isaev, who helped me to step out of my comfort zone and explore new scientific territories, and Mathilde Jégo for her outstanding assistance during her master's thesis.

Thanks to Prof. Dr. Wolfgang Frieß, Prof. Dr. Gerhard Winter, and Prof. Dr. Olivia Merkel for providing the best working atmosphere at the Department of Pharmaceutical Technology and Biopharmaceutics and for the valuable input and discussions within several progress reports and talks.

I want to thank Dr. Johann Klare from the University of Osnabrück for providing us with the EPR spectrometer and supporting our measurements in Osnabrück. Additionally, I extend my gratitude to Prof. Dr. Bracher and Karl Sauvageot-Witzku from the Bracher Group for their support in the synthesis of deuterated sucrose. I also thank Dr. Lars Allmendinger for performing the NMR analysis to investigate the deuteration rate.

Furthermore, many thanks to AK Frieß, AK Merkel, and AK Winter for reviving several social activities such as Oktoberfest visits, summer and winter parties, the annual Ski trip, and so much more. I was very happy to see colleagues becoming close friends and building meaningful and ongoing relationships.

Finally, and most importantly, I want to thank my parents, Luciano and Martina, and my sister Nina for their endless support, understanding, and love. Thank you for always believing in me and encouraging me in my decisions, which have helped me to unfold.

Table of Content

Chapter I Introduction

Protein drugs, especially monoclonal antibodies (mAbs), play an important role in the treatment of numerous severe diseases.[1–4] Freeze-drying, or lyophilization, is a common method to minimize the chemical and physical degrad of protein drugs by removing water without the need for elevated temperatures.[5,6] The freeze drying process is characterized by three stages: freezing, primary drying, and secondary drying. Freezing significantly affects the final product's quality, as it involves supercooling, cryoconcentration, crystallization, which induce severe stress on proteins.[7] During primary drying, approximately 80-90% of the water is removed at reduced pressure from a slightly warmed frozen product. The product temperature during this phase is critical because temperatures above the glass transition temperature of the amorphous freeze concentrate (T_g') the molecular mobility as well as the interactions between proteins and reaction partners are enhanced. Correspondingly, lyoprotectants and cryoprotectants with high T_g' are preferred. The duration of primary drying depends not only on the product temperature and the vacuum, but also on the formulation, total solid content, fill volume, and container heat transfer.[8] During secondary drying, the remaining water is removed at room temperature and slightly above, achieving a final moisture content of typically around 1% or less. Both freezing and drying induce significant stress on the protein molecules, and typically sugars, sugar alcohols, amino acids, surfactants, and buffer systems are the formulation components that ensure adequate protein stability. This chapter discusses the mechanisms of protein stabilization in the dried state and reviews common and novel analytical techniques used to evaluate protein stability.

I.1 General Aspects of Stability of Protein Lyophilizates

I.1.1 Physical instability of protein lyophilizates

The preservation of protein structure is essential.[9] Removal of water deprives the protein of its stabilizing hydrogen bond rich environment. As protein molecules lose their native structure, their attractive self-interaction increases as hydrophobic structural elements become exposed, potentially resulting in aggregation. Aggregation is considered a critical quality attribute and can negatively impact efficacy and safety. In the lyophilized products, aggregation may be enhanced due to the high protein concentration in the freeze concentrated and the final matrix. Changes in pH, ionic strength, and mechanical stress during freezing additionally impact conformational and colloidal stability.

I.1.2 Chemical instability of protein lyophilizates

In addition to physical degradation, chemical reactions with oxygen, water, excipients, and other protein molecules affect the integrity of protein drug products. Reducing sugars like glucose can react with primary or secondary amines such as lysine residues in proteins via the Maillard reaction, leading to N-glycosylated amines and potentially significant protein inactivation as well as discoloration.[10,11] Reducing sugars can also be generated by the hydrolysis of sucrose at higher temperatures and lower pH.[12,13] Furthermore, inter- or intramolecular disulfide or other covalent bonds, like amides, can potentially form.[14] Deamidation, the conversion of asparagine residues to aspartic or isoaspartic acid and glutamine residues to glutamic acid, alters the overall protein charge and charge distribution, which affects protein self-interaction, aggregation, and function. Deamidation becomes enhanced at higher pH values, as well as elevated temperature and residual moisture.[15] The presence of water around a protein molecule can promote hydrolysis of peptide bonds, potentially leading to protein fragmentation. Additionally, oxidation due to exposure to oxygen and light is an important chemical instability, specifically affecting methionine, cysteine, or tryptophan residues.

I.1.3 Macroscopic and microscopic changes

A pharmaceutically elegant cake appearance is crucial for marketed lyophilized drug products. Cracks, detachment from the vial wall, and shrinkage can occur due to tension in the product and container. Complete cake collapse may result from product temperatures exceeding T_g' during primary drying, whereas meltback can be traced back to leftover ice at the end of primary drying.

I.2 Means of Protein Stabilization in Freeze Dried Drug Products

Achieving protein drug stability is a central element of pharmaceutical product development. This needs to be ensured at the intended storage temperature over the lifetime of the product. Regulations concerning drug product stability can be found in various pharmacopeias, including the United States Pharmacopeia (USP), the European Pharmacopoeia (Ph. Eur.), and other authoritative sources, such as guidelines issued by the International Council for Harmonization (ICH). In addition to maintaining stability under the intended storage conditions, a final drug product must also demonstrate short-term stability at temperatures outside the recommended range. This ensures the product remains effective and safe during brief deviations, such as those that may occur during minor disruptions in the cold chain. Information regarding these stability requirements is typically included in the Summary of Product Characteristics, which is part of the medicinal product listings maintained by regulatory

authorities such as the European Medicines Agency (EMA) and the U.S. Food and Drug Administration (FDA). Accelerated stability studies, guided by the ICH Q1A(R2) guideline on "Stability Testing of New Drug Substances and Products," involve storing samples at elevated temperatures and/or humidity levels to accelerate degradation processes.[16,17] This enables predictions of the product behavior under the intended storage at a lower temperature. In case of protein lyophilizates, cryo- and lyoprotectants, surfactants, and buffers are key excipients to achieve adequate stability, with different impacts of these excipients during freezing, drying, and storage.[18]

I.2.1 Mechanisms of stabilization in the lyophilized state

Two theories are mainly brought in to explain protein stabilization in the freeze-dried matrix: water replacement and vitrification. The water replacement hypothesis suggests that excipients like sugars act as a substitute hydrogen bond donor upon water removal, preserving the native structure of the protein. The vitrification theory proposes that a rigid network formed by excipients in the solid state decreases protein mobility, thereby maintaining the protein structure. These theories are the basis for studying parameters such as the glass transition temperature (T_g) of the formulation, the crystalline or amorphous character of the matrix, and the accessibility and mobility of the protein molecules in the solid state.

While these theories offer valuable insights, some questions have not been fully answered yet, like the exact impact of excipient size, excipient to protein ratio, and the moisture content on protein stability. While medium molar ratios have been studied, low ratios, which are more relevant for high-concentration mAb formulations or when other excipients are present, remain less explored, as they limit the amount of lyoprotectant that can be added due to the osmolality limit.[19–23] Additionally, the interplay of excipient type and size with moisture content demands further studies to elucidate the relationship of hydrogen bond stabilization, matrix rigidity and mobility, as well as protein accessibility.

I.2.2 The impact of moisture content

The residual moisture content after lyophilization significantly impacts both physical and chemical protein stability. Water acts directly as a reactant and indirectly as a plasticizer, lowering T_g, increasing molecular mobility, and through this reducing protein stability. Moisture uptake of the amorphous matrix during storage can result from water released from the rubber stopper, ingress through the container, or dehydration of excipients like mannitol hemihydrate.[24,25] At the other end, extremely low moisture content may pose a risk due to extreme loss of stabilizing hydrogen bonds and increasing voids, considered as overdrying.

Therefore, identifying and maintaining the optimal residual moisture content, typically between approx. 0.5 and 2%, is crucial. The residual moisture content is essentially a function of the secondary drying temperature.

I.2.3 Excipients in freeze dried drug products

I.2.3.1 Disaccharides and HP-ß-Cyclodextrin

Sugars such as sucrose and trehalose form amorphous matrices upon freeze-drying and form hydrogen bonds with protein molecules, making them the lyoprotectants of choice. The amount added to protein formulations that are parenterally applied is limited by the isotonicity requirement.[26,27] Yet, it is widely accepted that more lyoprotectant equals a higher protein stability.[19] Sucrose (T_g of 74 °C and a T_g' of -32 °C) is most commonly utilized.[28,29] A typical sucrose concentration of approx. 7.5% [w/V] results in an excipient to mAb molar ratio of approx. 330:1 in 100 g/l mAb formulations.

Trehalose is the second most common disaccharide used in lyophilization. It shows a higher T_g of approx. 110 °C and has a higher resistance against crystallization.[30,31]

Hydroxypropyl-β-cyclodextrin (HPβCD) is used in freeze dried formulations as a stabilizing amorphous bulking agent and lyoprotectant due to its high T_g' of approx. -10 °C.[32] More interestingly, HPβCD has been proposed to function as a surfactant, stabilizing proteins against interfacial stresses at the ice surface.[33]

I.2.3.2 Polyols

Mannitol, a sugar alcohol, is commonly used as a bulking agent in lyophilization due to its high tendency to crystallize. This helps form an elegant cake structure and allows for primary drying at much higher product temperatures.[25] Additionally, at low concentrations, mannitol can act as an additional lyoprotectant if kept in an amorphous state.[34]

Glycerol plays a unique role as a stabilizing excipient. Due to its low T_g' of -88 °C, it must be used in combination with excipients that have higher T_g' values, such as disaccharides.[35–37] The small size and the high mobility of glycerol allow for advantageous filling of voids created upon water removal, accessing the protein surface, inhibiting local molecular motions, and thus stabilizing the protein conformation.[38]

I.2.3.3 Amino acids

In solution, arginine can act as a viscosity reducing agent (VRA) by shielding protein charges and thereby reducing non-specific protein interactions.[39,40] In lyo, arginine can build hydrogen bonds with proteins, thus improving protein stabilization based on the water replacement theory.[37,41] Additionally, depending on the arginine counter ion, a positive impact on the protein stability and/or glass transition temperature can be achieved.[42]

I.2.3.4 Surfactants

Surfactants such as polysorbate 20 and 80 and poloxamer 188 are commonly used to reduce interfacial stresses while freeze drying.[43] The surfactant molecules are enriched at the ice-liquid, the air-liquid, and the air-lyophilizate interface, preventing protein adsorption, which triggers aggregation.[44] Additionally, surfactants may interact with proteins directly, preventing intermolecular interactions.[45] However, polysorbate 20 and 80 are prone to oxidation and hydrolysis, whereas poloxamer 188 has shown incompatibilities with siliconized primary packaging.[46,47]

I.2.3.5 Buffer and pH-value

Buffers are essential in protein formulations as they maintain a stable pH, which is necessary to guarantee stabilization. The pH affects chemical reactions, colloidal interactions, and the conformational stability of proteins. Therefore, selecting an appropriate buffer system and the right pH-value is crucial. Common buffer systems used in liquid formulations, like phosphate, citrate, or histidine, show a temperature-dependent pH-shift with temperature change. In addition, upon freezing, the pH can drastically change in the case of sodium phosphate buffer due to the different solubility of the phosphate salts.[48]

I.2.4 Monitoring protein physical stabilization in lyophilizates

The physical protein stability in lyophilizates is typically studied after reconstitution by analysis of aggregate formation and higher order structure. Size exclusion chromatography (SEC) is widely used to quantify the formation of dimers and small higher molecular weight species. Sample dilution and the aggregate dissociation in the eluent can bias results.[49–51] Light obscuration (LO) and flow imaging microscopy complement SEC by examining subvisible particles, and visible particles are assessed by visual inspection.[52] The size gap between SEC and subvisible particles can be covered in a crude way by turbidity analysis. To gain a comprehensive understanding of the protein higher-order conformations, such as secondary and

tertiary structures, methods like Circular Dichroism (CD), Fourier Transform Infrared (FTIR) spectroscopy, Raman spectroscopy, and Intrinsic Fluorescence spectroscopy are used.[53–55]

The local stabilizing environment in the lyophilizates can be assessed by different tools. Differential scanning calorimetry (DSC) is used to measure T_g, which correlates with the relaxation of the protein matrix and mobility in an amorphous solid. Two types of relaxations are described, namely temperature-dependent α-relaxation, commonly associated with T_g, and β-relaxations, which occur at temperatures below T_g and represent substantial motions of a protein upon heating.[56,57] Wang et al. proposed that protein mobility and density in the solid state are linked with protein aggregation, indicating that protein stability is also influenced by β-relaxation.[58,59] A high T_g alone does not guarantee long-term stability; hence, additional solid-state analytical techniques and parameters are necessary. Terahertz Time-Domain Spectroscopy (THz-TDS) provides additional information about protein mobility and "free volume" within the sucrose matrix by examining the impact of remaining water molecules.[60,61]

Solid-state hydrogen-deuterium exchange mass spectrometry (ssHDX-MS) probes protein stability by examining the exchange of hydrogens in the amide backbone against deuterium, in the case of lyophilizates, by exposing them to D_2O vapor.[62–64] The global deuterium exchange rate is related to the accessibility of the amides and the protein mobility. Therefore, differences in the mass increase, whether observed at the intact protein level globally or at the local peptide level after enzymatic digestion, can be linked to changes in the protein structure.[65] Liquid-observed vapor exchange nuclear magnetic resonance spectroscopy (LOVE NMR) follows a similar principle but is limited by the need for a protein backbone assignment and a ^{14}N-enriched protein, making it less practical for universal use.[66,67]

Solid-state Fourier transform infrared spectroscopy (ssFTIR) and solid-state raman spectroscopy are used to investigate the protein structure in the solid state.[68,69] ssFTIR tracks changes in secondary and tertiary structures, such as α-helix and β-sheet, and can be coupled with an HDX approach.[70–72] Raman spectroscopy detects protein-protein interactions and secondary structures in the solid state.[73] Small-angle X-ray scattering (SAXS) and small-angle neutron scattering (SANS) are complementary scattering techniques that can be utilized for global nano-structural analysis of proteins. Whereas SAXS is based on contrasts in electron density, SANS is based on nucleus scattering governed by the respective scattering isotope, which enables the use of selective contrast matching by deuteration.[74–76]

Besides the mentioned novel but established methods, electron paramagnetic resonance spectroscopy (EPR) shows potential. It allows for analysis of a specific local distance of interest and structural properties of proteins, as shown for metallo- and membrane proteins.[77,78] EPR measurement of trehalose and sucrose matrices at different hydration levels showed that trehalose forms a homogeneous amorphous matrix, while sucrose can form a more heterogeneous matrix, including crystalline clusters and water-rich regions, leading to higher mobility, which could explain the efficient inhibition of matrix-embedded proteins.[20,21] In general, the relationship between magnetic moment, energy, and magnetic field is similar between EPR and NMR.[79] EPR operates by using the magnetic properties of electrons and varies the magnetic field with a constant frequency, similar to nuclear magnetic resonance (NMR) spectroscopy but at microwave frequencies (3-400 GHz). Since most proteins lack unpaired electron pairs, labeling is necessary to make the protein and defined distances of interest observable via EPR.[80,81]

I.3 References

[1] S. Crescioli, H. Kaplon, A. Chenoweth, L. Wang, J. Visweswaraiah, J.M. Reichert, Antibodies to watch in 2024, mAbs 16 (2024) 2297450.

[2] M.S. Kinch, Z. Kraft, T. Schwartz, Monoclonal antibodies: Trends in therapeutic success and commercial focus, Drug discovery today 28 (2023) 103415.

[3] Z. Ku, X. Ye, G.T. Salazar, N. Zhang, Z. An, Antibody therapies for the treatment of COVID-19, Antibody Therapeutics 3 (2020) 101–108.

[4] F. Jameel, A. Alexeenko, A. Bhambhani, G. Sacha, T. Zhu, S. Tchessalov, L. Kumar, P. Sharma, E. Moussa, L. Iyer, R. Fang, J. Srinivasan, T. Tharp, J. Azzarella, P. Kazarin, M. Jalal, Recommended Best Practices for Lyophilization Validation-2021 Part I: Process Design and Modeling, AAPS PharmSciTech 22 (2021) 221.

[5] A. Juckers, P. Knerr, F. Harms, J. Strube, Effect of the Freezing Step on Primary Drying Experiments and Simulation of Lyophilization Processes, Processes 11 (2023) 1404.

[6] J.F. Carpenter, M.J. Pikal, Chang, Byeong, S, T.W. Randolph, Rational Design of Stable Lyophilized Protein Formulations: Some Practical Advice, Pharmaceutical Research 14 (1997) 969–975.

[7] J.C. Kasper, W. Friess, The freezing step in lyophilization: physico-chemical fundamentals, freezing methods and consequences on process performance and quality attributes of biopharmaceuticals, European Journal of Pharmaceutics and Biopharmaceutics 78 (2011) 248–263.

[8] L. Leys, B. Vanbillemont, P.J. van Bockstal, J. Lammens, G. Nuytten, J. Corver, C. Vervaet, T. de Beer, A primary drying model-based comparison of conventional batch freeze-drying to continuous spin-freeze-drying for unit doses, European Journal of Pharmaceutics and Biopharmaceutics 157 (2020) 97–107.

[9] T.K. Das, A. Sreedhara, J.D. Colandene, D.K. Chou, V. Filipe, C. Grapentin, J. Searles, T.R. Christian, L.O. Narhi, W. Jiskoot, Stress Factors in Protein Drug Product Manufacturing and Their Impact on Product Quality, Journal of Pharmaceutical Sciences 111 (2022) 868–886.

[10] F. Ghaderi, F. Monajjemzadeh, Review of the physicochemical methods applied in the investigation of the maillard reaction in pharmaceutical preparations, Journal of Drug Delivery Science and Technology 55 (2020) 101362.

[11] M.C. Manning, D.K. Chou, B.M. Murphy, R.W. Payne, D.S. Katayama, Stability of protein pharmaceuticals: an update, Pharmaceutical Research 27 (2010) 544–575.

[12] J.D. Meyer, R. Nayar, M.C. Manning, Impact of bulking agents on the stability of a lyophilized monoclonal antibody, European journal of pharmaceutical sciences 38 (2009) 29–38.

[13] S. Ohtake, K. Izutsu, D. Lechuga-Ballesteros (Eds.), Drying technologies for biotechnology and pharmaceutical applications, Wiley-VCH, Weinheim, 2020.

[14] K.M. Hutterer, R.W. Hong, J. Lull, X. Zhao, T. Wang, R. Pei, M.E. Le, O. Borisov, R. Piper, Y.D. Liu, K. Petty, I. Apostol, G.C. Flynn, Monoclonal antibody disulfide reduction during manufacturing: Untangling process effects from product effects, mAbs 5 (2013) 608–613.

[15] Y. Du, A. Walsh, R. Ehrick, W. Xu, K. May, H. Liu, Chromatographic analysis of the acidic and basic species of recombinant monoclonal antibodies, mAbs 4 (2012) 578–585.

[16] E. Shalaev, S. Ohtake, E.M. Moussa, J. Searles, S. Nail, C.J. Roberts, Accelerated Storage for Shelf-Life Prediction of Lyophiles: Temperature Dependence of Degradation of Amorphous Small Molecular Weight Drugs and Proteins, Journal of Pharmaceutical Sciences 112 (2023) 1509–1522.

[17] ICH Harmonised Tripartite Guideline Stability. ICH, Q1A(R2): Stability testing of new drug substances and products, 2003.

[18] A. Arsiccio, R. Pisano, Clarifying the role of cryo- and lyo-protectants in the biopreservation of proteins, Physical chemistry chemical physics PCCP 20 (2018) 8267–8277.

[19] J.L. Cleland, X. Lam, B. Kendrick, J. Yang, T.-H. Yang, D. Overcashier, D. Brooks, C. Hsu, J.F. Carpenter, A specific molar ratio of stabilizer to protein is required for storage stability of a lyophilized monoclonal antibody, Journal of Pharmaceutical Sciences 90 (2001) 310–321.

[20] M. Malferrari, A. Nalepa, G. Venturoli, F. Francia, W. Lubitz, K. Möbius, A. Savitsky, Structural and dynamical characteristics of trehalose and sucrose matrices at different hydration levels as probed by FTIR and high-field EPR, Physical chemistry chemical physics PCCP 16 (2014) 9831–9848.

[21] M. Malferrari, A. Savitsky, W. Lubitz, K. Möbius, G. Venturoli, Protein Immobilization Capabilities of Sucrose and Trehalose Glasses: The Effect of Protein/Sugar Concentration Unraveled by High-Field EPR, The journal of physical chemistry letters 7 (2016) 4871–4877.

[22] L.L. Chang, D. Shepherd, J. Sun, D. Ouellette, K.L. Grant, X.C. Tang, M.J. Pikal, Mechanism of protein stabilization by sugars during freeze-drying and storage: native structure preservation, specific interaction, and/or immobilization in a glassy matrix?, Journal of Pharmaceutical Sciences 94 (2005) 1427–1444.

[23] Andya JD, Hsu CC, Shire SJ, Mechanisms of Aggregate Formation and Carbohydrate Excipient Stabilization of Lyophilized Humanized Monoclonal Antibody Formulations, AAPS PharmSci 5 (2003) 1–11.

[24] J. Sonje, S. Thakral, B. Mayhugh, G. Sacha, S. Nail, J. Srinivasan, R. Suryanarayanan, Mannitol hemihydrate in lyophilized protein formulations:Impact of its dehydration during storage on sucrose crystallinity and protein stability, International Journal of Pharmaceutics 624 (2022) 121974.

[25] S. Thakral, J. Sonje, R. Suryanarayanan, Anomalous behavior of mannitol hemihydrate: Implications on sucrose crystallization in colyophilized systems, International Journal of Pharmaceutics 587 (2020) 119629.

[26] W. Wang, Tolerability of hypertonic injectables, International Journal of Pharmaceutics 490 (2015) 308–315.

[27] W.H. Reinhart, N.Z. Piety, J.S. Goede, S.S. Shevkoplyas, Effect of osmolality on erythrocyte rheology and perfusion of an artificial microvascular network, Microvascular research 98 (2015) 102–107.

[28] A. Simperler, A. Kornherr, R. Chopra, P.A. Bonnet, W. Jones, W.D.S. Motherwell, G. Zifferer, Glass transition temperature of glucose, sucrose, and trehalose: an experimental and in silico study, The Journal of Physical Chemistry B 110 (2006) 19678–19684.

[29] T. Kharatyan, S. Igawa, S.R. Gopireddy, T. Ogawa, T. Kodama, R. Scherließ, N.A. Urbanetz, Impact of post-freeze annealing on shrinkage of sucrose and trehalose lyophilisates, International Journal of Pharmaceutics 641 (2023) 123051.

[30] K.D. Roe, T.P. Labuza, Glass Transition and Crystallization of Amorphous Trehalose-sucrose Mixtures, Int. J. of Food Properties 8 (2005) 559–574.

[31] H.R. Costantino, J.G. Curley, S. Wu, C.C. Hsu, Water sorption behavior of lyophilized protein–sugar systems and implications for solid-state interactions, International Journal of Pharmaceutics 166 (1997) 211–221.

[32] C. Haeuser, P. Goldbach, J. Huwyler, W. Friess, A. Allmendinger, Be Aggressive! Amorphous Excipients Enabling Single-Step Freeze-Drying of Monoclonal Antibody Formulations, Pharmaceutics 11 (2019) 616.

[33] T. Serno, R. Geidobler, G. Winter, Protein stabilization by cyclodextrins in the liquid and dried state, Advanced drug delivery reviews 63 (2011) 1086–1106.

[34] S. Thakral, J. Sonje, B. Munjal, B. Bhatnagar, R. Suryanarayanan, Mannitol as an Excipient for Lyophilized Injectable Formulations, Journal of Pharmaceutical Sciences 112 (2023) 19–35.

[35] K. Shirai, K. Watanabe, H. Momida, First-principles study of the specific heat of glass at the glass transition with a case study on glycerol, Journal of physics. Condensed matter an Institute of Physics journal 34 (2022) 375902.

[36] L. Yu, D.S. Mishra, D.R. Rigsbee, Determination of the glass properties of D-mannitol using sorbitol as an impurity, Journal of Pharmaceutical Sciences 87 (1998) 774–777.

[37] P. Stärtzel, Arginine as an Excipient for Protein Freeze-Drying: A Mini Review, Journal of Pharmaceutical Sciences 107 (2018) 960–967.

[38] M. Roussenova, J.-C. Andrieux, M.A. Alam, J. Ubbink, Hydrogen bonding in maltooligomer-glycerol-water matrices: Relation to physical state and molecular free volume, Carbohydrate polymers 102 (2014) 566–575.

[39] M. Prašnikar, M. Bjelošević Žiberna, N. Kržišnik, R. Roškar, I. Grabnar, A. Žula, P. Ahlin Grabnar, Additive effects of the new viscosity-reducing and stabilizing excipients for monoclonal antibody formulation, International Journal of Pharmaceutics 674 (2025) 125451.

[40] H.L. Svilenov, A. Kulakova, M. Zalar, A.P. Golovanov, P. Harris, G. Winter, Orthogonal Techniques to Study the Effect of pH, Sucrose, and Arginine Salts on Monoclonal Antibody Physical Stability and Aggregation During Long-Term Storage, Journal of Pharmaceutical Sciences 109 (2020) 584–594.

[41] P. Stärtzel, H. Gieseler, M. Gieseler, A.M. Abdul-Fattah, M. Adler, H.-C. Mahler, P. Goldbach, Freeze drying of L-arginine/sucrose-based protein formulations, part I: influence of

formulation and arginine counter ion on the critical formulation temperature, product performance and protein stability, Journal of Pharmaceutical Sciences 104 (2015) 2345–2358.

[42] P. Stärtzel, H. Gieseler, M. Gieseler, A.M. Abdul-Fattah, M. Adler, H.-C. Mahler, P. Goldbach, Freeze drying of L-arginine/sucrose-based protein formulations, part I: influence of formulation and arginine counter ion on the critical formulation temperature, product performance and protein stability, Journal of Pharmaceutical Sciences 104 (2015) 2345–2358.

[43] H.L. Kim, A. McAuley, B. Livesay, W.D. Gray, J. McGuire, Modulation of protein adsorption by poloxamer 188 in relation to polysorbates 80 and 20 at solid surfaces, Journal of Pharmaceutical Sciences 103 (2014) 1043–1049.

[44] T.A. Khan, H.-C. Mahler, R.S.K. Kishore, Key interactions of surfactants in therapeutic protein formulations: A review, European Journal of Pharmaceutics and Biopharmaceutics 97 (2015) 60–67.

[45] A. Arsiccio, J. McCarty, R. Pisano, J.-E. Shea, Effect of Surfactants on Surface-Induced Denaturation of Proteins: Evidence of an Orientation-Dependent Mechanism, The Journal of Physical Chemistry B 122 (2018) 11390–11399.

[46] A.J. Castañeda Ruiz, M.A. Shetab Boushehri, T. Phan, S. Carle, P. Garidel, J. Buske, A. Lamprecht, Alternative Excipients for Protein Stabilization in Protein Therapeutics: Overcoming the Limitations of Polysorbates, Pharmaceutics 14 (2022).

[47] A. Martos, W. Koch, W. Jiskoot, K. Wuchner, G. Winter, W. Friess, A. Hawe, Trends on Analytical Characterization of Polysorbates and Their Degradation Products in Biopharmaceutical Formulations, Journal of Pharmaceutical Sciences 106 (2017) 1722–1735.

[48] P. Kolhe, E. Amend, S.K. Singh, Impact of freezing on pH of buffered solutions and consequences for monoclonal antibody aggregation, Biotechnology progress 26 (2010) 727–733.

[49] J. den Engelsman, P. Garidel, R. Smulders, H. Koll, B. Smith, S. Bassarab, A. Seidl, O. Hainzl, W. Jiskoot, Strategies for the assessment of protein aggregates in pharmaceutical biotech product development, Pharmaceutical Research 28 (2011) 920–933.

[50] H.-C. Mahler, W. Friess, U. Grauschopf, S. Kiese, Protein aggregation: pathways, induction factors and analysis, Journal of Pharmaceutical Sciences 98 (2009) 2909–2934.

[51] R. Chaudhuri, Y. Cheng, C.R. Middaugh, D.B. Volkin, High-throughput biophysical analysis of protein therapeutics to examine interrelationships between aggregate formation and conformational stability, The AAPS journal 16 (2014) 48–64.

[52] D.K. Sharma, D. King, P. Oma, C. Merchant, Micro-flow imaging: flow microscopy applied to sub-visible particulate analysis in protein formulations, The AAPS journal 12 (2010) 455–464.

[53] T.T. Mutukuri, N.E. Wilson, L.S. Taylor, E.M. Topp, Q.T. Zhou, Effects of drying method and excipient on the structure and physical stability of protein solids: Freeze drying vs. spray freeze drying, International Journal of Pharmaceutics 594 (2021) 120169.

[54] C. Bertucci, M. Pistolozzi, A. de Simone, Circular dichroism in drug discovery and development: an abridged review, Analytical and bioanalytical chemistry 398 (2010) 155–166.

[55] N. Kuhar, S. Sil, S. Umapathy, Potential of Raman spectroscopic techniques to study proteins, Spectrochimica acta. Part A, Molecular and biomolecular spectroscopy 258 (2021) 119712.

[56] M.T. Ruggiero, M. Krynski, E.O. Kissi, J. Sibik, D. Markl, N.Y. Tan, D. Arslanov, W. van der Zande, B. Redlich, T.M. Korter, H. Grohganz, K. Löbmann, T. Rades, S.R. Elliott, J.A. Zeitler, The significance of the amorphous potential energy landscape for dictating glassy dynamics and driving solid-state crystallisation, Physical chemistry chemical physics PCCP 19 (2017) 30039–30047.

[57] M. Batens, T.A. Shmool, J. Massant, J.A. Zeitler, G. van den Mooter, Advancing predictions of protein stability in the solid state, Physical chemistry chemical physics PCCP 22 (2020) 17247–17254.

[58] B. Wang, M.T. Cicerone, Y. Aso, M.J. Pikal, The impact of thermal treatment on the stability of freeze-dried amorphous pharmaceuticals: II. Aggregation in an IgG1 fusion protein, Journal of Pharmaceutical Sciences 99 (2010) 683–700.

[59] M.T. Cicerone, J.F. Douglas, β-Relaxation governs protein stability in sugar-glass matrices, Soft Matter 8 (2012) 2983.

[60] J. Kölbel, M.L. Anuschek, I. Stelzl, S. Santitewagun, W. Friess, J.A. Zeitler, Dynamical Transition in Dehydrated Proteins, The journal of physical chemistry letters 15 (2024) 3581–3590.

[61] T.A. Shmool, P.J. Woodhams, M. Leutzsch, A.D. Stephens, M.U. Gaimann, M.D. Mantle, G.S. Kaminski Schierle, C.F. van der Walle, J.A. Zeitler, Observation of high-temperature macromolecular confinement in lyophilised protein formulations using terahertz spectroscopy, International journal of pharmaceutics: X 1 (2019) 100022.

[62] E.M. Moussa, N.E. Wilson, Q.T. Zhou, S.K. Singh, S. Nema, E.M. Topp, Effects of Drying Process on an IgG1 Monoclonal Antibody Using Solid-State Hydrogen Deuterium Exchange with Mass Spectrometric Analysis (ssHDX-MS), Pharmaceutical Research 35 (2018) 12.

[63] L. Kumar, K.B. Chandrababu, S.M. Balakrishnan, A. Allmendinger, B. Walters, I.E. Zarraga, D.P. Chang, P. Nayak, E.M. Topp, Optimizing the Formulation and Lyophilization Process for a Fragment Antigen Binding (Fab) Protein Using Solid-State Hydrogen-Deuterium Exchange Mass Spectrometry (ssHDX-MS), Molecular Pharmaceutics 16 (2019) 4485–4495.

[64] B.S. Moorthy, I.E. Zarraga, L. Kumar, B.T. Walters, P. Goldbach, E.M. Topp, A. Allmendinger, Solid-State Hydrogen-Deuterium Exchange Mass Spectrometry: Correlation of Deuterium Uptake and Long-Term Stability of Lyophilized Monoclonal Antibody Formulations, Molecular Pharmaceutics 15 (2018) 1–11.

[65] M. Domnowski, K. Lo Presti, J. Binder, J. Reindl, L. Lehmann, F. Kummer, M. Wolber, M. Satzger, M. Dehling, J. Jaehrling, W. Frieß, Generation of mAb Variants with Less Attractive Self-Interaction but Preserved Target Binding by Well-Directed Mutation, Molecular Pharmaceutics (2020).

[66] C.J. Crilly, J.A. Brom, M.E. Kowalewski, S. Piszkiewicz, G.J. Pielak, Dried Protein Structure Revealed at the Residue Level by Liquid-Observed Vapor Exchange NMR, Biochemistry 60 (2021) 152–159.

[67] C.J. Crilly, J.E. Eicher, O. Warmuth, J.M. Atkin, G.J. Pielak, Water's Variable Role in Protein Stability Uncovered by Liquid-Observed Vapor Exchange NMR, Biochemistry 60 (2021) 3041–3045.

[68] A.M. Abdul-Fattah, V. Truong-Le, L. Yee, L. Nguyen, D.S. Kalonia, M.T. Cicerone, M.J. Pikal, Drying-induced variations in physico-chemical properties of amorphous pharmaceuticals and their impact on stability (I): stability of a monoclonal antibody, Journal of Pharmaceutical Sciences 96 (2007) 1983–2008.

[69] S.U. Sane, R. Wong, C.C. Hsu, Raman spectroscopic characterization of drying-induced structural changes in a therapeutic antibody: correlating structural changes with long-term stability, Journal of Pharmaceutical Sciences 93 (2004) 1005–1018.

[70] K. Dauer, C. Werner, D. Lindenblatt, K.G. Wagner, Impact of process stress on protein stability in highly-loaded solid protein/PEG formulations from small-scale melt extrusion, International journal of pharmaceutics: X 5 (2023) 100154.

[71] R. Fang, W. Obeidat, M.J. Pikal, R.H. Bogner, Evaluation of Predictors of Protein Relative Stability Obtained by Solid-State Hydrogen/Deuterium Exchange Monitored by FTIR, Pharmaceutical Research 37 (2020) 168.

[72] S. Sinha, Y. Li, T.D. Williams, E.M. Topp, Protein conformation in amorphous solids by FTIR and by hydrogen/deuterium exchange with mass spectrometry, Biophysical Journal 95 (2008) 5951–5961.

[73] N. Nitika, H. Chhabra, A.S. Rathore, Raman spectroscopy for in situ, real time monitoring of protein aggregation in lyophilized biotherapeutic products, International journal of biological macromolecules 179 (2021) 309–313.

[74] M.M. Castellanos, A. McAuley, J.E. Curtis, Investigating Structure and Dynamics of Proteins in Amorphous Phases Using Neutron Scattering, Computational and Structural Biotechnology Journal 15 (2017) 117–130.

[75] J.E. Curtis, A. McAuley, H. Nanda, S. Krueger, Protein structure and interactions in the solid state studied by small-angle neutron scattering, Faraday Discussions 158 (2012) 285-99; 351-70.

[76] J.E. Curtis, H. Nanda, S. Khodadadi, M. Cicerone, H.J. Lee, A. McAuley, S. Krueger, Small-angle neutron scattering study of protein crowding in liquid and solid phases: lysozyme in aqueous solution, frozen solution, and carbohydrate powders, The Journal of Physical Chemistry B 116 (2012) 9653–9667.

[77] J. Eisermann, M. Hoffmann, F.A. Schöffmann, M. Das, C. Vargas, S. Keller, D. Hinderberger, Molecular-Level Interactions of Nanodisc-Forming Copolymers Dissected by EPR Spectroscopy, Macromolecular Chemistry and Physics 222 (2021) 2100051.

[78] I.D. Sahu, G.A. Lorigan, Electron Paramagnetic Resonance as a Tool for Studying Membrane Proteins, Biomolecules 10 (2020).

[79] I. Gertsenshteyn, M. Giurcanu, P. Vaupel, H. Halpern, Biological validation of electron paramagnetic resonance (EPR) image oxygen thresholds in tissue, The Journal of physiology 599 (2021) 1759–1767.

[80] J. Dröden, M. Drescher, Rapid Scan Electron Paramagnetic Resonance Spectroscopy Is a Suitable Tool to Study Intermolecular Interactions of Intrinsically Disordered Protein, Biology 12 (2023).

[81] L. Galazzo, E. Bordignon, Electron paramagnetic resonance spectroscopy in structural-dynamic studies of large protein complexes, Progress in nuclear magnetic resonance spectroscopy 134-135 (2023) 1–19.

Chapter II Aim and objective of the thesis

A better understanding of the protein drug stability in the lyophilizates is crucial for the rational development of optimal formulations. In this context, the application of novel stabilizing excipients and novel analytical methods is of interest to elucidate the mechanism of stabilization in the lyophilized matrix.

This thesis should give insights into the molecular environment, mobility, accessibility, and ultimately stability of protein molecules in lyophilizates. To this end, the impact of the amount, type, and size of excipient, as well as residual moisture content, was analyzed. Low molar ratios of common excipients such as sucrose and mannitol, as well as novel excipients in varying sizes, maltose, maltotriose, maltotetraose, and their mixtures, were tested using mAb and HSA combined with well-defined residual moisture contents. For this purpose, a spiking technique was established to adjust the moisture content post-lyophilization precisely.

Two novel methods, solid state hydrogen deuterium exchange (ssHDX) mass spectrometry and electron paramagnetic resonance (EPR) spectroscopy, were established to correlate the protein accessibility and folding in the solid state, as well as the nearest environment around the protein and excipient to protein interaction.

Chapter III describes the development and establishment of the residual moisture spiking technique used in several approaches throughout this thesis. Hamilton microliter syringes were used to precisely and individually adjust the moisture content of lyophilizates to set a specific moisture level in samples from the same lyophilization cycle. Additionally, this technique was used to spike deuterium oxide in the ssHDX approaches, leading to a highly controlled deuterium incorporation under relevant storage and packing conditions.

In **Chapter IV**, a mAb was lyophilized using sucrose at different low molar ratios to investigate the existence of a minimal molar stabilization threshold and whether “the more the better” holds true at such low stabilizer to protein ratios. Additionally, the influence of buffer, surfactant, and excipient type was elucidated at the low molar ratios.

Next, in **Chapter V**, HSA was lyophilized using excipients of different sizes to address the “the bigger the better” theory and to gain a deeper understanding of protein stabilization in lyophilizates. Larger excipient molecules may enhance protein stabilization by forming a rigid matrix within the lyocake and promoting vitrification of the protein. In contrast, smaller excipients can more effectively occupy voids around the protein and replace water molecules. Glucose, maltose, maltotriose, and maltotetraose, as well as mixtures thereof, were

characterized for the stabilization potential while considering the influence of the residual moisture content. Additionally, an ssHDX approach was established and applied to compare the protein accessibility with protein monomer retention upon storage.

Chapter VI summarizes the establishment of EPR as a novel method in the pharmaceutical technological field to gain insights into the protein structural preservation and the molecular environment of protein molecules in the solid state. For this purpose, HSA was spin-labelled HSA and lyophilized with deuterated sucrose. Electron spin echo envelope modulation (ESEEM) was used to investigate the nearest environment of the HSA label in the freeze dried state with a focus on the sucrose content. Double-electron resonance (DEER) was used to investigate the distance between HSA molecules. The results were compared by aggregate and structure analysis by SEC and CD.

Chapter VII is a summary and conclusion of this thesis, highlighting the impact of the amount, size, and type of excipient and the impact of residual moisture for an increased formulation space of lyophilized protein drugs. Finally, the novel techniques, which were established to investigate the protein structure in the solid state, are briefly discussed.

Chapter III Adjustment of specific residual moisture levels in completely freeze-dried protein formulations by controlled spiking of small water volumes

This chapter is published as: Lo Presti, K.; Frieß, W. Adjustment of specific residual moisture levels in completely freeze-dried protein formulations by controlled spiking of small water volumes. *European Journal of Pharmaceutics and Biopharmaceutics* 169 (2021) 292-296.

Note from the authors: To establish a coherent numbering and pagination within this document the numbers of references, figures, and tables were adapted. Apart from minor changes, the version included in this thesis is identical to the published article.

The published article can be accessed online via:

https://doi.org/10.1016/j.ejpb.2021.10.011

III.1 Abstract

The residual moisture (RM) level strongly impacts the stability of freeze-dried biopharmaceuticals. On the one hand, the RM should not be too high to keep the reaction potential of water molecules low and to avoid a decrease in the glass transition temperature through the plasticizing effect of water. On the other hand, overdrying has been described to negatively impact protein stability. Consequently, an optimal RM has to be established and justified for approval by authorities. Therefore, end products with different RM are analyzed over storage. The different RM levels are typically obtained by slightly varying the lyophilization process itself; but deviations from the original process are critical. Additionally, samples can be taken during lyophilization runs, e.g. at the end of primary drying or after the ramp into secondary drying. This, however, does not allow for good control over the RM. Here we present the adaption of a headspace water spiking technique using a microliter syringe to precisely increase and adjust the RM. This technique is suitable to reproducibly introduce water in the microliter scale to achieve RM of less than 1% [w/w] with high precision depending on the dry cake weight. In addition, we show that by using different fill volumes and cake densities, an equal three-dimensional water distribution throughout the whole cake can be achieved. Furthermore, potential limitations and risks in manual RM introduction are discussed.

Keywords: Lyophilization; Residual Moisture; Spiking; Moisture Distribution; Antibody; Stability Testing

III.2 Graphical Abstract

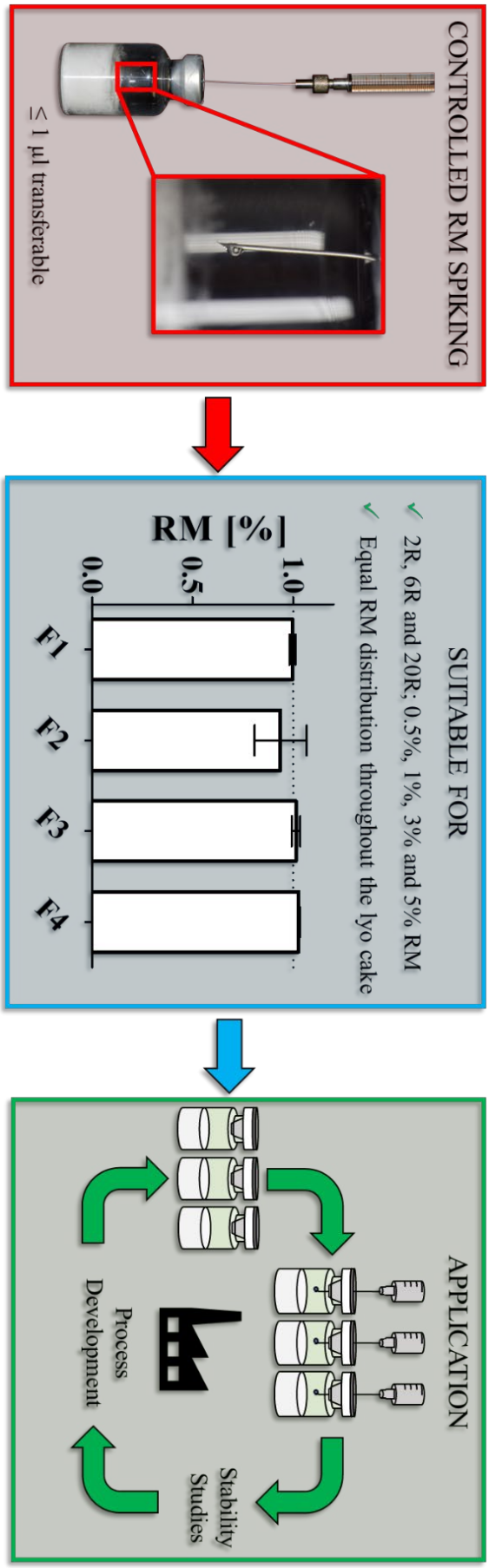

III.3 Introduction

Residual moisture (RM) in lyophilized biopharmaceutical drug products has a crucial impact in protein stability and cake structure [1,2]. The RM shall not be too high to keep the water molecule concentration as chemical reaction partner low and to avoid a decrease of the glass transition temperature by the plasticizing effect of water [3,4]. But the RM shall not be too low since overdrying could negatively impact protein stability [5]. RM of commercial lyophilized products usually varies between ≤1.0% to 3 % [w/w] [6,7]. Consequently, an optimal RM has to be established and justified for approval by authorities. Thus, end products with different RM are analyzed over storage. Controlled adjustment of RM may allow for better comparison of samples obtained with different formulations and different processes or simply from different batches.

The different RM levels are typically obtained by slightly varying the lyophilization process itself; but deviations from the original process are critical. In addition, this comes with high time and material consumption. Alternatively, samples are taken during lyophilization runs, e.g. at the end of primary drying or after the ramp into secondary drying, which does not give a good control over the RM. Open storage in controlled low humidity chambers is another option [8]. But again, water uptake is strongly formulation dependent and is hard to control it precisely. Thus, a technique to introduce a defined RM in lyophilizates is needed to waive multiple lyophilization cycles and to adjust RM in vials resulting from the same batch.

Water spiking with a microliter syringe has been described by Metrohm to establish near-infrared spectroscopy as a tool for RM analysis [9,10]. To establish this method as a strong tool in pharmaceutical process development and stability studies, further investigations of this technique were needed. We therefore aimed at providing confidence into the method as tool for research and development of lyophilizates of biologics. We monitored the water spiking procedure for its practical pharmaceutical application checking precision and reproducibility, analyzing the impact of cake density, studying the RM distribution throughout the freeze-dried cake, and evaluating possible limitations.

III.4 Materials and Methods

III.4.1 Materials

A monoclonal IgG1 antibody in 20 mM histidine buffer pH 6 at a stock concentration of more than 100 mg/ml (mAb) was used. D-mannitol and sucrose were purchased from Sigma-Aldrich (St. Louis, MO), L-histidine hydrochloride monohydrate and polysorbate 20 were purchased from Merck KGaA, Darmstadt, Germany. Spiking and diluting was performed using highly purified water (HPW) prepared with a UF system (Sartorius Arium Pro; Sartorius, Göttingen, Germany). 5 different formulations were investigated (Table III.1). All analyses were performed in triplicates.

Table III.1: Formulations tested

Formulation	mAb [mg/ml]	Buffer	Sucrose [mg/ml]	Mannitol [mg/ml]
F1	50	20 mM L-His/HisHCl pH 6; 0.02% PS 20	40	-
F2	50		80	-
F3	50		8	32
F4	50		27	53
F5	100		100	-

III.4.2 Generation of lyophilizates

1 ml of formulation F1-F4 were lyophilized in 2R, 3 ml of F1-F4 in 6R vials (Bünder Glas GmbH, Bünde, Germany), and 10 ml of formulation 5 in 20R vials (Fiolax®, Schott AG, Mainz, Germany) (Table 1). Vials were loosely closed with pre-dried rubber stoppers (West Pharmaceutical Services, Inc., Exton, PA). Freeze-drying was performed on an FTS Lyostar 3 equipped with a comparative pressure system (SP Scientific, Stone Ridge, USA). After 30 min equilibration at 5 °C, the shelf temperature was decreased to -45 °C at 0.5 K/min followed by a 3 h hold. During primary drying a vacuum of 70 mTorr was applied at -30 °C shelf temperature (ramp of 0.25 K/min). The end of primary drying was detected by a difference of 5% in the comparative pressure measurement. At that point the vacuum was set to 40 mTorr and the shelf temperature was ramped to 10 °C at 0.25 K/min. After a 1 h hold, the temperature was further increased to 30 °C at 0.25 K/min and the vacuum was set at 20 mTorr. These conditions were held for 3 h. Finally, the shelf temperature was increased to 70°C at 0.25 K/min. The conditions were held for 24 h. Venting and vial closing was performed with nitrogen at 450 Torr. Immediately after lyophilization the vials were crimped.

III.4.3 Spiking of residual moisture

Lyophilized samples were spiked using Hamilton Microliter syringes (7000 needle series, needle point style 2, Hamilton Bonaduz AG, Bonaduz, Switzerland) with total volumes of 0.5 µl, 1 µl, 5 µl, 10 µ and 100 µl. Transferred volumes were adjusted by eye. Consequently, transferable volumes of less than 0.01 µl measured by visual judgment are possible. The desired volume of HPW was calculated according to the theoretical solid content of the completely freeze-dried samples and spiked in as shown in Figure III.1. 2R samples were spiked with 0.93 µl and 1.33 µl and 6R samples with 2.79 µl and 3.99 µl to generate 1% RM samples. Additionally, 20R samples containing 0.5%, 3% and 5% RM were generated using volumes of 10.16 µl, 60.93 µl and 101.55 µl, respectively. The latter was spiked by introducing 100 µl first, followed by 1.55 µl using the 5 µl syringe.

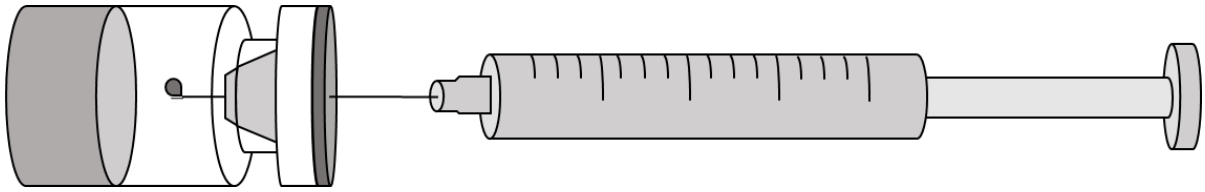

Figure III.1: Residual moisture spiking procedure using Hamilton Microliter syringes. Droplet was injected into the headspace and evaporated completely before removal of the syringe

HPW was introduced at room temperature by pinching the needle through the capped vial standing in upright position, ejecting the water droplet approx. 1 cm above the cake and letting the droplet completely evaporate from the tip of the needle. The syringe was removed and the prick was additionally sealed with Parafilm® and samples stored for at least 24 h at 4 °C before RM measurements.

III.4.4 Analysis of Residual moisture by Karl Fischer titration

RM and RM distribution was analyzed with a headspace Karl Fischer titration (Aqua 40.00, Analytik Jena GmbH, Jena, Germany). Samples were placed into an oven with 120 °C and heated until complete extraction of present water. As a control, a pure water standard (Aquastar water standard oven 1.0, Merck KGaA) was analyzed before each sample set. The RM introduced by spiking was calculated by subtracting the RM of non-spiked samples. Whole cakes in 2R vials were directly analyzed in the original vials. Additionally, selected cakes as well as fractions of cakes were removed from the vial as described in 3.5 and analyzed.

III.4.5 Investigation of water distribution and recovery

The RM distribution within cakes was characterized by dissecting vial cakes and analyzing the RM of the segments. For this purpose, the spiked vials were cut open using a glass cutting device (Dremel® Model 300 with glass cutting attachment, DREMEL Europe, the Netherlands) in a glove box under nitrogen environment with residual air humidity of less than 4%. The laid open 2R and 6R vial cakes were cut horizontally using a scalpel. 20R vial cakes were dissected as shown in Figure III.2. Furthermore, laid open cakes were transferred in new 2R vials, grinded using a spatula and analyzed.

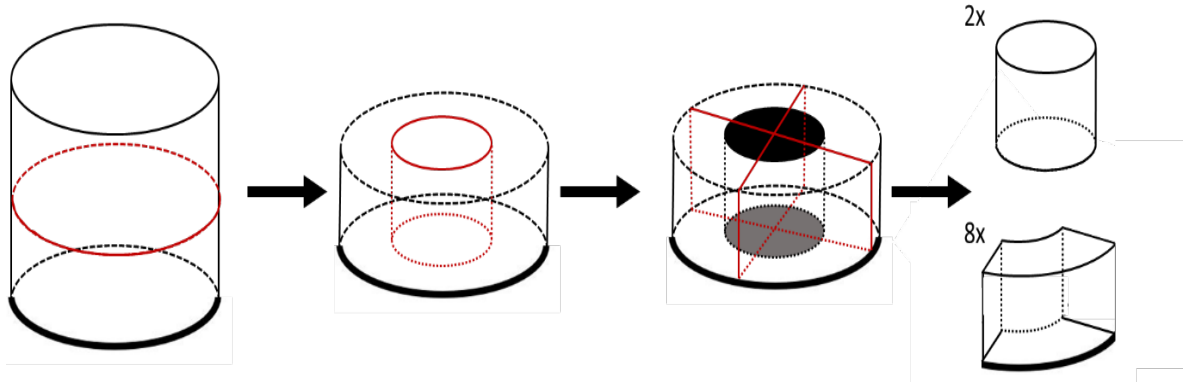

Figure III.2: Sample preparation procedure of 20R vials. The product cake is cut into a top and a bottom half and additionally separated into 4 outer and one inner area to achieve a 3D model of the RM distribution. Due to the low solid content, 2R and 6R samples were only separated into a top and a bottom half to investigate water distribution.

III.5 Results and Discussion

III.5.1 Residual moisture after spiking 1% in 2R vial samples

The RM content after freeze drying was ≤ 0.18%, ≤ 0.50%, and ≤ 0.1% [w/w] for 2R, 6R and 20R vial samples. No significant impact of the formulation could be identified. After spiking formulations F1 through F4 with approx. 1 µl, the increase in RM was 1.0% + < 0.05 for F1, F3, and F4, and 0.94% ± 0.13 for F2, the formulation with the highest sucrose content (Figure III.3). Thus, the described method is suitable to adjust low RM level cakes of only approx. 100 mg which reflects a typical biologic product with an amorphous sugar matrix and buffer.

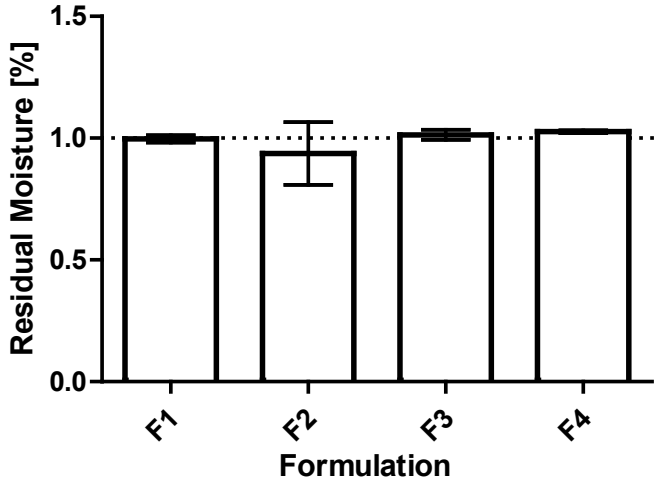

Figure III.3: RM content of lyophilized 2R vial samples spiked with 1.0% water without further sample preparation.

III.5.2 Residual moisture distribution

Analysis of the moisture distribution showed comparable results for the top and the bottom half of cakes in 2R and 6R vials (Figure III.4). No trend was seen that F2 would behave differently and the 2R vial cakes with a total solid content between 93 mg and 133 mg showed the targeted spiked in RM of 1.0% in the top and bottom half (Figure III.4a). Cakes in 6R vials with a 3 times higher solid content revealed similar results (Figure III.4b).

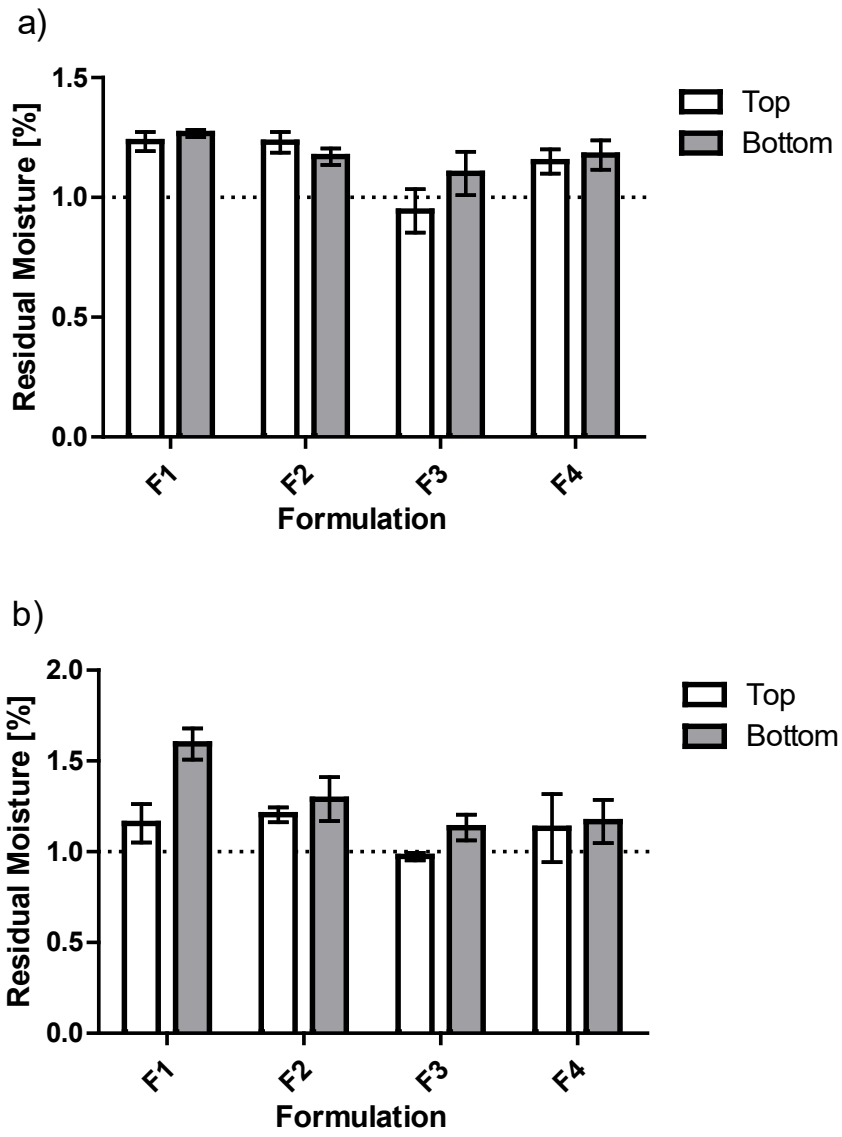

Figure III.4: RM content of top and bottom half of lyophilized (a) 2R and (b) 6R vial samples spiked with 1.0% water.

RM scattered around 1%, with tendencies towards slightly higher RM. The bottom half of F1 showed slightly higher RM content of approx. 1.6%. The combined RM of top and bottom half of each formulation was higher than targeted. This slight increase can be explained by the time-consuming sample preparation in the glovebox and potential environmental humidity uptake. More challenging RM distribution analysis was performed by testing the RM of formulation F5 with approx. 2 g solid in 20R vials. Samples adjusted to 0.5% RM by injecting 10.16 µl showed comparable water distribution through the whole cake at the value between 0.4% and 0.5% (Figure III.5a). 20R vials adjusted to 3% displayed variations of the RM content in the different segments between 2.2 and 3.0% (Figure III.5b), and this offset to the target values was even more distinct for 5% RM spiking with 3.5% to 4.3% RM in the different segments (Figure III.5c).

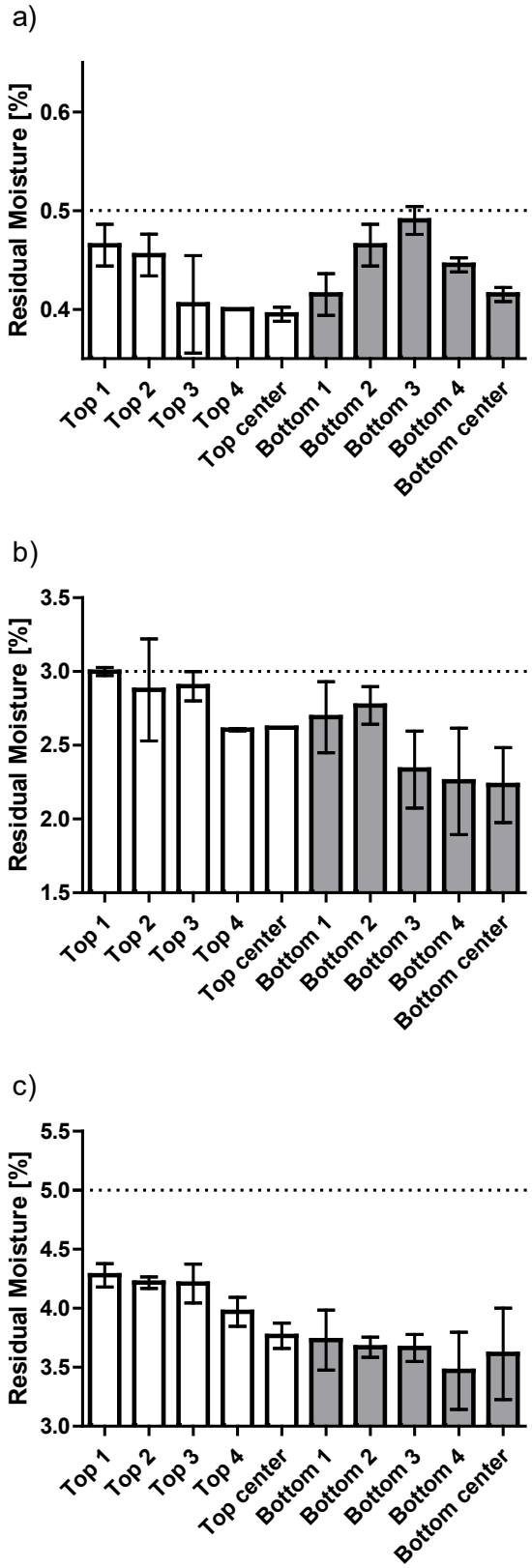

Figure III.5: RM content of different fragments (see Figure III.2) of lyophilized 20R samples spiked with (a) 0.5%, (b) 3%, and (c) 5% water.

Fluctuation in RM seemed independent of the investigated area, but strongly connected with the operating time under the glovebox. The RM decreased from the first prepared sample "top 1" to the last prepared sample "bottom center", leading to the conclusion that low relative humidity in the glovebox (≤ 4%) and long preparation times led to a water loss. To further investigate this effect, 6R placebo lyophilizates were adjusted to 8% RM, opened under the glovebox and weighed for 20 min. The mass continuously decreased by approx. 0.5% every 5 min. This result not only explains the decreased overall RM in the dissected segments as well as the differences between the segments; it also highlights the fact that any open handling of lyophilizates before RM analysis, being unprotected or in a humidity reduced glovebox should be avoided and if necessary, be performed as quick as possible. The effect was markedly more pronounced for cakes with higher RM of 5% which more rapidly loose water in the dry glove box atmosphere compared to the 3% RM cake. For the 1% RM cake we noticed the opposite, an increase in RM in the nitrogen flushed glove box. Ultimately, it can be expected that also the formulation affects this equilibration effect of the unprotected cake exposed to any atmosphere outside the vial.

In summary, the transfer of minimal water volumes of less than 1 µl into the head space of a vial allows highly reproducible adjustment of the RM of lyophilizates. Grinding before Karl Fischer measurements demonstrates water incorporation into the lyocake itself and not into the existing pores. The water rapidly evenly distributes throughout the cakes. We demonstrated this from 1% RM level for 93 mg cakes with an injection volume below 1 µl up to 5% RM level for 2 g cakes injecting approx. 100 µl. Consequently, this technique is applicable for a broad range of typical biologic lyophilization products and is an accurate, fast, and reproducible alternative to lyophilization process variations. Since RM modification can be performed independently after lyophilization, comparable initial conditions are adjustable in stability testing. Thus, comparison of different formulations or batches as well as process parameters and specifications can be investigated, compared, and rated.

III.6 References

References

[1] E.D. Breen, J.G. Curley, D.E. Overcashier, C.C. Hsu, S.J. Shire, Effect of Moisture on the Stability of a Lyophilized Humanized Monoclonal Antibody Formulation, Pharmaceutical Research 18 (2001) 1345-1353.

[2] M.J. Hageman, The Role of Moisture in Protein Stability, Drug Development and Industrial Pharmacy 14 (1988) 2047–2070.

[3] S. Ohtake, S. Feng, E. Shalaev, Effect of Water on the Chemical Stability of Amorphous Pharmaceuticals: 2. Deamidation of Peptides and Proteins, Journal of Pharmaceutical Sciences 107 (2018) 42–56.

[4] S. Feng, G.H.J. Peters, S. Ohtake, C. Schöneich, E. Shalaev, Water Distribution and Clustering on the Lyophilized IgG1 Surface: Insight from Molecular Dynamics Simulations, Molecular Pharmaceutics 17 (2020) 900–908.

[5] C.C. Hsu, C.A. Ward, R. Pearlman, H.M. Nguyen, D.A. Yeung, J.G. Curley, Determining the optimum residual moisture in lyophilized protein pharmaceuticals, Developments in Biological Standardization 74 (1992) 255-70.

[6] K.A. Gaidhani, M. Harwalkar, D. Bhambere, P.S. Nirgude, Lyophilization/Freeze Drying - A Review, World Journal of Pharmaceutical Research 4 (2015) 516–543.

[7] A. Duralliu, P. Matejtschuk, P. Stickings, L. Hassall, R. Tierney, D.R. Williams, The Influence of Moisture Content and Temperature on the Long-Term Storage Stability of Freeze-Dried High Concentration Immunoglobulin G (IgG), Pharmaceutics 12 (2020).

[8] L. Greenspan, Humidity fixed points of binary saturated aqueous solutions, Journal of Research of the National Bureau of Standards Section A: Physics and Chemistry 81A (1977) 89–96.

[9] Metrohm, Analysis of residual moisture in a lyophilized pharmaceutical product by near-infrared spectroscopy. Application Bulletin 358/1e.

[10] R.P. Affleck, D. Khamar, K.M. Lowerre, N. Adler, S. Cullen, M. Yang, T.R. McCoy, Near Infrared and Frequency Modulated Spectroscopy as Non-invasive methods for Moisture Assessment of Freeze-Dried Biologics, Journal of Pharmaceutical Sciences 110 (2021) 3395–3402.

Chapter IV "The more, the better?" - The impact of sugar-to-protein molar ratio in freeze-dried monoclonal antibody formulations on protein stability

This chapter is published as: Lo Presti, K.; Jègo, M.; Frieß, W. "The more, the better?" - The impact of sugar-to-protein molar ratio in freeze-dried monoclonal antibody formulations on protein stability. *Molecular Pharmaceutics* 21 (2024) 6484-6490

Note from the authors: To establish a coherent numbering and pagination within this document the numbers of references, figures, and tables were adapted. Apart from minor changes, the version included in this thesis is identical to the published article.

The published article can be accessed online via:

https://doi.org/10.1021/acs.molpharmaceut.4c01174

IV.1 Abstract

Lyophilization is widely used to ensure the stability of protein drugs by minimizing chemical and physical degradation in the dry solid state. To this end, proteins are typically formulated with sugars which form an amorphous immobilizing matrix and stabilizing hydrogen bonds replacing water molecules. The optimal amount of sugar required and protein stability at low molar excipient-to-protein molar ratios is not well understood. We investigated this by focusing on the physical stability of formulations reflecting highly concentrated monoclonal antibody (mAb) lyophilizates at low sucrose to mAb ratios between 25:1 to 360:1. Additionally, the impact of different excipient types, buffer concentration, and polysorbate was studied. The mAb stability was evaluated over up to three months at 25 °C and 40 °C. We investigated the "the more, the better" approach regarding excipient usage in protein formulation and the existence of a potential stabilizing threshold. Our findings show efficient monomeric content preservation even at low molar ratios which could be explained based on the water replacement theory. We identified an exponential correlation between the sucrose to protein molar ratio and aggregate formation and found that there is no molar ratio threshold to achieve minimum stabilization. Sucrose demonstrated the best stabilization effect. Both mannitol, used as a cryoprotectant at low concentrations, and arginine reduced aggregation compared to pure mAb formulation. The higher ionic strength of 5 mM histidine buffer enhanced protein stability compared to 0.1 mM histidine buffer, which was more pronounced at lower molar ratios. The addition of polysorbate 20 contributed an additional interfacial stabilizing effect, complementing the cryo- and lyoprotective properties of sucrose. Overall, a model could be developed to optimize the

quantity of sugar required for protein stabilization and facilitate a more rational design of protein lyophilizates. The molar ratio of sugar to protein for high concentration mAb products is limited by the acceptable tonicity but we showed that sufficient stabilization can be achieved even at low molar ratios.

Keywords: lyophilization, long-term stability, molar ratio, monoclonal antibody, sucrose, arginine, mannitol, excipient, high concentration, aggregation, water replacement

IV.2 Graphical Abstract

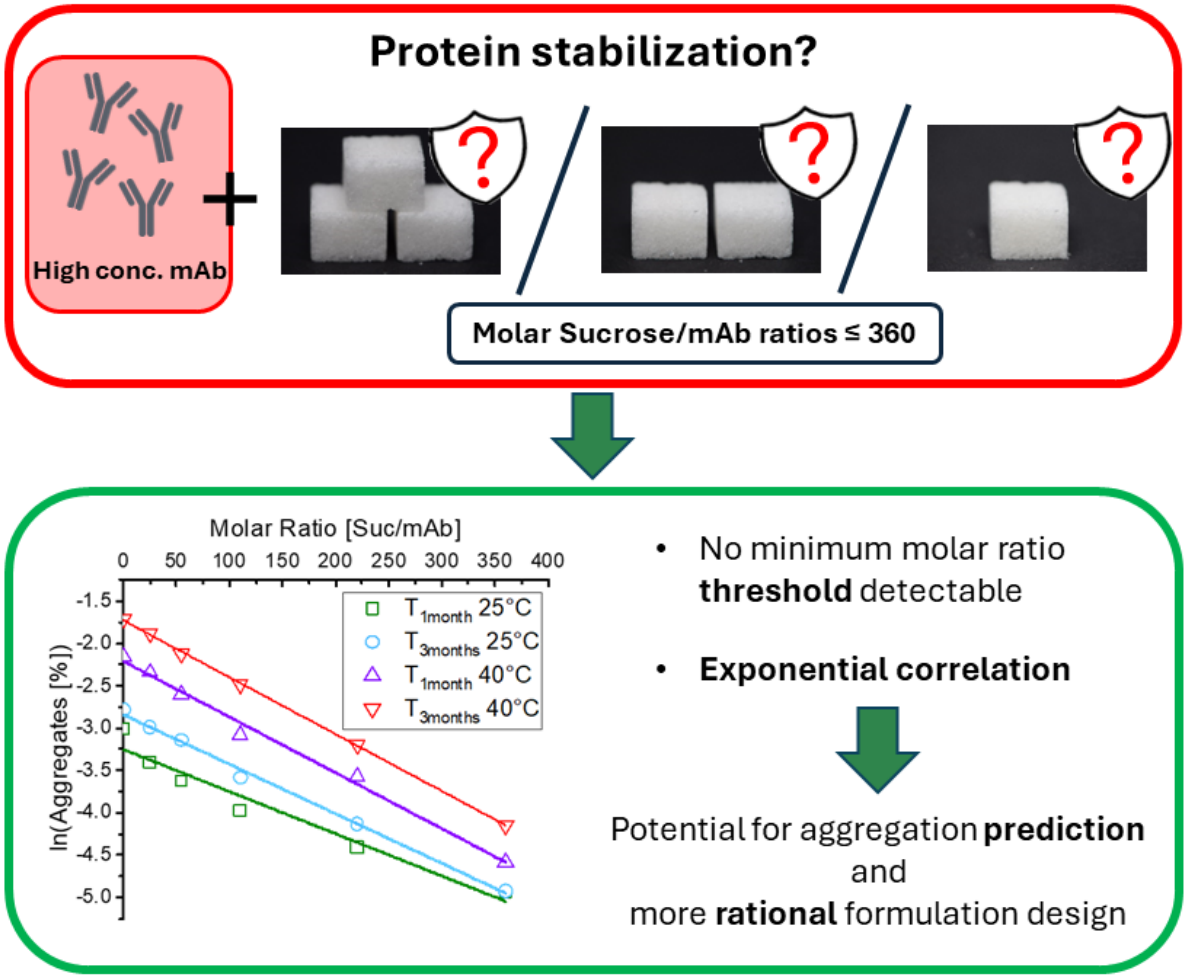

IV.3 Introduction

It is essential to preserve the chemical and physical integrity of protein drugs in pharmaceutical formulations to assure safety and efficacy.[1,2] If the stability in aqueous solutions is not sufficient, lyophilization is commonly used to reduce the rates of both chemical and physical degradation.[3,4] Sugars such as trehalose and sucrose are the primary cryo- and lyoprotectants of choice in protein lyophilizates.[5,6] Two main hypotheses are utilized to explain the mechanisms by which sugars stabilize proteins in the dry state. Firstly, the sugar molecules build hydrogen bonds with the protein molecules in the dry state, replacing removed water molecules in this function and maintaining the native structure.[7] Secondly, the vitrification theory proposes that the viscosity of the amorphous sugar matrix formed with the protein molecules drastically reduces mobility below the glass transition temperature leading to a lower unfolding propensity within the energy landscape in combination with steric hindrance.[8]

It was shown that varying excipient type, sugar to protein ratio, and excipient size affect protein stability which can be explained via either theory.[9–12] Chang et al. found that increasing weight ratios of sucrose to mAb or rHSA led to improved structure preservation and reduced aggregation formation, as investigated by FTIR.[13] Cleland et al. proposed that for a 25 g/l mAb, a minimum molar ratio of 360:1 is necessary to achieve sufficient stabilization against aggregation and deamidation in lyophilizates.[14] Furthermore, Andya et al. showed that increasing the molar sucrose to protein ratio decreases the formation of soluble aggregates of freeze dried rhuMAb.[15]

At the upper end, osmolality sets a limit to the amount of sugars that can be used.[16] While osmolalities of 500 mM and higher could be considered, an isotonic solution is most preferred.[17] For a 150 g/l (1 mM) mAb solution with a 40 mosmol buffer, approximately 260 mM sucrose can be used, resulting in a low sucrose to protein molar ratio of 260:1 This highlights the practical limitations of the "the more the better" approach, particularly in highly concentrated protein formulations and those that include multiple excipients. Bulking agents like mannitol are widely used and often exceed the concentration of sucrose, further restricting the additional amount of sugar that can be used.[18] Furthermore, reducing the amount of sugar offers more flexibility for incorporating additional excipients that might be necessary for stabilization of e.g. methionine oxidation or viscosity reduction.

In this work, we investigated the effect of sucrose at molar ratios from 25:1 to 360:1 in highly concentrated mAb (50 g/l) formulations on the protein stability. Our investigation involved assessing aggregate formation using SEC and monitoring subvisible particle formation.

We aimed to identify potential molar ratio thresholds to stabilize lyophilizates and compared the impact of excipient type by additionally investigating mannitol and arginine HCl as common bulking and stabilization excipients.[19,20] We examined the impact of the ionic strength of the buffer system on protein stability at low excipient to protein molar ratios comparing 5 mM histidine and 0.1 mM histidine buffers.[21] Lastly, we investigated the stabilization impact of polysorbate 20 as a surfactant to assess the extent of additional stabilization via protection of the interface at low excipient to protein molar ratios.[14,22]

IV.4 Material and Methods

IV.4.1 Materials

A monoclonal IgG_1 antibody stock solution (derived from a CHO cell line) of approx. 200 g/l was prepared by dialyzing against 0.1 mM and 5 mM histidine buffer, respectively. L-histidine hydrochloride, arginine HCl, di-potassium hydrogen phosphate, and polysorbate 20 were purchased from Merck KGaA (Darmstadt, Germany). Sucrose was obtained from Caelo (Caesar &Loretz, Hilden, Germany) and mannitol was bought from Sigma-Aldrich (Steinheim am Albruch, Germany). Potassium dihydrogen phosphate was purchased from Grussing GmbH (Filsum, Germany). Highly purified water was prepared with a UF system (Sartorius Arium Pro; Sartorius, Gottingen, Germany). All samples were filtered using 0.2 µm PES membrane syringe filters (VWR International, Radnor, PA, USA).

IV.4.2 Lyophilization

1 ml of sample solution was filled into 2R glass vials (Bünder Glas, Bünde, Germany) and semi-stoppered with single vent lyophilization stoppers (13-mm Lyo Nova Pure RS 1356 4023/50 G West Pharmaceuticals, Eschweiler, Germany). Thermocouples were placed into the different formulations to monitor product temperature, and all samples were freeze dried in the same cycle. Samples were lyophilized using an FTS Lyostar 3 equipped with a comparative pressure system (SP Scientific, Stone Ridge, NY, USA). After 30 min of equilibration at 5 °C, the shelf temperature was decreased to -45 °C with a ramp of 0.5 °C/min and held for 3 h. Primary drying was performed at 0.1 mbar and -25 °C after a temperature ramp of 0.25 °C/min. The end of primary drying was detected within 48 h by a 5 mTorr (=0067 mbar) difference using comparative pressure measurement. Secondary drying was executed at 0.066 mbar at a shelf temperature of 25 °C with a ramp of 0.25 C/min. After 24 h, the vials were stoppered under a nitrogen atmosphere at 800 mbar. Dried samples were crimped with Flipp-Off® caps (ChemoLine, Sankt Augustin, Germany) and stored at 5 °C until further use.

IV.4.3 Formulations

Samples were analyzed before (T_{liquid}) and immediately after (T_{lyo}) lyophilization. The freeze-dried samples were stored at 25 °C and 40 °C for up to 3 months. The conditions were selected to assess stability within a reasonable timeframe at temperatures reflecting accelerated storage conditions compared to the typically intended storage temperature of 5 °C. Lyophilized samples were reconstituted with 1 ml of HPW for analysis. Four sets of formulations were investigated to study various factors affecting stability: the sucrose to mAb molar ratio (Table IV.1), the effects of sucrose, mannitol, and arginine HCl at very low molar ratios (Table IV.2), the role of buffer concentration to test the impact of low ionic strength using 0.1 mM His instead of 5 mM His buffer (Table IV.3), and the impact of the presence of surfactants (Table IV.4). Although slightly higher concentrations of 10 mM to 20 mM may be more typical for mAb drug products, we selected lower buffer concentrations to highlight the effects of the low sugar amounts and to avoid pH shifts.

Table IV.1: Formulations to investigate the impact of sucrose-to-protein molar ratio.

Molar ratio [excipient/protein]	Sucrose			mAb [g/l]	Buffer
	[g/l]	[mM]	Wt%		
360	41.1	120	45.1%	50	5 mM His pH 6.5 0.02% PS20
220	20.5	60	29.1%		
110	10.3	30	17.1%		
55	5.1	15	9.3%		
25	2.6	7.5	4.9%		
-*	-	-	0%		

**Corresponds to the mAb-only formulation*

Table IV.2: Formulations to study the influence of excipient type.

Molar ratio [excipient/protein]	Sucrose			Mannitol			Arginine HCl			mAb [g/l]	Buffer
	[g/l]	[mM]	Wt%	[g/l]	[mM]	Wt%	[g/l]	[mM]	Wt%		
25	2.6	7.5	4.9	-	-	-	-	-	-	50	5 mM His pH 6.5 0.02% PS20
25	-	-	-	1.4	7.5	2.7	-	-	-		
25	-	-	-	-	-	-	1.3	7.5	2.5		
-*	-	-	-	-	-	-	-	-	-		

**Corresponds to the mAb-only formulation*

Table IV.3: Formulations to study the influence of ionic strength of the buffer system.

Molar ratio [excipient/protein]	Sucrose			Mannitol			Arginine HCl			mAb [g/l]	Buffer
	[g/l]	[mM]	Wt%	[g/l]	[mM]	Wt%	[g/l]	[mM]	Wt%		
55	5.1	15	9.3	-	-	-	-	-	-	50	0.1 mM His pH 6.5 0.02% PS20
25	2.6	7.5	4.9	-	-	-	-	-	-		
25	-	-	-	1.4	7.5	2.7	-	-	-		
25	-	-	-	-	-	-	1.3	7.5	2.5		
-*	-	-	-	-	-	-	-	-	-		

**Corresponds to the mAb-only formulation*

Table IV.4: Formulations to study the impact of surfactant

Molar ratio [excipient/protein]	Sucrose		mAb [g/l]	Buffer
	[g/l]	[mM]		
55	5.1	15	50	5 mM His pH 6.5
25	2.6	7.5		

IV.4.4 Analysis of residual moisture by Karl Fischer titration

The residual moisture (RM) of lyophilizates was analyzed using a headspace Aqua 40.00 Karl Fischer titration system (Vario, Elektrochemie Halle, Halle, Germany). As control, a pure water standard (Aquastar water standard oven 1.0, Merck KGaA) was analyzed. Approx. 20 mg of lyophilizate were transferred into 2R vials under a nitrogen environment (r.h. $\leq$ 4.5%). Then, samples were heated at 120 °C until residual moisture extraction was complete.

IV.4.5 X-Ray powder diffraction

X-ray powder diffraction (XRD) was performed on a Miniflex (II) (Rigaku Corporation, Tokyo, Japan) with Cu Kα radiation at a scan rate of 10° min^{-1} from 2° to 60° 2θ at room temperature.

IV.4.6 Monomeric content analysis by size exclusion chromatography

The monomer content was determined by size exclusion chromatography (SEC) with an Agilent 1200 HPLC system, equipped with a diode array detector (Agilent Technologies, Santa Clara, CA, USA). A TSKgel G3000 SWxl column (Tosoh Bioscience, Griesheim, Germany) was employed as stationary phase, and 150 mM potassium phosphate buffer at pH 6.45 as mobile phase at 0.4 ml/min. Before injection, the reconstituted samples were centrifuged for 4 min at 13,000xG using a HeraeusTM MegafugeTM 16R (Thermo Fisher Scientific Inc., Waltham, MA, USA), and 0.5 mg mAb was injected. A gel filtration chromatography standard (Bio-Rad Laboratories, Hercules, CA, USA) was used routinely to validate the obtained chromatograms. The data was analyzed using Agilent OpenLAB Data Analysis Software 2.1.

IV.4.7 Protein-protein interaction analysis by dynamic light scattering

A DynaPro Plate Reader II (Wyatt Technology, Santa Barbara, CA, USA) was used to determine the interaction parameter k_D. Samples were filtered, 25 µl were transferred into a 384 microwell plate (Corning Inc., Kennebunk, USA), sealed with silicone oil to avoid evaporation, and measured as triplicates with 20 acquisitions for 5 s at 25 °C. The mutual diffusion coefficient was calculated by Dynamics software version 8.8 (Wyatt Technology, Santa Barbara, CA, USA) for 10 different protein concentrations between 0.1- 1 mg/ml. k_D was then determined from the concentration-dependent slope of the mutual diffusion coefficient and transferred into the estimated osmotic second viral coefficient A_2^* according to Menzen et al.[23]

IV.5 Results and Discussion

IV.5.1 Residual Moisture (RM), T_g and XRPD analysis of the lyophilizates

The RM values were below 0.8% for all formulations. Overall, all samples formed elegant cakes. Due to the low solid content, the 25:1 samples showed cake shrinkage (Figure IV.1). T_g values could not be evaluated due to the low excipient content, a challenge encountered in similar studies involving protein-rich glasses.[24] Duddu et al. observed that reducing the sugar-to-protein ratio increases the T_g of the lyophilizate.[25] Simperler et al. measured a T_g of approx. 60 °C for sucrose, while Pikal et al. extrapolated the glass transition for “pure protein” to theoretical values exceeding 100 °C.[24,26] Consequently, it is expected that the formulations studied will have a Tg above 60 °C, which is markedly higher than the storage temperatures of 25 °C and 40 °C.

Correspondingly, no cake change or even collapse was observed over 3 months at 40 °C. XRPD showed a fully amorphous cake structure for all samples at T_{lyo} and after storage.

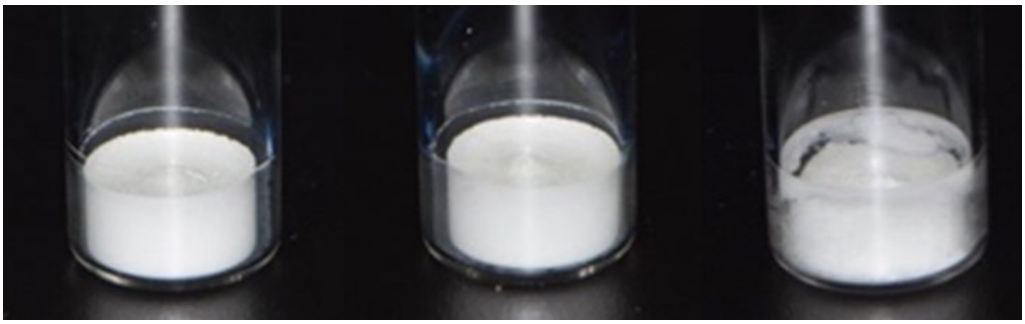

Figure IV.1: Macroscopic image of samples containing a 25:1 ratio of sucrose, mannitol, or arginine (left to right).

IV.5.2 Protein stability

IV.5.2.1 The influence of sugar to mAb ratio on stability

We varied the molar ratio of sucrose to mAb and the initial monomer content was >99.4% before lyophilization (T_{lyo}) in all formulations (Figure IV.2). After lyophilization, all formulations showed good monomer retention exceeding 99%, except for the sugar-free lyophilizate with only 97%. After storage at 25 °C for 1 month, a decrease in monomer content was observed across all formulations. After 3 months, the monomer content had further decreased and ranged between >99% (360:1) and 95% (25:1) for the sucrose containing formulations. Samples stored at 40 °C experienced a more rapid decline in monomer content; After 1 month, the high sugar to protein molar ratio of 360:1 resulted in a preservation of 99%, while at 25:1 the value dropped to 90%, and the formulation without sucrose had the lowest monomer content of 88.4%. The decrease in monomer content continued over 3 months, making the differences between the formulations more pronounced. The 360:1 ratio sample maintained a monomer content of 98.4%, the 25:1 ratio sample dropped to 85.4%, and the sucrose-free formulation to 82%. The results demonstrate a clear relationship between the molar ratio of sucrose to mAb and protein aggregation. The 360:1 ratio provides very good stabilization, but even the low 25:1 ratio shows good and improved mAb stability when compared to the sucrose-free formulation.

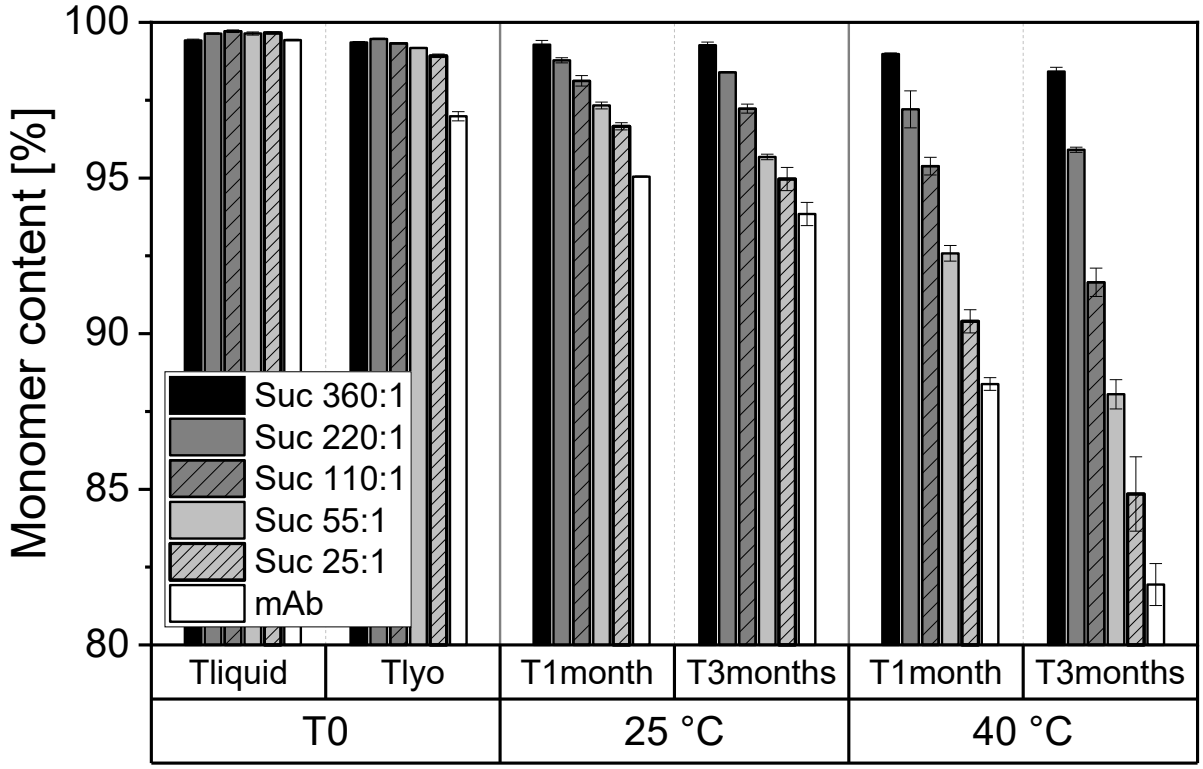

Figure IV.2: Monomer content in SEC at different sucrose to mAb ratios before and after storage at 25 °C and 40 °C for 1 and 3 months.

Detailed analysis of the aggregate formation demonstrates a linear decay on a semi-logarithmic scale ($R^2_{25°C/1mo}$= 0.9530; $R^2_{25°C/3mo}$= 0.9956; $R^2_{40°C/1mo}$= 0.9924; $R^2_{40°C/3mo}$= 0.9997) at both temperatures and at both sample time points of the monomer content as a function of the sucrose to protein molar ratio (Figure IV.3). This illustrates the absence of a threshold for the stabilizing effect provided by the sugar molecules. While protein stabilization improves exponentially with higher sucrose to protein molar ratio, even the low molar ratio 25:1 demonstrates enhanced protein stability compared to the sucrose-free formulation. Thus, the "the more the better" approach is justified. However, adjusting a minimum amount of sucrose can significantly expand the formulation space.

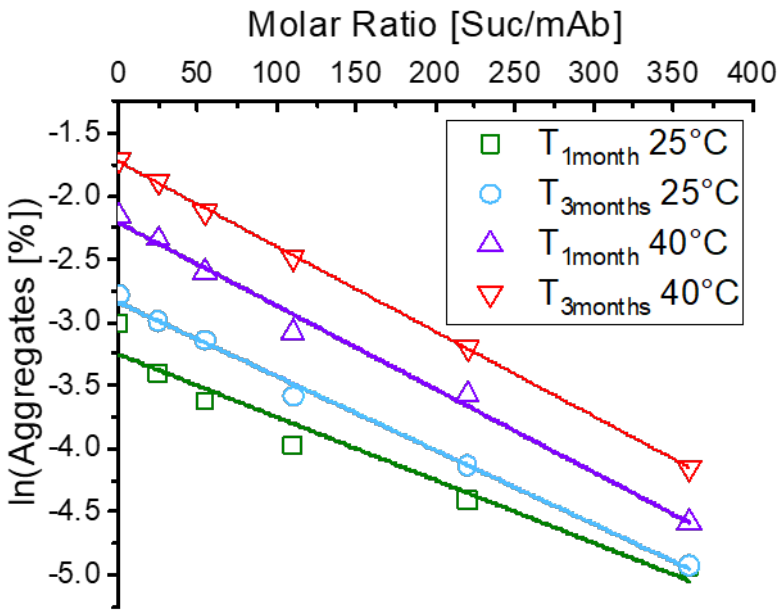

Figure IV.3: Mab aggregation vs sucrose to protein molar ratio.

For further investigations, additional temperature conditions and time points could be used for an Arrhenius plot-like kinetic model. The correlation between protein stability and molar ratio enables the interpolation and extrapolation of protein stability to molar ratios beyond 360:1, unexplored temperatures, and time points. Determining the minimum molar ratio needed to ensure effective protein stabilization can guide the decision of including additional excipients like mannitol as a crystalline bulking agent and at which concentration. The crystalline mannitol scaffold provides mechanically robust, pharmaceutically elegant cakes and can enable faster primary drying at higher product temperatures.[18] Anko et al. demonstrated that higher mannitol to sucrose ratio in a lyophilized mAb formulation significantly enhanced the mannitol crystallization tendency.[27] Cao et al. suggested that a higher sucrose content results in slower reconstitution of highly concentrated protein formulations with mannitol.[28] Kulkarni et al. found that faster reconstitution was closely linked to both crystallinity and protein concentration.[29] It should be noted that more comprehensive investigations, including various formulations, proteins, and excipients, are necessary before establishing a general guideline.

The exponential correlation triggers the question concerning the stabilization mechanism of sugars. According to the water-replacement theory, low molar ratios can result in unoccupied hydrogen bonds, potentially favoring partial unfolding of the protein. It was shown that exceeding molar ratios of 360:1 leads to very low changes in aggregation rates and that the occupation of hydrogen bonds improves the preservation of the protein's native

structure.[14,15] Moreover, if the sucrose content is too low, the spacing between protein molecules decreases. In addition, the increased number of unoccupied hydrogen bonds enhances protein mobility, which can lead to unfolding and relaxation within the energy landscape.[30,31] Terahertz time-domain spectroscopy can provide more detail into the changes in protein mobility and "free volume" within the sucrose matrix by adding information on the impact of remaining water molecules.[32,33] Reconstitution of the relaxed proteins could trigger protein aggregation, which may be reduced by higher sucrose concentrations which increase the inter-molecular distances. Techniques such as solid-state hydrogen-deuterium exchange (ssHDX) and liquid-observed vapor exchange nuclear magnetic resonance (LOVE NMR) analyze native structure preservation, the accessibility to H_2O, and water replacement.[34,35] In ssHDX, the extent of deuterium incorporation in the solid state showed a linear correlation with the aggregation propensity during storage, particularly with higher deuterium incorporation in formulations containing lower concentrations of sucrose.[36] Brom et al showed in LOVE NMR measurements that the protection of protein by sugars correlates with the number of intramolecular hydrogen bonds, polar solvent-accessible surface area, and hydrogen bond-competent side chains which is in line with the water replacement theory.[37] Based on molar sucrose-to-protein ratios from 1000:1 to 10,000:1 and electron paramagnetic resonance spectroscopy, it was proposed that sucrose's ability to form hydrogen bonds is the key characteristic for achieving protein structure preservation and establishing long-range homogeneous connectivity within the matrix.[38,39]

IV.5.2.2 The impact of excipient type and stabilization mechanism

Mannitol is commonly used as a crystalline bulking agent for better cake appearance and faster reconstitution. At low fraction of the total solids, mannitol remains amorphous.[27] In this study, mannitol was chosen for its role as a smaller, non-reducing, amorphous matrix forming excipient, rather than as a crystalline bulking agent. Its smaller size may allow for improved water replacement and better stabilization than sucrose.[40,41] At the 1.4 g/l in our lyophilizates, mannitol stayed amorphous, as confirmed via XRD analysis, and could act as a cryo- and lyoprotectant rather than a bulking agent.[18] Despite its T_g of around 10 °C, the low molar ratio and the high T_g of the pure mAb rendered the formulation suitable for our storage conditions.

Arginine is rarely used in commercial formulations and, in our study, functions similarly to mannitol as a smaller alternative to sucrose. Its ability to enhance the vitrification of an

amorphous matrix is compared to the stabilization seen in sucrose-containing formulations.[42] Arginine HCl is a suitable alternative to sucrose in protein lyophilization due to various factors, including a higher T_g and ruling out glycation and formulations containing 4% (w/w) arginine HCl and 50 g/l of mAb, corresponding to a molar ratio of approximately 570:1, demonstrated similar protein stability to sucrose.[43] No cake collapse was observed in all formulations (Figure IV.1). The influence of excipient type was compared at a molar ratio of 25:1 (Figure IV.4).

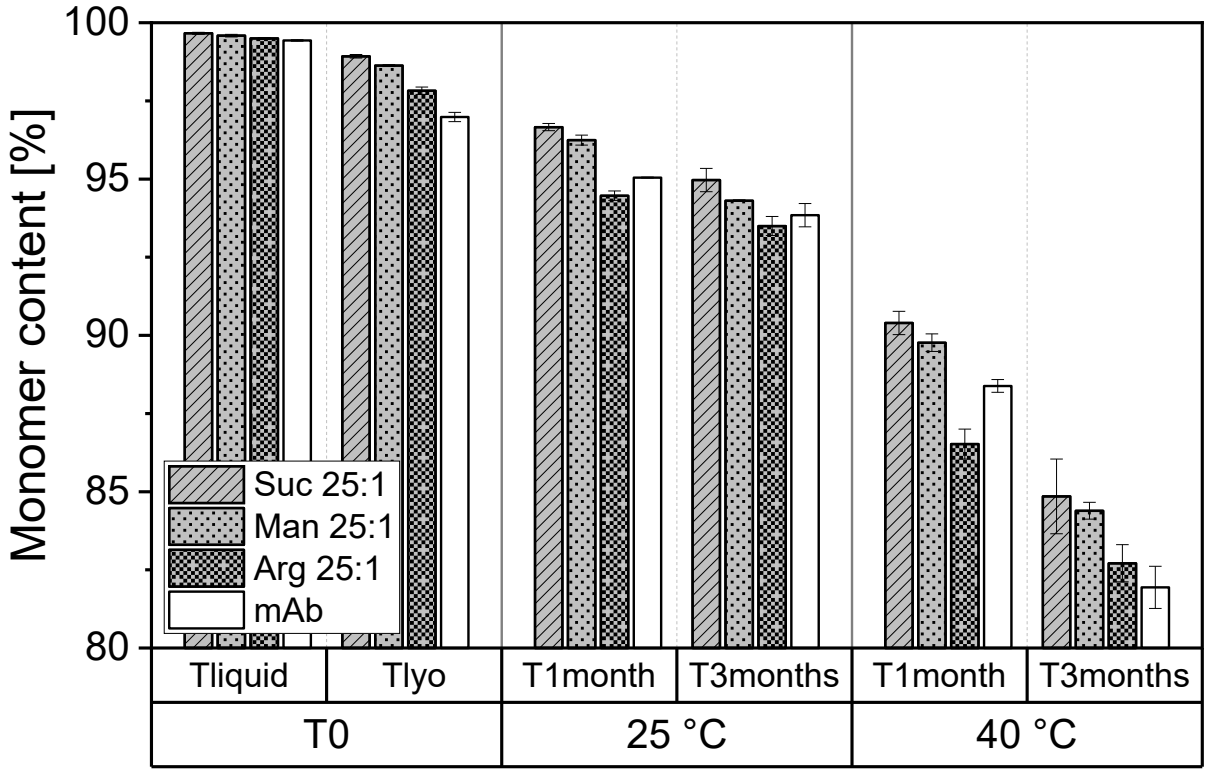

Figure IV.4: Monomer content in SEC of mAb formulated with sucrose, mannitol, and arginine HCl at ratios of 25:1 before and after storage at 25 °C and 40 °C for 1 and 3 months.

The stabilizing effect of sucrose, mannitol, and arginine HCl was compared at a molar ratio to protein of 25:1. Due to lower molecular weight, the lyophilizates with mannitol and arginine HCl contain only approx. 1.4 g/l excipient compared to 2.6 g/l for sucrose (Table 2). All formulations show similar stability. Mannitol samples stored for three months at 40 °C show a monomer content of approx. 84% and therefore an improvement over the excipient-free mAb formulation (82%). Like sucrose, its hydroxyl groups can stabilize the protein through hydrogen bonding. Furthermore, because of its smaller size, mannitol reduces the spacing between proteins and decreases hydrogen bonding, consequently restricting the protein relaxation as demonstrated with glycerol.[44,45] Arginine HCl shows slightly less stabilizing capacity (approx. 83%). Thus, arginine's ability to enhance the vitrification of the amorphous matrix may be less efficient for protein stabilization at low concentrations compared to the hydrogen bonding interactions provided by sucrose and mannitol.[42]

IV.5.2.3 The influence of the buffer strength on protein stability

In addition, we studied the impact of buffer concentration on protein stability at low stabilizer to protein ratio to provoke effects. (Figure IV.5). Consistent with previous findings, formulations with 5 mM histidine exhibiting higher ionic strength showed overall superior protein stability as compared to 0.1 mM histidine.[46,47] 10 mM to 20 mM histidine are typically utilized in commercial drug products. We selected lower buffer concentrations to avoid pH shifts and to highlight the influence of the charge shielding effect, which arises from higher ion concentration, on protein stability more clearly. Net repulsive protein interactions in solution are represented by a positive osmotic second virial coefficient A_2^*, whereas attractive protein interactions are reflected by a negative A_2^* value.[23] All formulations showed positive A_2^* values indicating repulsive protein interaction. At 0.1 mM histidine, the repulsive interactions are markedly stronger, with A_2^* values of 1.3E-02 and 2.4E-02 for sucrose and mannitol at molar ratios of 25:1. The pure protein solutions with minimal histidine exhibit the highest level of repulsion, with A_2^* =4.3E-02. In contrast, the A_2^* values in 5 mM histidine solution are lower with 5.3E-04 for sucrose and 5.1E-03 for mannitol. This is in accordance with the results of Bluemel et al..[48] Thus, the stability difference cannot be explained by the mAb self-interaction but potentially by a cryoprotective effect of histidine.[47] The concentration of histidine during the freezing phase could level out differences in mAb self-interaction observed in the starting liquid.

Even at low histidine concentrations, the sucrose-to-protein molar ratio impacts protein stability. No threshold molar ratio was identified, indicating that already with small amounts of sugar a stabilization effect sets in which may be sufficient depending on protein sensitivity, storage conditions, and protein concentration.

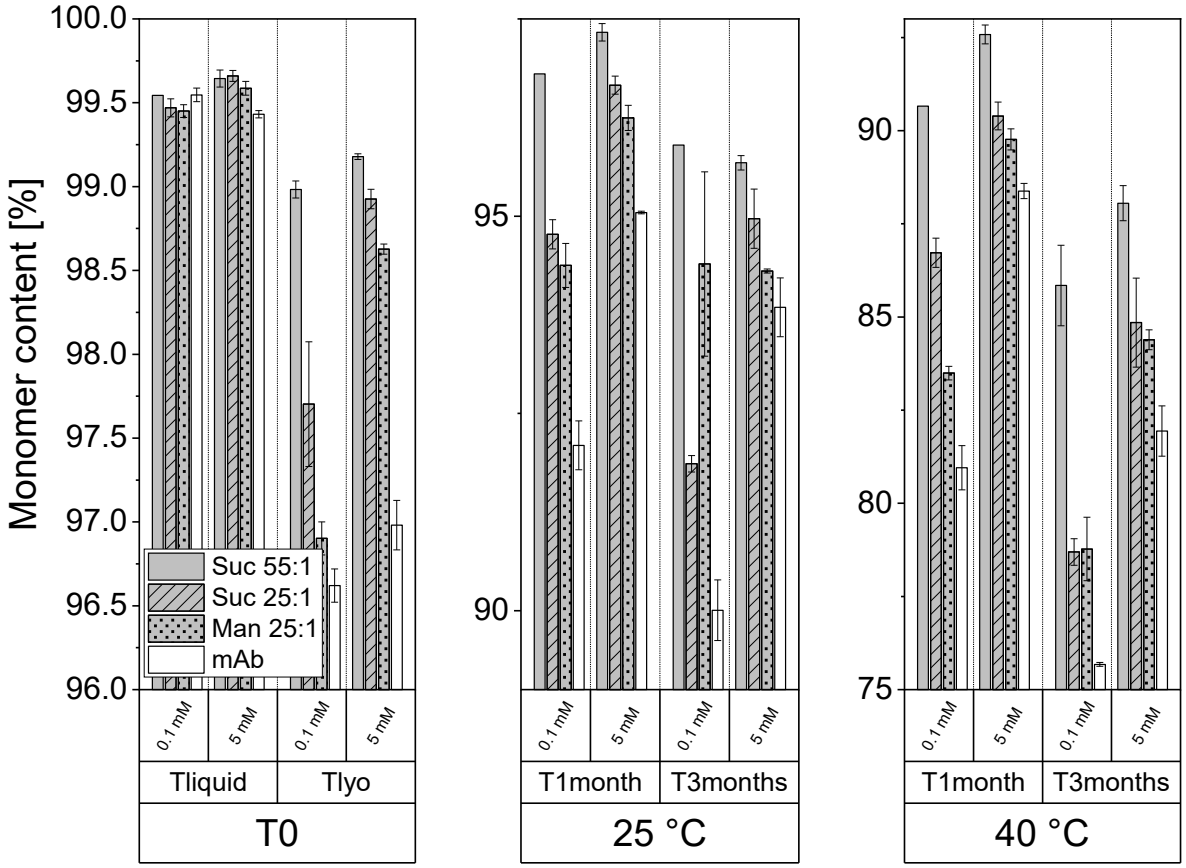

Figure IV.5: Monomer content of mAb formulated in 0.1 mM or 5 mM histidine buffer pH 6.5 with 55:1 sucrose, 25:1 sucrose, 25:1 mannitol, and pure mAb before and after storage at 25 °C and 40 °C for 1 and 3 months.

IV.5.2.4 The influence of the presence of surfactant on protein stability

Sucrose stabilizes proteins during lyophilization as a cryo- and lyoprotectant based on vitrification and water replacement. But what is the impact of sugar on the destabilization of the protein molecules at the formed liquid-ice and dry matrix-air interface? To this end, we examined the impact of polysorbate 20 at sucrose to mAb molar ratios of 55:1 and 25:1 (Figure IV.6).

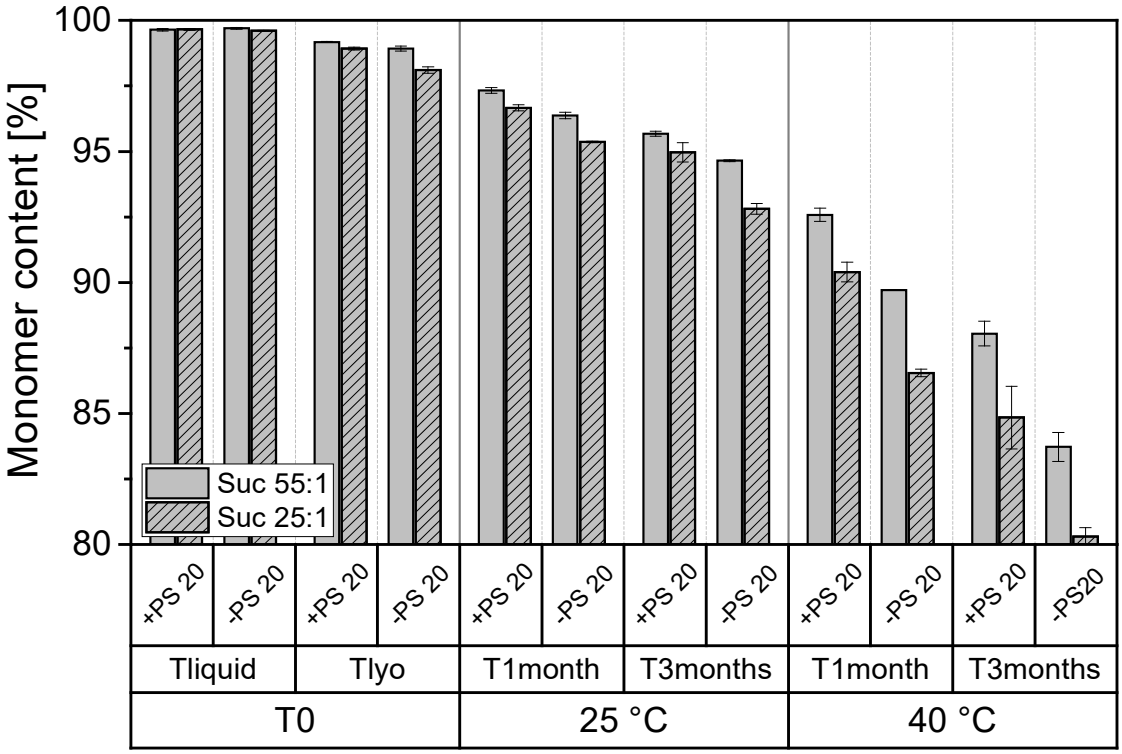

Figure IV.6: Monomer content of mAb formulated without and with 0.02% PS 20 with 55:1 sucrose and 25:1 sucrose before and after storage at 25 °C and 40 °C for 1 and 3 months.

Formulations without polysorbate 20 showed slightly lower protein stability. The most pronounced difference was observed after 3 months at 40 °C with a reduction from 88.1% to 83.7% at a molar ratio of 55:1 and from 84.9% to 80.3% at a molar ratio of 25:1. The absence of polysorbate 20 had a greater impact on protein stability at a molar ratio of 25:1 compared to 55:1. Polysorbate 20 enhances stability through interfacial protection of the mAb in addition to the hydrogen bonding effect of sucrose. In the presence of polysorbate 20, the mAb stability still depends on the molar ratio of sucrose to protein.

IV.6 Conclusion and Outlook

This study aimed to examine the impact of low molar ratios of sucrose to protein on mAb aggregation in lyophilizates, focusing on ratios ranging from 25:1 to 360:1. While previous studies have investigated excipient use at higher molar ratios, our study aimed to explore the lower end of the excipient-to-protein ratio spectrum. We found that sucrose to protein molar ratios of 360:1 already provide very good overall protein stabilization. Low ratios still render a stabilizing effect compared to the excipient-free mAb formulation. The chosen model protein exhibits overall good stability. Studying a diverse range of mAbs with varying stability profiles could offer a further understanding of excipient efficacy and concentration optima. Our results reveal the existence of an exponential relationship between protein aggregation in SEC and the sucrose to protein molar ratio. This correlation suggests the absence of a critical minimal molar ratio threshold to achieve a beneficial effect. This may allow cautious extrapolating to not-tested ratios e.g. in case of interest in a very low sucrose concentration accelerate reconstitution time of highly concentrated protein formulations. Nevertheless, further investigations are needed to establish a generalized predictive model. The improvement in stability with higher sucrose concentrations supports the “the more, the better” approach and the water replacement theory. At low molar ratios, mannitol, despite its smaller size, demonstrates a mAb stabilization comparable to sucrose. In contrast, arginine, despite its good glass formation, provides less protein stability, which points towards the importance of the hydrogen bond-based positive impact of sucrose. The protein stability varies with buffer concentrations, but the sucrose-to-protein molar ratio is always a significant factor. Surfactant contributes an interfacial stabilization effect beyond hydrogen bonding. Our findings suggest that even low excipient concentrations substantially improve protein stability. Reducing the amount of lyoprotective excipients could open the formulation space to include additional excipients by increasing the delta to the isotonicity level. These additional excipients may be highly valuable to control protein self-interaction to improve stability or reduce viscosity, e.g. with salts or more buffer, or to achieve faster drying, better cake appearance, or faster reconstitution e.g. with mannitol.

IV.7 References

[1] T.K. Das, A. Sreedhara, J.D. Colandene, D.K. Chou, V. Filipe, C. Grapentin, J. Searles, T.R. Christian, L.O. Narhi, W. Jiskoot, Stress Factors in Protein Drug Product Manufacturing and Their Impact on Product Quality, Journal of Pharmaceutical Sciences 111 (2022) 868–886.

[2] S. Gupta, W. Jiskoot, C. Schöneich, A.S. Rathore, Oxidation and Deamidation of Monoclonal Antibody Products: Potential Impact on Stability, Biological Activity, and Efficacy, Journal of Pharmaceutical Sciences 111 (2022) 903–918.

[3] K.B. Preston, T.W. Randolph, Stability of lyophilized and spray dried vaccine formulations, Advanced drug delivery reviews 171 (2021) 50–61.

[4] A.M. Abdul-Fattah, D. Lechuga-Ballesteros, D.S. Kalonia, M.J. Pikal, The impact of drying method and formulation on the physical properties and stability of methionyl human growth hormone in the amorphous solid state, Journal of Pharmaceutical Sciences 97 (2008) 163–184.

[5] J. Li, H. Wang, L. Wang, D. Yu, X. Zhang, Stabilization Effects of Saccharides in Protein Formulations: a Review of Sucrose, Trehalose, Cyclodextrins and Dextrans, European journal of pharmaceutical sciences 192 (2023) 106625.

[6] J.D. Meyer, R. Nayar, M.C. Manning, Impact of bulking agents on the stability of a lyophilized monoclonal antibody, European journal of pharmaceutical sciences 38 (2009) 29–38.

[7] F. Jameel (Ed.), Principles and Practices of Lyophilization in Product Development and Manufacturing, 1st ed. 2023 ed., Springer International Publishing; Imprint Springer, Cham, 2023.

[8] S. Groël, T. Menzen, G. Winter, Prediction of Unwanted Crystallization of Freeze-Dried Protein Formulations Using α-Relaxation Measurements, Pharmaceutics 15 (2023) 1–19.

[9] C. Haeuser, P. Goldbach, J. Huwyler, W. Friess, A. Allmendinger, Impact of dextran on thermal properties, product quality attributes, and monoclonal antibody stability in freeze-dried formulations, European Journal of Pharmaceutics and Biopharmaceutics 147 (2020) 45–56.

[10] B.S. Larsen, J. Skytte, A.J. Svagan, H. Meng-Lund, H. Grohganz, K. Löbmann, Using dextran of different molecular weights to achieve faster freeze-drying and improved storage stability of lactate dehydrogenase, Pharmaceutical Development and Technology 24 (2019) 323–328.

[11] B. Wang, S. Tchessalov, M.T. Cicerone, N.W. Warne, M.J. Pikal, Impact of sucrose level on storage stability of proteins in freeze-dried solids: II. Correlation of aggregation rate with protein structure and molecular mobility, Journal of Pharmaceutical Sciences 98 (2009) 3145–3166.

[12] K.M. Ziegler, Untersuchungen zur Stabilisierung und Interaktion von Cetuximab mit nicht-ionischen Tensiden, Munich, 2013.

[13] L.L. Chang, D. Shepherd, J. Sun, D. Ouellette, K.L. Grant, X.C. Tang, M.J. Pikal, Mechanism of protein stabilization by sugars during freeze-drying and storage: native structure preservation, specific interaction, and/or immobilization in a glassy matrix?, Journal of Pharmaceutical Sciences 94 (2005) 1427–1444.

[14] J.L. Cleland, X. Lam, B. Kendrick, J. Yang, T.-H. Yang, D. Overcashier, D. Brooks, C. Hsu, J.F. Carpenter, A specific molar ratio of stabilizer to protein is required for storage stability of a lyophilized monoclonal antibody, Journal of Pharmaceutical Sciences 90 (2001) 310–321.

[15] Andya JD, Hsu CC, Shire SJ, Mechanisms of Aggregate Formation and Carbohydrate Excipient Stabilization of Lyophilized Humanized Monoclonal Antibody Formulations, AAPS PharmSci 5 (2003) 1–11.

[16] W.H. Reinhart, N.Z. Piety, J.S. Goede, S.S. Shevkoplyas, Effect of osmolality on erythrocyte rheology and perfusion of an artificial microvascular network, Microvascular research 98 (2015) 102–107.

[17] W. Wang, Tolerability of hypertonic injectables, International Journal of Pharmaceutics 490 (2015) 308–315.

[18] S. Thakral, J. Sonje, B. Munjal, B. Bhatnagar, R. Suryanarayanan, Mannitol as an Excipient for Lyophilized Injectable Formulations, Journal of Pharmaceutical Sciences 112 (2023) 19–35.

[19] M.H.H. AbouGhaly, J. Du, S.M. Patel, E.M. Topp, Effects of ionic interactions on protein stability prediction using solid-state hydrogen deuterium exchange with mass spectrometry (ssHDX-MS), International Journal of Pharmaceutics 568 (2019) 118512.

[20] A. Hawe, W. Friess, Impact of freezing procedure and annealing on the physico-chemical properties and the formation of mannitol hydrate in mannitol-sucrose-NaCl formulations, European Journal of Pharmaceutics and Biopharmaceutics 64 (2006) 316–325.

[21] A. Al-Hussein, H. Gieseler, Investigation of histidine stabilizing effects on LDH during freeze-drying, Journal of Pharmaceutical Sciences 102 (2013) 813–826.

[22] D. Awotwe-Otoo, C. Agarabi, G.K. Wu, E. Casey, E. Read, S. Lute, K.A. Brorson, M.A. Khan, R.B. Shah, Quality by design: impact of formulation variables and their interactions on quality attributes of a lyophilized monoclonal antibody, International Journal of Pharmaceutics 438 (2012) 167–175.

[23] T. Menzen, W. Friess, Temperature-ramped studies on the aggregation, unfolding, and interaction of a therapeutic monoclonal antibody, Journal of Pharmaceutical Sciences 103 (2014) 445–455.

[24] M.J. Pikal, D.R. Rigsbee, M.L. Roy, Solid state chemistry of proteins: I. glass transition behavior in freeze dried disaccharide formulations of human growth hormone (hGH), Journal of Pharmaceutical Sciences 96 (2007) 2765–2776.

[25] S.P. Duddu, P.R. Dal Monte, Effect of Glass Transition Temperature on the Stability of Lyophilized Formulations Containing a Chimeric Therapeutic Monoclonal Antibody, Pharmaceutical Research 14 (1997) 591–595.

[26] A. Simperler, A. Kornherr, R. Chopra, P.A. Bonnet, W. Jones, W.D.S. Motherwell, G. Zifferer, Glass transition temperature of glucose, sucrose, and trehalose: an experimental and in silico study, The Journal of Physical Chemistry B 110 (2006) 19678–19684.

[27] M. Anko, M. Bjelošević, O. Planinšek, U. Trstenjak, M. Logar, P. Ahlin Grabnar, B. Brus, The formation and effect of mannitol hemihydrate on the stability of monoclonal antibody in the lyophilized state, International Journal of Pharmaceutics 564 (2019) 106–116.

[28] W. Cao, S. Krishnan, M.S. Ricci, L.-Y. Shih, D. Liu, J.H. Gu, F. Jameel, Rational design of lyophilized high concentration protein formulations-mitigating the challenge of slow reconstitution with multidisciplinary strategies, European journal of pharmaceutics and biopharmaceutics official journal of Arbeitsgemeinschaft fur Pharmazeutische Verfahrenstechnik e.V 85 (2013) 287–293.

[29] S.S. Kulkarni, R. Suryanarayanan, J.V. Rinella, R.H. Bogner, Mechanisms by which crystalline mannitol improves the reconstitution time of high concentration lyophilized protein formulations, European journal of pharmaceutics and biopharmaceutics official journal of Arbeitsgemeinschaft fur Pharmazeutische Verfahrenstechnik e.V 131 (2018) 70–81.

[30] N. Chieng, M.T. Cicerone, Q. Zhong, M. Liu, M.J. Pikal, Characterization of dynamics in complex lyophilized formulations: II. Analysis of density variations in terms of glass dynamics and comparisons with global mobility, fast dynamics, and Positron Annihilation Lifetime Spectroscopy (PALS), European Journal of Pharmaceutics and Biopharmaceutics 85 (2013) 197–206.

[31] V. Kocherbitov, T. Arnebrant, Hydration of lysozyme: the protein-protein interface and the enthalpy-entropy compensation, Langmuir the ACS journal of surfaces and colloids 26 (2010) 3918–3922.

[32] J. Kölbel, M.L. Anuschek, I. Stelzl, S. Santitewagun, W. Friess, J.A. Zeitler, Dynamical Transition in Dehydrated Proteins, The journal of physical chemistry letters 15 (2024) 3581–3590.

[33] T.A. Shmool, P.J. Woodhams, M. Leutzsch, A.D. Stephens, M.U. Gaimann, M.D. Mantle, G.S. Kaminski Schierle, C.F. van der Walle, J.A. Zeitler, Observation of high-temperature macromolecular confinement in lyophilised protein formulations using terahertz spectroscopy, International journal of pharmaceutics: X 1 (2019) 100022.

[34] N.E. Wilson, T.T. Mutukuri, D.Y. Zemlyanov, L.S. Taylor, E.M. Topp, Q.T. Zhou, Surface Composition and Formulation Heterogeneity of Protein Solids Produced by Spray Drying, Pharmaceutical Research 37 (2019) 14.

[35] C.J. Crilly, J.E. Eicher, O. Warmuth, J.M. Atkin, G.J. Pielak, Water's Variable Role in Protein Stability Uncovered by Liquid-Observed Vapor Exchange NMR, Biochemistry 60 (2021) 3041–3045.

[36] B.S. Moorthy, I.E. Zarraga, L. Kumar, B.T. Walters, P. Goldbach, E.M. Topp, A. Allmendinger, Solid-State Hydrogen-Deuterium Exchange Mass Spectrometry: Correlation of Deuterium Uptake and Long-Term Stability of Lyophilized Monoclonal Antibody Formulations, Molecular Pharmaceutics 15 (2018) 1–11.

[37] J.A. Brom, R.G. Petrikis, G.J. Pielak, How Sugars Protect Dry Protein Structure, Biochemistry 62 (2023) 1044–1052.

[38] M. Malferrari, A. Nalepa, G. Venturoli, F. Francia, W. Lubitz, K. Möbius, A. Savitsky, Structural and dynamical characteristics of trehalose and sucrose matrices at different hydration levels as probed by FTIR and high-field EPR, Physical chemistry chemical physics PCCP 16 (2014) 9831–9848.

[39] M. Malferrari, A. Savitsky, W. Lubitz, K. Möbius, G. Venturoli, Protein Immobilization Capabilities of Sucrose and Trehalose Glasses: The Effect of Protein/Sugar Concentration Unraveled by High-Field EPR, The journal of physical chemistry letters 7 (2016) 4871–4877.

[40] M.T. Cicerone, J.F. Douglas, β-Relaxation governs protein stability in sugar-glass matrices, Soft Matter 8 (2012) 2983.

[41] W.F. Tonnis, M.A. Mensink, A. de Jager, K. van der Voort Maarschalk, H.W. Frijlink, W.L.J. Hinrichs, Size and molecular flexibility of sugars determine the storage stability of freeze-dried proteins, Molecular Pharmaceutics 12 (2015) 684–694.

[42] P. Stärtzel, Arginine as an Excipient for Protein Freeze-Drying: A Mini Review, Journal of Pharmaceutical Sciences 107 (2018) 960–967.

[43] I. Seifert, A. Bregolin, D. Fissore, W. Friess, The Influence of Arginine and Counter-Ions: Antibody Stability during Freeze-Drying, Journal of Pharmaceutical Sciences 110 (2021) 2017–2027.

[44] J. Horn, J. Schanda, W. Friess, Impact of fast and conservative freeze-drying on product quality of protein-mannitol-sucrose-glycerol lyophilizates, European Journal of Pharmaceutics and Biopharmaceutics 127 (2018) 342–354.

[45] D. Averett, M.T. Cicerone, J.F. Douglas, J.J. de Pablo, Fast relaxation and elasticity-related properties of trehalose-glycerol mixtures, Soft Matter 8 (2012) 4936.

[46] A. Al-Hussein, H. Gieseler, The effect of mannitol crystallization in mannitol-sucrose systems on LDH stability during freeze-drying, Journal of Pharmaceutical Sciences 101 (2012) 2534–2544.

[47] B. Chen, R. Bautista, K. Yu, G.A. Zapata, M.G. Mulkerrin, S.M. Chamow, Influence of Histidine on the Stability and Physical Properties of a Fully Human Antibody in Aqueous and Solid Forms, Pharmaceutical Research 20 (2003) 1952–1960.

[48] O. Bluemel, J.W. Buecheler, A. Hauptmann, G. Hoelzl, K. Bechtold-Peters, W. Friess, The effect of mAb and excipient cryoconcentration on long-term frozen storage stability - part 2: Aggregate formation and oxidation, International journal of pharmaceutics: X 4 (2022) 100109.

Chapter V "Bigger, the Better?" – The Influence of Sugar Size and Residual Moisture on Protein Stability and Accessibility in Lyophilizates

This chapter is published as: Lo Presti, K.; Frieß, W. "Bigger, the Better?" – The Influence of Sugar Size and Residual Moisture on Protein Stability and Accessibility in Lyophilizates. *Molecular Pharmaceutics 22 (2025) 5952–5958*

Note from the authors: To establish a coherent numbering and pagination within this document, the numbers of references, figures, and tables were adapted. Apart from minor changes, the version included in this thesis is identical to the submitted article.

The published article can be accessed online via:

https://doi.org/10.1021/acs.molpharmaceut.5c00596

V.1 Abstract

Lyophilization is a key technology to improve long term stability of protein drug products, traditionally using the disaccharides sucrose and trehalose for cryo- and lyoprotection. Monosaccharides are less favored due to low glass transition temperature and Maillard reaction potential. Additionally, trisaccharides and tetrasaccharides typically do not play significant roles as they are often not approved for parenteral use and have been associated with lower protein stabilization. Key stability parameters include preserved protein structure, solid-state accessibility, and monomer content. This study explores the long-term monomer retention of human serum albumin (HSA) in lyophilizates at 2-8 °C, 25 °C, and 40 °C by investigating the effect of a series of mono- to tetra saccharide based on glucose (glucose, maltose, maltotriose, and maltotetraose) as well as glucose maltose and glucose maltotriose mixtures. We varied the residual moisture (RM) content (1%, 1.5%, and 2%) post-lyophilization to understand the effects of water replacement, vitrification, and matrix mobility on protein stability. The molar ratios of maltose to HSA were set at 360:1 and 180:1 to investigate the impact of sugar concentration at overall low sugar ratios. Solid-state hydrogen-deuterium exchange mass spectrometry (ssHDX MS) was performed on a QDa benchtop mass spectrometer to evaluate protein accessibility and structural preservation, using RMs of 1% D2O, 2% D2O, and 1% D2O + 1% H2O. The larger the sugar, the lower its stabilizing potential and the higher the protein accessibility, indicating insufficient water replacement. Increasing the RM from 1% to 1.5% and 2% enhanced stability, highlighting the superiority of residual water molecules which was especially the case for the tri and tetra saccharides. Mixtures of small and large sugars showed

stabilization benefits in maintaining monomer content and structural preservation, indicating a good balance of water replacement and vitrification. Overall, the ssHDX MS findings of samples with head-space spiked D2O did correspond with monomer retention, indicating that it could be a valuable tool for characterization and understanding the stabilizing capacity of lyophilized formulations. Our findings highlight the importance of RM control for optimal stability as well as the importance of the sugar size on lyoprotection based on water replacement, and the potential of sugar mixtures to optimize the stability of lyophilized proteins.

Keywords: ssHDX-MS, solid state, lyophilization, residual moisture, glucose, sugar, protein stability

V.2 Graphical Abstract

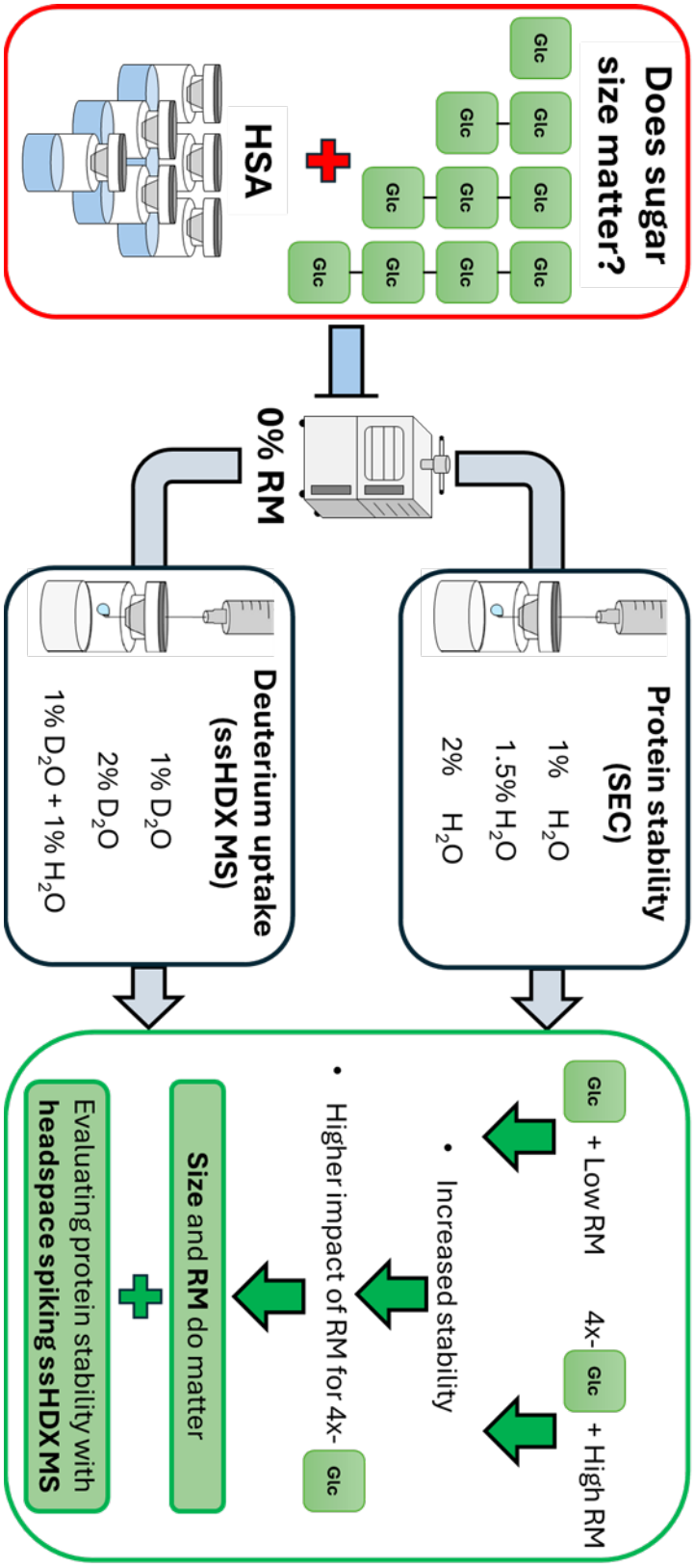

V.3 Introduction

Lyophilization is a key technology to achieve stable protein drug products.[1] Non-reducing disaccharides like sucrose and trehalose are typically used as lyo- and cryoprotectants as they form amorphous matrices with high glass transition temperatures (T_g) and water replacement potential. Both smaller and larger sugars or polyol-type excipients like glycerol, raffinose, lactosucrose or HPß-cyclodextrins have protein stabilization capacity.[2–4]

Two main hypotheses explain the lyoprotective effect of sugars. The water replacement theory suggests that sugar molecules preserve the native structure of proteins by compensating for the removal of water molecules via hydrogen bond formation.[5] According to the vitrification theory, the rigid amorphous matrix reduces protein mobility and unfolding.[6]

While glycerol presents challenges during lyophilization, such as increased mobility and subsequently lower T_g in the lyocake, HPß-CD exhibit surface-stabilizing effects in addition to their lyo and cryoprotective characteristics.[7–9] Reducing the size from oligosaccharides to disaccharides can potentially enhance water replacement and protein stabilization.[10,11] Additionally, smaller excipient sizes can reduce free volume and create a more compact matrix, which restricts protein relaxation and improves stability.[12,13]

In this work, we gained further insights into the impact of residual moisture (RM), overdrying, and hydrogen bonding on the protein stability when using different sugar sizes. To this end, we freeze dried human serum albumin (HSA) with various glucose oligosaccharides. Mixtures of glucose with maltose or maltotriose were used to investigate synergistic effects that balance water replacement and vitrification. Furthermore, an exponential relationship between the disaccharide to protein molar ratio and protein aggregation has been demonstrated, and different proteins are structurally better preserved at higher sucrose to protein ratios and show less aggregation in lyophilizates.[14–16] To address the impact of molar ratio, we investigated the maltose to HSA stability at molar ratios of sugar to protein of 360:1 and 180:1.

Furthermore, an optimal moisture of lyophilizates is important for protein stability. If the water content exceeds a monolayer around the protein, decomposition is accelerated due to higher protein flexibility and the mobilization of reactants by less tightly bound water.[17] Above certain water content thresholds, protein deamidation becomes substantially enhanced.[18] Additionally, an increased RM leads to a decrease in the glass transition temperature and therefore challenges in protein stability and cake integrity.[19] In contrast, overdrying can increase long term stability issues.[18,20,21] To investigate the influence of residual moisture

and excipients on protein stability, we adjusted moisture levels to 1%, 1.5%, and 2% post-lyophilization using a Hamilton syringe spiking approach.[22]

For further understanding, we investigated the protein accessibility in the solid state by solid state hydrogen deuterium exchange mass spectrometry (ssHDX MS) [23,24] We adapted and improved the common desiccator with a saturated humidity ssHDX MS approach by spiking D_2O post-lyophilization and using a simple benchtop mass spectrometer. Changes in global deuterium uptake across formulations and moisture levels were compared with the aggregation formation upon storage.

V.4 Material and Methods

V.4.1 Materials

Highly purified recombinant human serum albumin (198 g/L) (HSA) formulated in a 144 mM sodium phosphate buffer at pH 7 and 14 mg/L polysorbate 80 was provided by Albumedix (Nottingham, UK). For polysorbate removal, HSA was precipitated using a saturated ammonium sulfate solution (Bernd Kraft, Duisburg, Germany) and reconstituted in 1 mM sodium phosphate buffer at pH 6.5 (Merck KGaA, Darmstadt, Germany). Polysorbate removal was checked by measuring the surface tension of the reconstituted protein solution using a drop shape analyzer (DSA25e, Krüss GmbH, Nürnberg, Germany). Maltose, maltotriose and maltotetraose were purchased from Nagase (NAGASE & CO., LTD., Osaka, Japan), glucose was purchased from Sigma-Aldrich (St. Louis, MO, USA) and HPW was prepared using a UF system (Sartorius Arium Pro, Sartorius, Göttingen, Germany). D_2O, acetonitrile, and trifluoracetic acid (TFA) were purchased from Sigma-Aldrich (St. Louis, MO, USA), and formic acid (FA) was obtained from VWR Chemicals (Darmstadt, Germany).

V.4.2 Formulations

Six different formulations were prepared, each consisting of 30 g/L HSA in 1 mM sodium phosphate buffer pH 6.5 and different sugars composed of various glucose modules (Figure V.1, Table V.1). In a pretest, pure glucose did not result in appropriate lyophilizates due to its low T_g' and T_g.

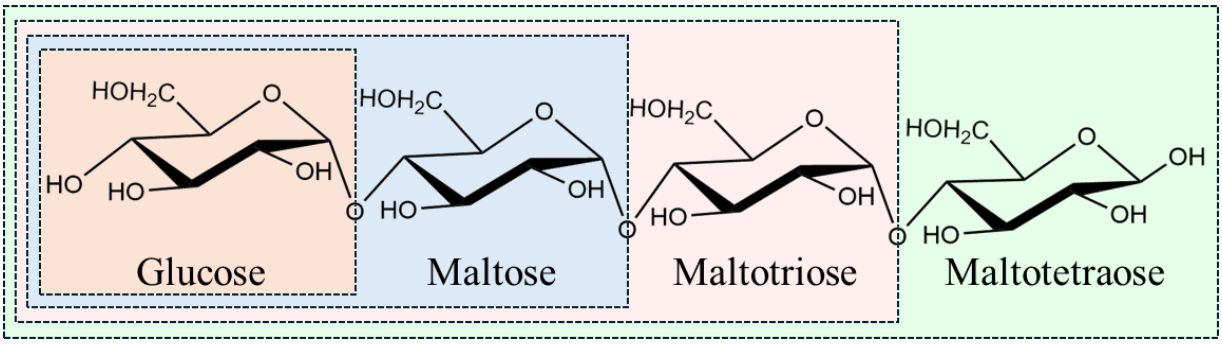

Figure V.1: Glucose "modules" of the used sugars (glucose (mono), maltose (di), maltotriose (tri), and maltotetraose (tetra)).

Table V.1: Formulations

Sample ID	Sugar	Molar ratio [excipient/protein]		Sugar [g/L]		Weight ratio [excipient/protein]		Glucose "modules"
Di	Maltose	360		55.6		1.85		720
Tri	Maltotriose	240		54.6		1.82		720
Tetra	Maltotetraose	180		54.1		1.80		720
Di_{low}	Maltose	180		27.8		0.93		360
Di+Mono	Maltose+Glucose	120	480	18.5	39	0.62	1.30	720
Tri+Mono	Maltotriose+Glucose	60	540	13.7	43.9	0.46	1.46	720

V.4.3 Lyophilization

500 µL formulation is lyophilized in 2R vials (Bünder Glas Bünde, Germany) using an Epsilon 2-6D LSCplus freeze dryer (Martin Christ Gefriertrocknungsanlagen, Osterode am Harz, Germany). The vials were semi-stoppered with single-vent lyophilization stoppers (13-mm Lyo Nova Pure RS 1356 4023/50 G West Pharmaceuticals, Eschweiler, Germany). Thermocouples were placed into the different formulations to monitor product temperature, and all samples were freeze dried in the same cycle. Samples were cooled to 5 °C for 60 min, then frozen to -55 °C within 3:40 h followed by a 4 h hold. Primary drying was conducted at 0.1 mbar and -25 °C shelf temperature, with a 5% difference in the comparative pressure measurement marking the end of primary drying. Secondary drying involved increasing the shelf temperature to 0 °C at 0.25 K/min, holding for 5 h, then ramping up to 25 °C at the same rate, and maintaining the vacuum at 0.05 mbar for an additional 6 h. Finally, the temperature was increased to 45 °C at 0.25 K/min and held for 24 h. Venting and vial closing were performed in a nitrogen environment at 800 mbar. Samples were crimp-sealed using “flip-off” caps (ChemoLine, Sankt Augustin, Germany), and stored at 4 °C until further use.

V.4.4 Analysis of residual moisture by Karl Fischer titration

A headspace Karl Fischer titration system (Aqua 40.00, Analytik Jena, Jena, Germany) was used to determine residual moisture content. Approx. 20 mg of freeze dried samples were transferred into 2R vials in a glovebox under nitrogen environment (r.h. ≤ 4%). Water extraction was performed at 100 °C, and an Aquastar water standard (Merck KGaA, Darmstadt, Germany) was analyzed as a control.

.

V.4.5 Residual moisture adjustment

Residual moisture was adjusted to 1%, 1.5%, and 2% post-lyophilization using a moisture spiking approach.[22] The required HPW amount was spiked into the vial headspace using zero dead volume syringes (Hamilton Bonaduz AG, Bonaduz, Switzerland) at 8 °C, considering the RM after lyophilization (< 0.5%). For ssHDX MS, samples were adjusted to 1% D_2O, 2% D_2O, and 1% D_2O + 1% H_2O via spiking followed by incorporation at 45 °C for 18 h. After incubation, samples were flash-frozen and stored at -70 °C until analysis.

V.4.6 Thermal analysis by differential scanning calorimetry

Thermal analysis of the lyophilizates was performed using a differential scanning calorimeter (DSC 821e from Mettler Toledo, Columbus, OH, USA). 10-15 mg were transferred into aluminum pans under nitrogen (r.h. ≤ 4%) and hermetically sealed. The samples were heated from -10 to 80 °C at 10 °C/min, cooled to -10 °C at 10 C/min, and reheated to 150 °C at 10 °C/min. The T_g was defined as the midpoint of the phase transition during the second.

V.4.7 Monomer content analysis by size exclusion chromatography

Samples spiked with H_2O were stored at 2-8 °C and 25 °C for 3 and 6 months, respectively, and at 40 °C for 1 and 3 months. Stored samples were reconstituted with 500 µl HPW and 10 µL sample analyzed by SEC with an Agilent 1200 HPLC system with a diode array detector (Agilent Technologies, Santa Clara, CA, USA) at 280 nm using a TSKgel G3000 SWxl column (Tosoh Bioscienc, Grießheim, Germany) and 150 mM potassium phosphate buffer at pH 6.45 with 0.4 mL/min as mobile phase.

V.4.8 Solid state hydrogen deuterium exchange mass spectrometry

The method development for the ssHDX MS approach utilized is explained in SI 1. Global deuterium uptake in D_2O-spiked samples was assessed by ssHDX MS on an Acquity UPLC I-Class system coupled with an Acquity Tunable UV detector, a benchtop Acquity QDa Detector, and an Acquity UPLC Protein BEH SEC column 200 Å (Waters Corporation, Milford, MA, USA) cooled to 5 °C using a Cera column cooler 250 (Tecan Trading AG, Männedorf, Swiss). The HSA eluted in approx. 18 min using a chilled mobile phase consisting of 80% water and 20% acetonitrile containing 0.1% FA and 0.05% TFA. Sample reconstitution was performed by adding 500 µL of ice-chilled quench buffer (0.1% FA in HPW) to the lyophilized sample. 1 µL of undiluted sample was injected into the system, and mass spectra were acquired over the range of *m/z* 900-1250. The resulting TICs were processed by subtracting, smoothing, and deconvoluting the mass envelopes using the MaxEnt1 software (Waters Corporation, Milford, MA, USA). Data evaluation was conducted by plotting the weighted arithmetic mean of all TICs that exceeded 90%, ensuring only high-quality data points contributed to the final analysis.

V.5 Results and Discussion

To gain insights into the impact of RM on the mobility of the amorphous matrix, to evaluate the risk of overdrying, and ultimately gain insights into the protein stability, HSA was freeze dried using different glucose-oligosaccharides combinations. Additionally, a novel headspace spiking ssHDX MS approach was developed to further investigate the protein stability depending on RM, sugar size, and sugar to protein ratio.

V.5.1 Physical properties of the lyophilizates

All samples formed elegant lyophilization cakes despite their varying, overall low solid content as well as showing RM levels below 0.5% (Figure V.2). Samples without glucose had T_g values above 100 °C, suitable for long term storage conditions. A clear T_g could not be detected, which is consistent with previous observations in protein-rich glasses where excipient content is low.[14,25] Nonetheless, according to Pikal et al., the T_g of nearly pure protein is expected to be above 100 °C.[25] In addition, no visible changes in cake appearance were observed across all reconstitution moisture levels and storage conditions, supporting the physical stability of the samples under the tested conditions. Additionally, Schugmann et al. showed T_g values of approx. 100 °C and higher for used oligosaccharides.[26] In contrast, mixed samples with glucose, Di+Mono and Tri+Mono, exhibited lower T_g values with 57.8 °C and 57 °C, respectively, due to glucose's low T_g.[27] These lyophilizates remained stable at 2-8 °C and 25 °C but showed shrinkage at 40 °C, which can be correlated to a potential decrease in T_g.[28] SsHDX samples showed no cake shrinkage or collapse after D_2O spiking and 18 h of storage at 45 °C.

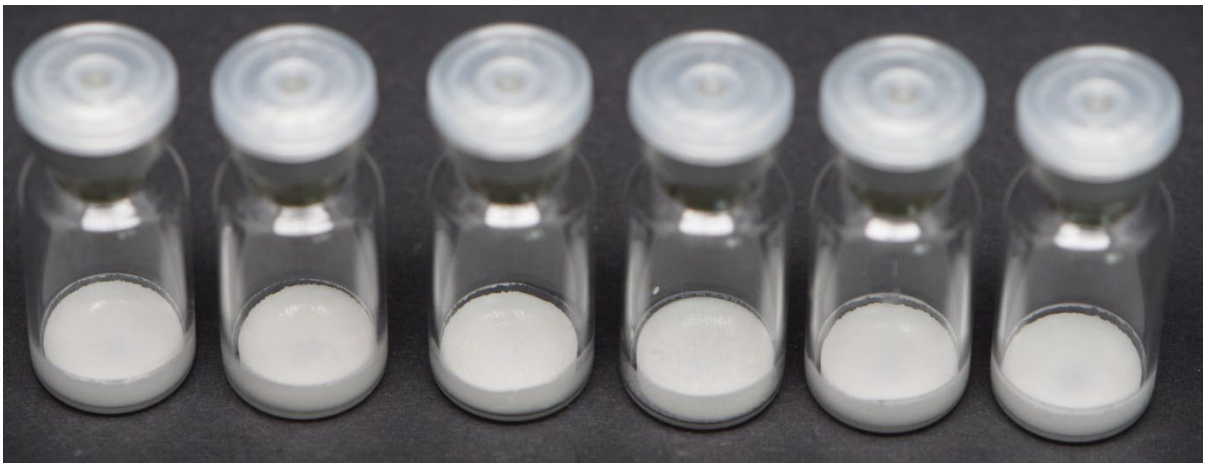

Figure V.2: Macroscopic image of lyophilizates from Di, Tri, Tetra, Di_{low}, Di+Mono, and Tri+Mono (left to right).

V.5.2 The influence of sugar size on monomer content

We varied the sizes of glucose oligosaccharides by adjusting the number of glucose "modules" and investigated mixtures of glucose with maltose and maltotriose for their protein stabilization potential. With this, we aimed to differentiate the effects of water replacement (potentially improved for small sugar molecules) and vitrification (with the superiority of larger sugar molecules).

All formulations showed a decrease in monomer content over time, more pronounced with longer storage periods. We did not observe low molecular weight (LMW) formation or fragmentation. Thus, changes in the monomer content are reflected in the formation of high molecular weight (HMW) species. The influence of sugar size on protein stability was most evident at 40 °C (Figure V.3). After one month, maltose formulations had a monomer content of 94.1% at 1% RM, compared to 92.3% for maltotetraose. After three months, the HSA monomer content decreased to 93.8%, and to 88.7% for maltose and maltotetraose lyophilizates, respectively. This general effect could be observed at 2-8 °C and 25 °C storage temperature as well (Figure V.4; Figure V.5). Formulations with smaller sugars showed better stability than those with larger sugars. Despite higher mobility in disaccharide matrices, water replacement leads to enhanced stabilization of the protein molecules.[10,13]

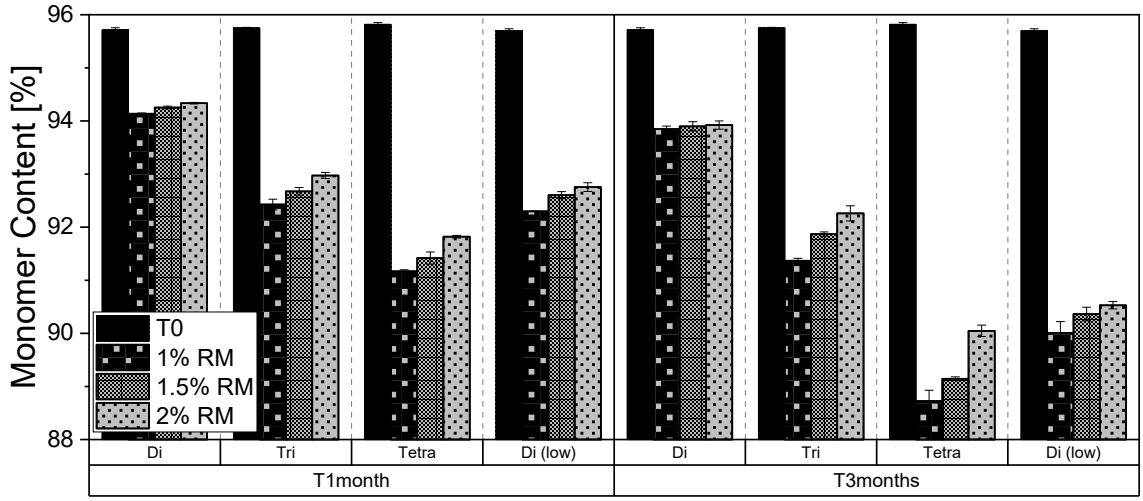

Figure V.3: Monomer content in SEC with different sugar sizes and molar sugar to HSA ratios before (T0) and after storage at 40 °C for 1 and 3 months.

At 2-8 °C, the glucose-containing formulations maintained the HSA monomer content after six months best, with approx. 94.7% (Figure V.5). This indicates a beneficial synergy between small hydrogen bond-forming sugars and larger vitrifying sugars, as previously reported by Hauser et al who studied different dextrans in combination with sucrose.[29] At 25 °C, the

stabilizing effect of mixed formulations became even more apparent (Figure V.4).). Due to its small size and high mobility, glucose can efficiently form hydrogen bonds and stabilize the protein structure by filling "voids" created by the removed water. The larger sugars form a stabilizing amorphous network, vitrifying the protein molecules with high T_g. After 6 months, the monomer content in the mixed systems was significantly decreased, representing the increased impact of residual moisture with higher temperatures on the monomer content (*see V.5.3*).[30,31]

.

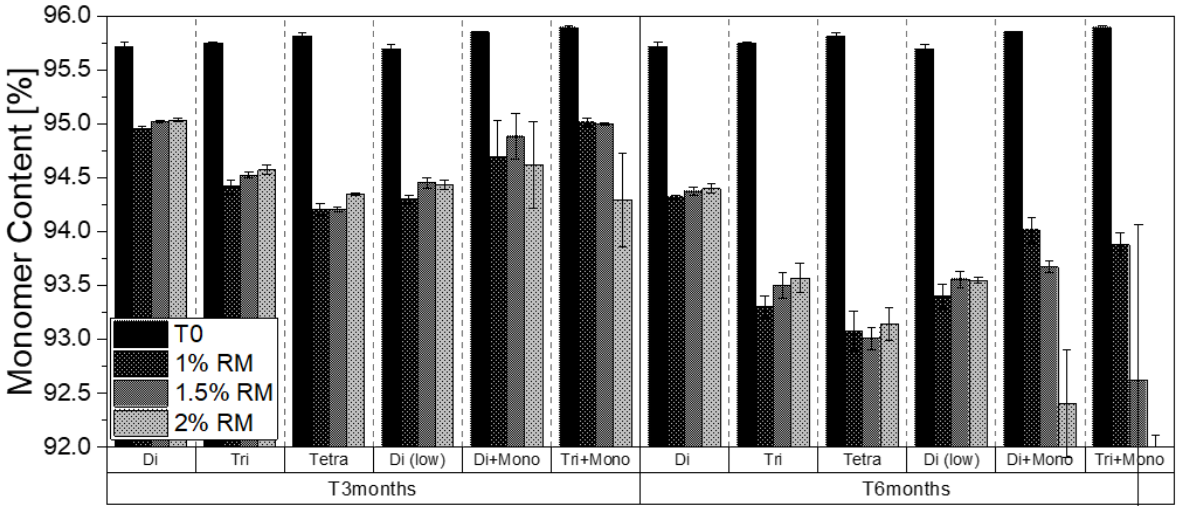

Figure V.4:Monomer content in SEC with different sugar sizes and molar sugar to HSA ratios before (T0) and after storage at 25 °C for 3 and 6 months.

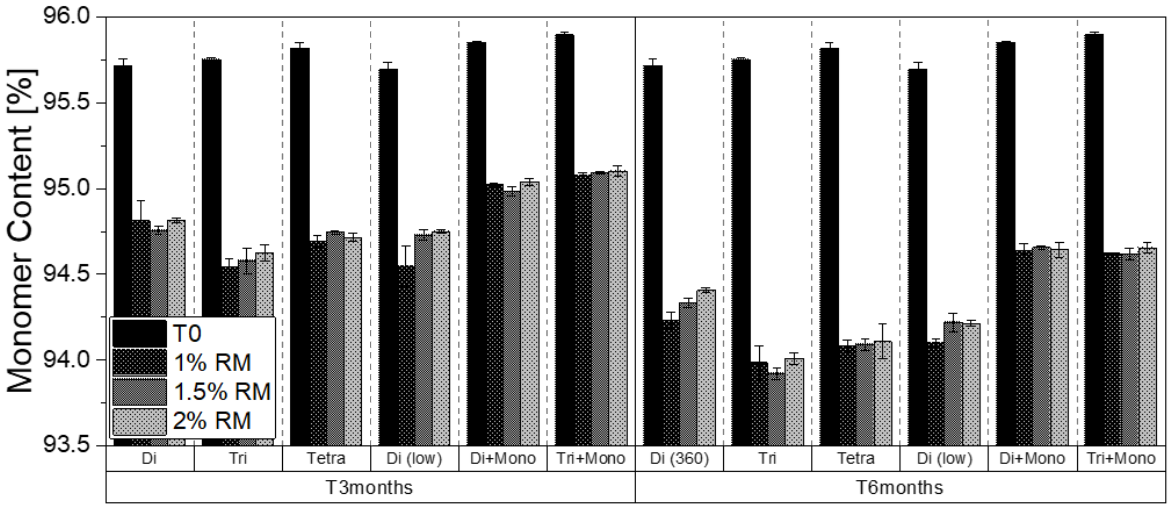

Figure V.5: Monomer content in SEC with different sugar sizes and molar sugar to HSA ratios before (T0) and after storage at 2-8 °C for 3 and 6 months.

V.5.3 The influence of residual moisture on monomer content

The influence of RM on protein stability becomes clearly noticeable at 40 °C (Figure V.4). The maltose formulation with a 360:1 ratio showed a slightly higher monomer retention with increasing RM with 94.14%, 94.25%, and 94.34% monomer content after 1 month at 1%, 1.5%, and 2% RM, respectively. In the maltotetraose formulation 91.2% to 91.8% monomer was retained after 1 month and 88.7% to 90% after 3 months when comparing 1% and 2% RM lyophilizates. The enhanced monomer retention in all glucose-free formulations with higher RM indicates the importance of a minimum level of water and the risks of overdrying. Better stabilization resulted from the combination of water-replacing sugars and remaining water molecules surrounding the protein, helping to maintain its native structure.[32,33] Additionally, the presence of water molecules reduces the T_g value, leading to increased mobility and structural relaxation. The latter effect could be beneficial by relieving internal stresses, potentially enhancing stability. The formulations based on larger sugar entities like maltotriose and maltotetraose benefit more from additional water molecules, as the sugar molecules themselves are less capable of hydrogen bonding compared to smaller ones. At 25 °C, an increased RM markedly enhanced the monomer loss in the mixed formulation with glucose, despite the better water replacement capacity (Figure V.4). We propose that this is due to the low initial T_g in glucose formulations, which further decreases with increasing RM, leading to cake collapse and protein degradation at 40 °C. At the lower temperature of 2-8 °C, RM has no detectable effect on monomer content (Figure V.3). Thus, the formulations demonstrate sufficient stabilization at the typical intended storage temperature for protein drug lyophilizates without requiring additional stabilizing H_2O molecules.

V.5.4 The influence of molar ratio on monomer content

Decreasing the molar ratio of maltose to protein from 360:1 to 180:1 reduced the monomer content at all temperatures and time points. Previous studies highlight the significant impact of stabilizer to protein molar ratios, especially at low values below 360:1.[14] After 3 months at 40 °C, the monomer content decreased from 93.8% at 1% RM for a 360:1 ratio to 90% for a 180:1 ratio. While increased residual moisture had minimal influence on the 360:1 sample, it slightly increased monomer retention for the 180:1 sample. The more pronounced effect of residual moisture at lower molar ratios is likely due to the reduced amount of stabilizing maltose and the resulting enhanced influence of hydrogen bonding from additional water molecules.

V.5.5 The influence of sugar size, molar ratio, and RM on the deuterium incorporation via ssHDX

To gain additional insights into the protein environment in the amorphous sugar glasses, we performed ssHDX MS measurements. The global HSA mass differed depending on the formulation (Figure V.6). The least mass increase [from 66,428 Da to 66,936 Da at 1% D_2O] was observed in the maltose lyophilizates. The weighted mean mass increased with sugar size, reaching 67,425 Da for maltotriose and 67,754 Da for maltotetraose at 1% D_2O. This mass increase can be estimated to be approximately. 32-38% of H-atoms exchanged by deuterium (assuming 585 amino acids x 6-7 hydrogen atoms in total). This difference in mass increase could be due to a higher accessibility of the protein to D_2O due to limited water replacement by the larger sugar molecule. It could also reflect the higher flexibility of the protein molecules in the matrices formed by the larger sugar molecules, which points to a higher unfolding potential. These results align with the SEC data and the higher stability in the matrices formed by the smaller sugars with higher water replacement and void-filling capacity.

Increasing the spiked D_2O content from 1% to 2% did not lead to more global deuterium uptake in the glucose-free formulations. Increasing the spiked D_2O amount raises the question, whether an increased deuterium uptake is related to the higher D2O concentration per se or its impact as a softener on glass mobility, Tg, and ultimately protein molecular mobility. To gain further insights, we increased RM using a mixture of 1% D_2O and 1% H_2O, avoiding additional D_2O that could influence deuterium incorporation. This approach led to a decrease in deuterium incorporation in glucose-free samples. For the 360:1 maltose sample, the HSA mass reached 66,936 Da compared to 2% D_2O with 66,725 Da; for the maltotetraose lyophilizates, the deuterium uptake was reduced by 332 Da to 67,422 Da only. This confirms the stability study findings that an increased RM content stabilizes the protein structure. Moreover, the stabilizing effect of RM was more pronounced in samples with larger sugars, likely due to their slightly limited hydrogen bonding properties.

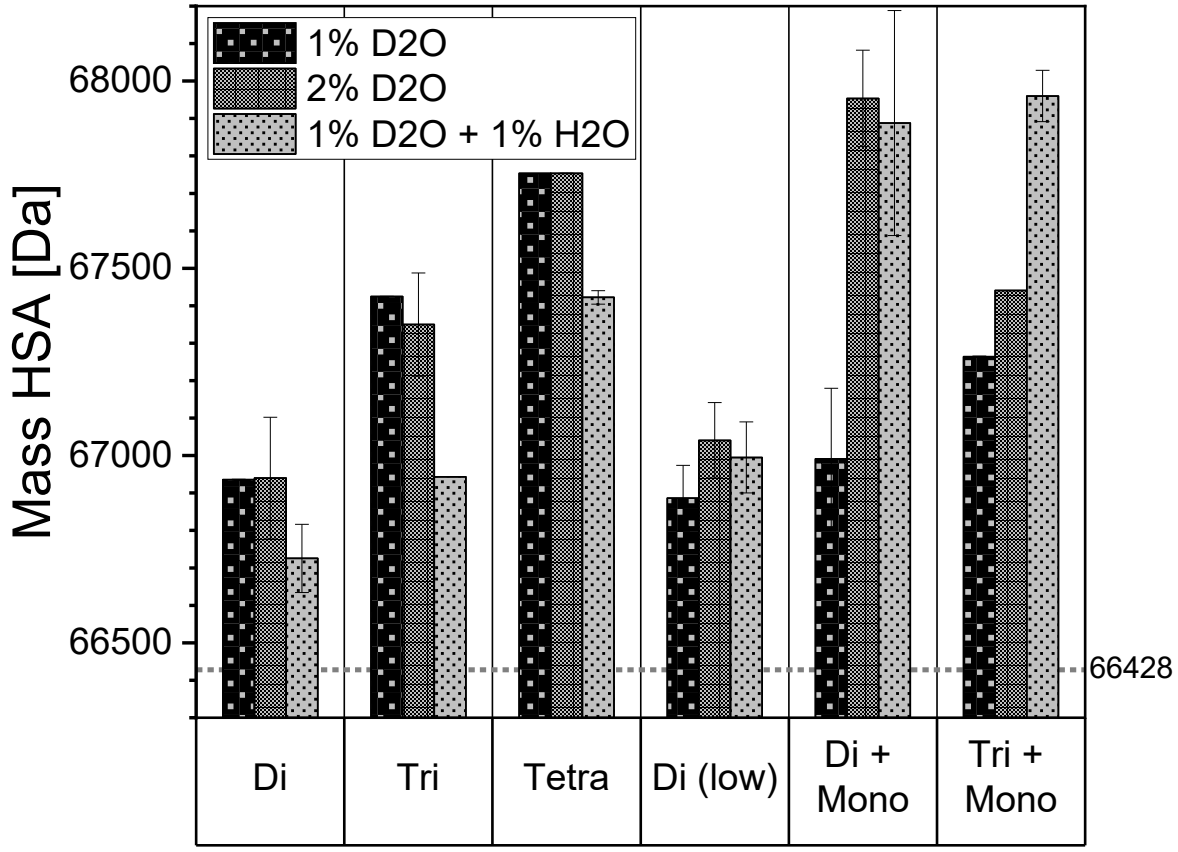

Figure V.6: Mass of HSA after spiking 1% D_2O, 2% D_2O, and 1% D_2O + 1% H2O and incubation at 45 °C for 18 h compared to the HSA control sample.

Glucose-containing formulations showed a different behavior. While a mixture of glucose and maltose showed comparable masses to the maltose samples at 66,831 Da, mixtures of glucose and maltotriose exhibited an even lower mass at 1% D_2O of 66,612 Da. This supports the hypothesis that varying excipient sizes within one sample can offer complementary properties and improve stability. Increasing the moisture content from 1% D_2O to 2% D_2O or 1% D_2O + 1% H_2O increased molecular weight. In mixtures of glucose and maltose, the HSA mass increased to 67,954 Da at 2% D_2O, in glucose-maltotriose mixtures to 67,778 Da. This initially surprising result can be explained by considering the low T_g of glucose and the increased moisture content. The T_g of the glucose mixtures of approx. 57 °C at 0% RM will be reduced with higher residual moisture, considering the rule of thumb that an increase of 1% RM will lead to a decreased T_g of 10 K.[34] The expected T_g at 2% RM should be at 37 °C and thus below the incubation temperature, leading to severe structural changes.

In addition to lowering T_g, glucose can cause glycation on HSA, introducing an additional mass-altering factor.[29,35] These additional variables are also evident in the increased

standard deviation of the glucose-containing samples. Consequently, interpreting ssHDX MS data becomes challenging when the moisture content exceeds 1%, but it remains consistent with the SEC results for samples stored at 40 °C. Maltose samples with 360:1 and 180:1 ratios show no differences in the deuterium uptake. It is important to note that due to the size of HSA, mass deconvolution and data interpretation reach their limit. Despite these challenges, we successfully implemented a novel, simple, and adaptable ssHDX MS approach using headspace spiking in combination with a small benchtop spectrometer. The ssHDX MS measurements provided structural insights into the sugar glass matrix surrounding the protein molecules, demonstrating that smaller sugars enhance protein stability by filling voids and forming hydrogen bonds. Larger sugars form more rigid glasses but are limited in the direct interaction with the protein molecule, leading to greater protein accessibility and potential structural destabilization. The lower monomer retention aligns well with the higher D/H substitution, supporting ssHDX as a rapid and sensitive method to evaluate the stabilizing potential of formulations under varying residual moisture conditions.

V.6 Conclusion and Outlook

In this study, we investigated the impact of sugar size, RM, and the molar sugar to protein ratio on HSA monomer retention upon storage. We compared glucose-based oligosaccharides, including maltose, maltotriose, maltotetraose, and glucose/maltose and glucose/maltotriose mixtures. Our findings indicate that sugar size significantly impacts protein stability. The use of larger sugars resulted in less monomer retention and increased deuterium incorporation, suggesting greater protein accessibility and flexibility in the solid state. Despite the formation of more rigid glasses, larger sugars are less effective in void filling and hydrogen bond formation upon water removal. Increasing the RM to 1%, 1.5%, and 2% improved HSA stability in all glucose-free formulations at higher temperatures, highlighting the beneficial effect of water molecules on protein stabilization and the importance of hydrogen bonding in the dry state, as well as the beneficial plasticizing effect of water. The stabilizing effect of higher RM was more pronounced in formulations containing larger sugars. This supports the hypothesis that the reduced capability of hydrogen bonding with the protein molecules due to less intimate interaction is the reason for lower stabilization capacity of larger sugars. Consequently, formulations based on larger sugars providing insufficient hydrogen bond-based stabilization preferably benefit from additional water molecules. In glucose-free formulations, ssHDX MS showed no change in deuterium incorporation when RM was increased from 1% D_2O to 2% D_2O, likely due to a trade-off between beneficial moisture content and increased deuterium uptake. Samples spiked with 1% D_2O + 1% H_2O showed decreased deuterium

uptake, supporting the hypothesis of improved stability with increased RM and enhanced interaction with water molecules. Glucose-oligosaccharide mixtures demonstrated higher monomer content after storage at 2-8 °C but were less stable at higher temperatures due to higher mobility as they show low T_g values. Increased RM did not enhance monomer retention of the mixtures, likely due to further T_g reduction and already good protein stabilization by water replacement. However, considering the effects of lower T_g and appropriate storage conditions, combining small and large sugars may provide high stability; such combinations could combine good water replacement and vitrification for drug products intended for storage at 2-8 °C. Formulations containing larger sugars benefit from higher RM content and carry a higher risk of lower protein stability when overdried. In contrast, lyophilizates containing smaller sugars benefit from lower RMs due to the T_g reducing properties of moisture challenging elevated storage temperatures. Highly concentrated mAb formulations often exhibit elevated T_g values, which may reduce the negative impact of RM-induced higher mobility. In such cases, carefully balancing sugar mixture composition and RM can help maximize stability. Furthermore, we demonstrated that the headspace spiking ssHDX MS approach is an effective tool for evaluating protein stability during early development. In addition to physical stability, future studies will address chemical stability, including potential modifications such as deamidation and oxidation, to complement the present results. Overall, the findings on the impact of sugar size and RM on protein stability in sugar-based lyophilizates can help to develop more effective stabilization strategies.

.

V.7 Supporting information

V.7.1 Assessing protein accessibility in lyophilizates by ssHDX MS

In pre-experiments, 5 g/l human growth hormone (MW 22126 Da) was lyophilized in 10 mM Tris Buffer pH 7.4 with 7% or 10% sucrose and with and without polysorbate 20. Additionally, sucrose to protein ratios were varied between 360:1 and 90:1.

In the pre-experiments, 1µL was injected, a Waters BEH SEC 200 Å column, maintained at 5 °C with a flow rate of 0.15 ml/min was used, and elution was performed at 80% H_2O and 20% ACN, with 0.1% formic acid and 0.05% trifluoroacetic acid. UV/Vis was performed at 280 nm, and the QDa mass detector was used.

A compromise of T and t is required to enable studies with a relevant D_2O level, an adequate time frame, and without physical changes in the lyophilizates.

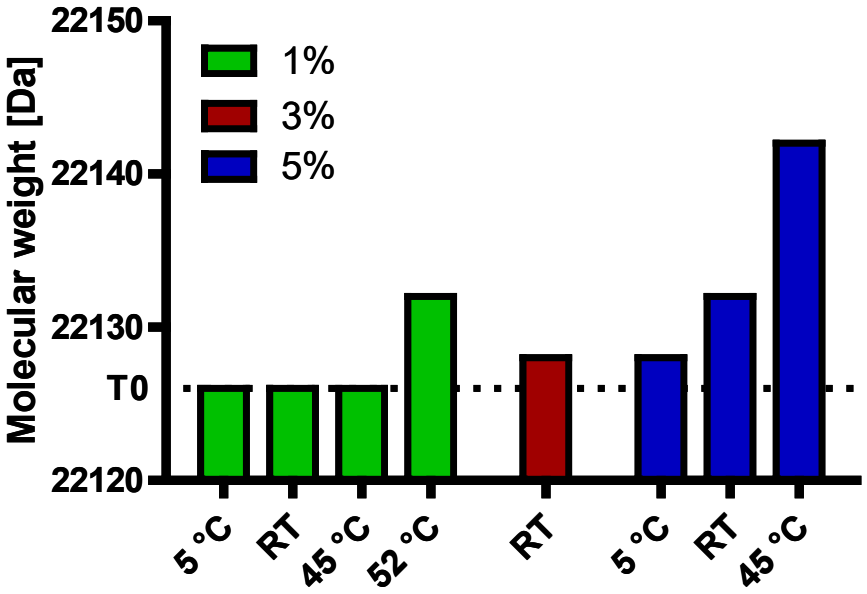

SI Figure V.1: Deuterium uptake of hGH vs RM_{D2O} content and temperature after one week.

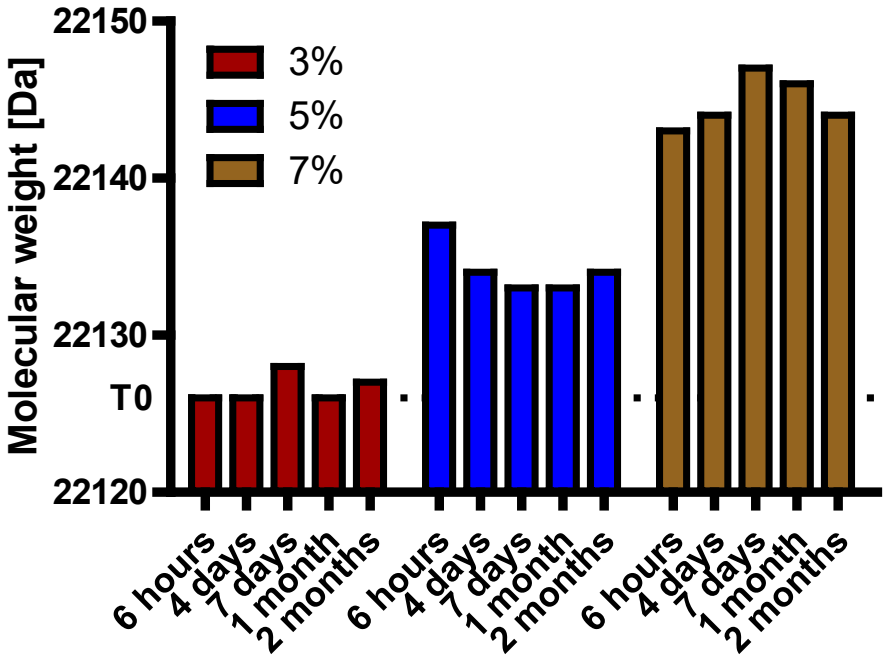

SI Figure V.2: Deuterium uptake of hGH vs time and RM_{D2O} at RT.

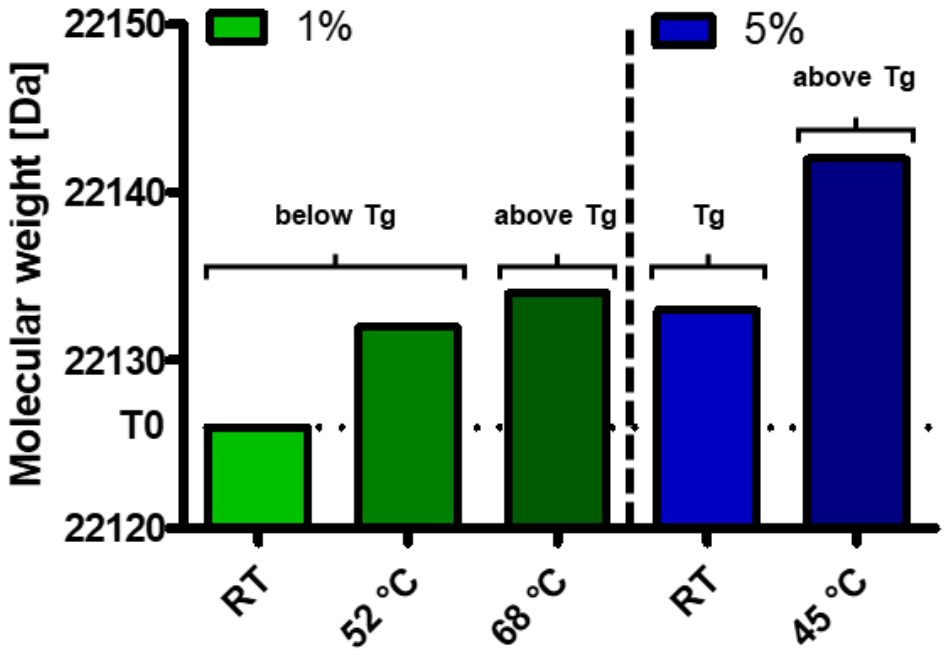

SI Figure V.3: Deuterium uptake above and below T_g

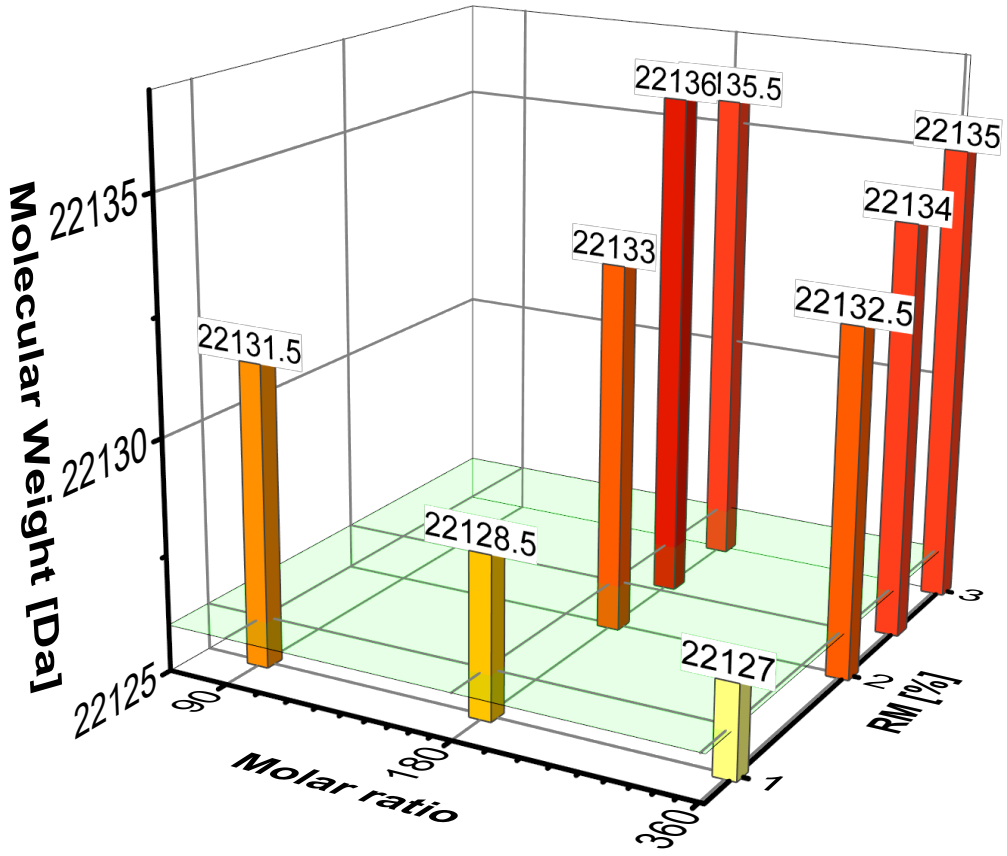

SI Figure V.4: Deuterium uptake vs. sucrose to protein molar ratio and RM_{D2O}.

Based on these findings, ssHDX was conducted at 45 °C with an incubation period of approximately 18 h in the main experiments

V.8 References

[1] A. Juckers, P. Knerr, F. Harms, J. Strube, Effect of the Freezing Step on Primary Drying Experiments and Simulation of Lyophilization Processes, Processes 11 (2023) 1404.

[2] J. Horn, J. Schanda, W. Friess, Impact of fast and conservative freeze-drying on product quality of protein-mannitol-sucrose-glycerol lyophilizates, European Journal of Pharmaceutics and Biopharmaceutics 127 (2018) 342–354.

[3] C. Haeuser, P. Goldbach, J. Huwyler, W. Friess, A. Allmendinger, Be Aggressive! Amorphous Excipients Enabling Single-Step Freeze-Drying of Monoclonal Antibody Formulations, Pharmaceutics 11 (2019) 616.

[4] J.C. Kasper, G. Winter, W. Friess, Recent advances and further challenges in lyophilization, European Journal of Pharmaceutics and Biopharmaceutics 85 (2013) 162–169.

[5] F. Jameel (Ed.), Principles and Practices of Lyophilization in Product Development and Manufacturing, 1st ed. 2023 ed., Springer International Publishing; Imprint Springer, Cham, 2023.

[6] S. Groël, T. Menzen, G. Winter, Calorimetric Investigation of the Relaxation Phenomena in Amorphous Lyophilized Solids, Pharmaceutics 13 (2021) 1735.

[7] K. Shirai, K. Watanabe, H. Momida, First-principles study of the specific heat of glass at the glass transition with a case study on glycerol, Journal of physics. Condensed matter an Institute of Physics journal 34 (2022) 375902.

[8] M. Roussenova, J.-C. Andrieux, M.A. Alam, J. Ubbink, Hydrogen bonding in maltooligomer-glycerol-water matrices: Relation to physical state and molecular free volume, Carbohydrate polymers 102 (2014) 566–575.

[9] T. Serno, R. Geidobler, G. Winter, Protein stabilization by cyclodextrins in the liquid and dried state, Advanced drug delivery reviews 63 (2011) 1086–1106.

[10] W.F. Tonnis, M.A. Mensink, A. de Jager, K. van der Voort Maarschalk, H.W. Frijlink, W.L.J. Hinrichs, Size and molecular flexibility of sugars determine the storage stability of freeze-dried proteins, Molecular Pharmaceutics 12 (2015) 684–694.

[11] M.T. Cicerone, J.F. Douglas, β-Relaxation governs protein stability in sugar-glass matrices, Soft Matter 8 (2012) 2983.

[12] M.T. Cicerone, C.L. Soles, Fast dynamics and stabilization of proteins: binary glasses of trehalose and glycerol, Biophysical Journal 86 (2004) 3836–3845.

[13] D. Averett, M.T. Cicerone, J.F. Douglas, J.J. de Pablo, Fast relaxation and elasticity-related properties of trehalose-glycerol mixtures, Soft Matter 8 (2012) 4936.

[14] K. Lo Presti, M. Jégo, W. Frieß, "The More, the Better?": The Impact of Sugar-to-Protein Molar Ratio in Freeze-Dried Monoclonal Antibody Formulations on Protein Stability, Mol. Pharmaceutics (2024) 6484–6490.

[15] J.L. Cleland, X. Lam, B. Kendrick, J. Yang, T.-H. Yang, D. Overcashier, D. Brooks, C. Hsu, J.F. Carpenter, A specific molar ratio of stabilizer to protein is required for storage stability of a lyophilized monoclonal antibody, Journal of Pharmaceutical Sciences 90 (2001) 310–321.

[16] L.L. Chang, D. Shepherd, J. Sun, D. Ouellette, K.L. Grant, X.C. Tang, M.J. Pikal, Mechanism of protein stabilization by sugars during freeze-drying and storage: native structure preservation, specific interaction, and/or immobilization in a glassy matrix?, Journal of Pharmaceutical Sciences 94 (2005) 1427–1444.

[17] M.J. Hageman, The Role of Moisture in Protein Stability, Drug Development and Industrial Pharmacy 14 (1988) 2047–2070.

[18] S. Ohtake, S. Feng, E. Shalaev, Effect of Water on the Chemical Stability of Amorphous Pharmaceuticals: 2. Deamidation of Peptides and Proteins, Journal of Pharmaceutical Sciences 107 (2018) 42–56.

[19] E. Bogdanova, S. Lages, T. Phan-Xuan, M.A. Kamal, A. Terry, A. Millqvist Fureby, V. Kocherbitov, Lysozyme-Sucrose Interactions in the Solid State: Glass Transition, Denaturation, and the Effect of Residual Water, Molecular Pharmaceutics 20 (2023) 4664–4675.

[20] C.C. Hsu, C.A. Ward, R. Pearlman, H.M. Nguyen, D.A. Yeung, J.G. Curley, Determining the optimum residual moisture in lyophilized protein pharmaceuticals, Developments in Biological Standardization 74 (1992) 255-70.

[21] A. Duralliu, P. Matejtschuk, P. Stickings, L. Hassall, R. Tierney, D.R. Williams, The Influence of Moisture Content and Temperature on the Long-Term Storage Stability of Freeze-Dried High Concentration Immunoglobulin G (IgG), Pharmaceutics 12 (2020) 303.

[22] K. Lo Presti, W. Frieß, Adjustment of specific residual moisture levels in completely freeze-dried protein formulations by controlled spiking of small water volumes, European Journal of Pharmaceutics and Biopharmaceutics 169 (2021) 292–296.

[23] B.S. Moorthy, I.E. Zarraga, L. Kumar, B.T. Walters, P. Goldbach, E.M. Topp, A. Allmendinger, Solid-State Hydrogen-Deuterium Exchange Mass Spectrometry: Correlation of Deuterium Uptake and Long-Term Stability of Lyophilized Monoclonal Antibody Formulations, Molecular Pharmaceutics 15 (2018) 1–11.

[24] L. Kumar, K.B. Chandrababu, S.M. Balakrishnan, A. Allmendinger, B. Walters, I.E. Zarraga, D.P. Chang, P. Nayak, E.M. Topp, Optimizing the Formulation and Lyophilization Process for a Fragment Antigen Binding (Fab) Protein Using Solid-State Hydrogen-Deuterium Exchange Mass Spectrometry (ssHDX-MS), Molecular Pharmaceutics 16 (2019) 4485–4495.

[25] M.J. Pikal, D.R. Rigsbee, M.L. Roy, Solid state chemistry of proteins: I. glass transition behavior in freeze dried disaccharide formulations of human growth hormone (hGH), Journal of Pharmaceutical Sciences 96 (2007) 2765–2776.

[26] M. Schugmann, P. Foerst, Systematic Investigation on the Glass Transition Temperature of Binary and Ternary Sugar Mixtures and the Applicability of Gordon-Taylor and Couchman-Karasz Equation, Foods (Basel, Switzerland) 11 (2022).

[27] A. Simperler, A. Kornherr, R. Chopra, P.A. Bonnet, W. Jones, W.D.S. Motherwell, G. Zifferer, Glass transition temperature of glucose, sucrose, and trehalose: an experimental and in silico study, The Journal of Physical Chemistry B 110 (2006) 19678–19684.

[28] E.D. Breen, J.G. Curley, D.E. Overcashier, C.C. Hsu, S.J. Shire, Effect of Moisture on the Stability of a Lyophilized Humanized Monoclonal Antibody Formulation, Pharmaceutical Research 18 (2001) 1345-1353.

[29] C. Haeuser, P. Goldbach, J. Huwyler, W. Friess, A. Allmendinger, Impact of dextran on thermal properties, product quality attributes, and monoclonal antibody stability in freeze-dried formulations, European Journal of Pharmaceutics and Biopharmaceutics 147 (2020) 45–56.

[30] M.T. Ruggiero, M. Krynski, E.O. Kissi, J. Sibik, D. Markl, N.Y. Tan, D. Arslanov, W. van der Zande, B. Redlich, T.M. Korter, H. Grohganz, K. Löbmann, T. Rades, S.R. Elliott, J.A. Zeitler, The significance of the amorphous potential energy landscape for dictating glassy dynamics and driving solid-state crystallisation, Physical chemistry chemical physics PCCP 19 (2017) 30039–30047.

[31] M. Batens, T.A. Shmool, J. Massant, J.A. Zeitler, G. van den Mooter, Advancing predictions of protein stability in the solid state, Physical chemistry chemical physics PCCP 22 (2020) 17247–17254.

[32] J.A. Brom, R.G. Petrikis, G.J. Pielak, How Sugars Protect Dry Protein Structure, Biochemistry 62 (2023) 1044–1052.

[33] S. Feng, G.H.J. Peters, S. Ohtake, C. Schöneich, E. Shalaev, Water Distribution and Clustering on the Lyophilized IgG1 Surface: Insight from Molecular Dynamics Simulations, Molecular Pharmaceutics 17 (2020) 900–908.

[34] B.C. Hancock, G. Zografi, The Relationship Between the Glass Transition Temperature and the Water Content of Amorphous Pharmaceutical Solids, Pharmaceutical Research 11 (1994) 471–477.

[35] L. Liu, Y. Liu, A. Xiao, S. Mei, Y. Xie, Influence of Human Serum Albumin Glycation on the Binding Affinities for Natural Flavonoids, Open Chemistry 17 (2019) 806–812.

Chapter VI Insights into folding and molecular environment of lyophilized proteins using pulsed electron paramagnetic resonance spectroscopy

This chapter is published as: Isaev[§], N.; Lo Presti[§], K.; Frieß, W. Chapter V Insights into folding and molecular environment of lyophilized proteins using pulsed electron paramagnetic resonance spectroscopy. *Molecular Pharmaceutics* 22 (2025) 424-432

[§]These authors contributed equally to this work

Note from the authors: To establish a coherent numbering and pagination within this document the numbers of references, figures, and tables were adapted. Apart from minor changes, the version included in this thesis is identical to the published article.

The published article can be accessed online via:

https://doi.org/10.1021/acs.molpharmaceut.4c01008

VI.1 Abstract

There is still insufficient understanding of how the characteristics of protein drugs are maintained in the solid state of lyophilizates, including aspects such as protein distances, local environment, and structural preservation. To this end, we evaluated protein folding and the molecules' nearest environment by electron paramagnetic resonance (EPR) spectroscopy. Double electron-electron resonance (DEER) probes distances of up to approx. 200 Å and is suitable to investigate protein folding, local concentration, and aggregation, whereas electron spin echo envelope modulation (ESEEM) allows to study the near environment within approx. 10 Å of the spin-label. We spin labeled HSA and freeze-dried different concentrations with 100 g/l deuterated sucrose. DEER showed distinct local concentration behaviors for two folding states, directly correlating folding percentage with inter-protein distance, reaching 2 nm at an HSA concentration of 84 g/l. Interestingly, 50% of the HSA molecules showed partial structural perturbation already at 2.6 g/l which corresponds to a molar ratio Suc/HSA of 7469. This percentage increased to 97% with increasing the HSA concentration to 84 g/l. The degree of the protein perturbation cannot be told, and no signs of unfolding are found after reconstitution. ESEEM demonstrated a higher sucrose concentration around the protein label as compared to the HSA environment in highly concentrated sucrose solutions. The partial unfolding detected in DEER could lead to label exposure and explain the enhanced sucrose detection in the intimate shell. Our work provides new insights regarding sucrose enrichment in the nearest shell of proteins upon lyophilization. In addition, the results indicate substantial partial structural

perturbation even in the presence of enormous supplies of stabilizing sugars. Thus, pulse EPR spectroscopy allows additional understanding of the solid state of protein lyophilizates which is complementary to SANS, FTIR, or ssNMR.

Keywords: EPR, solid state, lyophilization, protein unfolding, accessibility, sucrose, human serum albumin, DEER, ESEEM, local environment

VI.2 Graphical Abstract

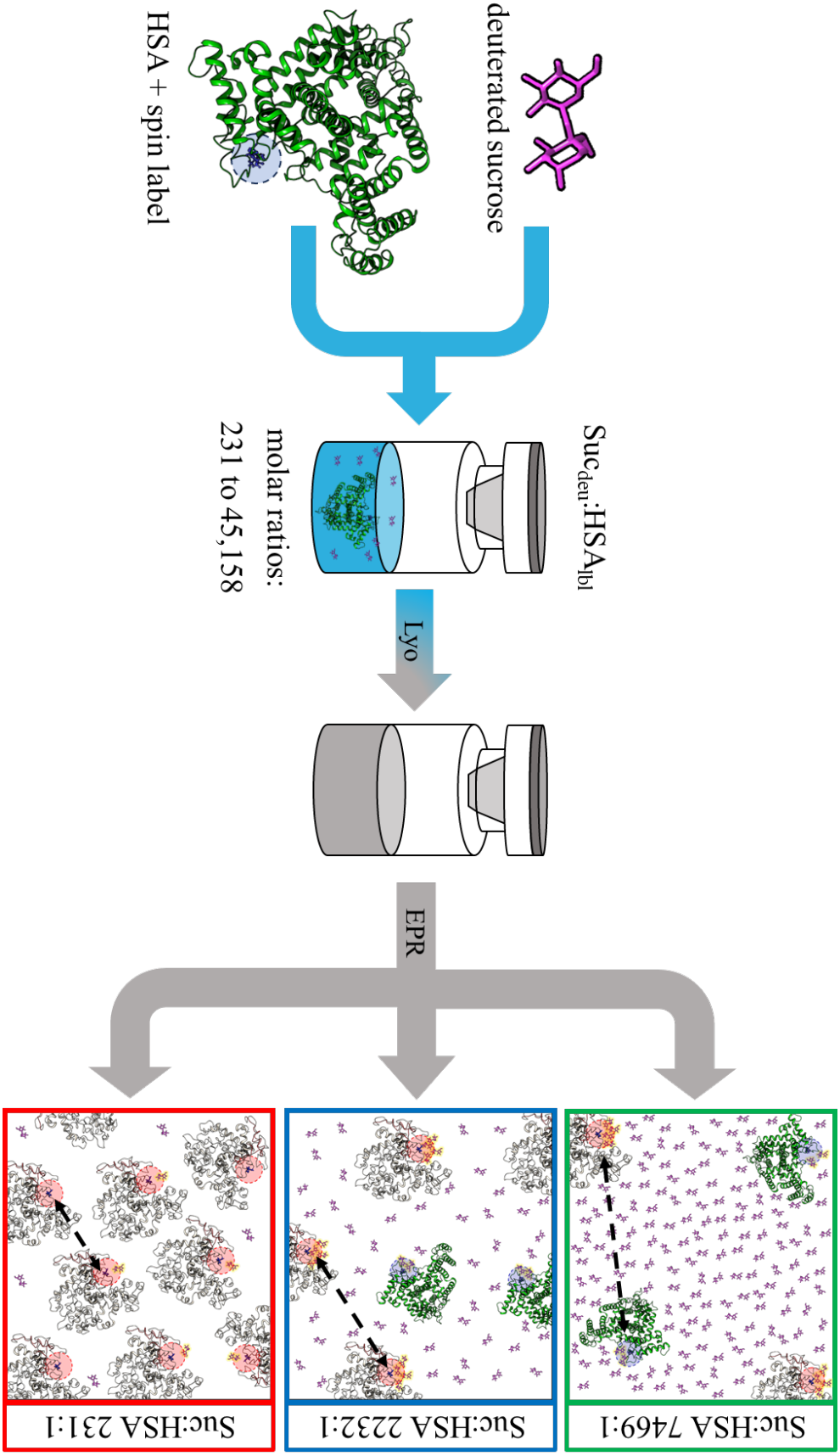

VI.3 Introduction

Lyophilization is common to increase the long-term stability of protein drugs but also nanoparticulate nucleic acid delivery systems.[1–3] How proteins are preserved in the solid state is not fully understood.[4,5] There are two main hypotheses. In the water replacement theory, water removal and resulting changes in the native structure are compensated by excipient molecules, most preferably sucrose or trehalose.[6] It is assumed that these excipients replace the protein-to-water hydrogen bonds with their own hydroxyl groups.[7] The vitrification hypothesis states that the native structure is preserved by the high viscosity and rigidity of the matrix in which the protein molecules are embedded hindering inter- and intramolecular movements.[8] Based on these theories, factors like the ability of an excipient to form hydrogen bonds with critical sites of the protein molecules or the ratio of stabilizing excipient to protein affect the preservation of the protein native structure during and after lyophilization.[9]

To gain deeper insights into the stabilizing mechanisms and molecular motions in the freeze-dried state, solid-state Fourier-transform infrared spectroscopy (ssFTIR), liquid observed vapor exchange nuclear magnetic resonance (LOVE NMR), solid-state hydrogen-deuterium exchange mass spectrometry (ssHDX-MS), and small angle neutron scattering (SANS) are used. ssFTIR is used to investigate the secondary structure in the solid state and track changes in the spectrum especially when coupled with an HDX approach.[10–12] LOVE NMR and ssHDX-MS provide information regarding protein folding and accessibility of the protein molecules‘ surface; they require a reconstitution step before the analysis giving more details on the accessible surface area of the protein.[13–16] SANS can be used to study the nanoscale structure of the protein environment in both liquid and solid state but it reaches its limits when it comes to the analysis of the protein shape itself.[17–19] In this study, we evaluated electron paramagnetic resonance (EPR) spectroscopy as a novel technique to gain additional insights into the structural changes of proteins in the solid state and the sugar molecules in the near protein environment to get a complete picture of protein drug lyophilizates.

EPR allows for the direct analysis of distances and structural properties of proteins with unpaired electron spins, such as metalloproteins or electron transfer chains like in photosystem II at 50-80 K.[20,21] However, most proteins lack unpaired electron spins and thus require spin labeling to be observable in EPR. (1-Oxyl-2,2,5,5-tetramethylpyrroline-3-methyl)methanethiosulfonate (MTSSL) is one of the most widely used spin labels. It binds to

free cysteine residues via disulfide bond formation at mild reaction conditions with almost 100% yield generating only a 185 Da protein modification (Figure VI.1).

EPR can be described by the same physics as NMR whereby electron spins show a 10^3-10^4 times larger magnetic moment compared to nuclear spins. The energy of EPR interspin interactions is proportional to the product of the magnetic moments of the interacting spins, resulting in interaction energies 10^6-10^8 times stronger than nuclear interactions. Thus, EPR can measure spin interactions over longer distances compared to NMR. The double electron-electron resonance (DEER) technique provides detailed information about nearby electron spins in 15-200 Å distance, and the electron spin echo envelope modulation (ESEEM) procedure gives information about nuclear spins within 10 Å of unpaired electrons. Both methods require cooling to temperatures between 50-80K. Thus, on the one hand, DEER and ESEEM reveal the local concentration of protein molecules and changes in the composition of their nearest 10 Å shell as shown in protein containing freeze concentrates.[22] On the other hand, DEER can characterize protein folding by investigating excluded volumes.[22–24]

In this work, we employed EPR as a novel tool in the pharmaceutical field to gain additional information about protein structure preservation, local (<200 Å) concentration changes, and the protein nearest environment in the solid state. We analyzed the protein structure and structural changes before lyophilization, in lyophilizates, and after reconstitution gain information on protein stability and the reversibility of changes in the protein structure occurring in the dried state. We tested the influence of the protein to excipient molar ratio on the protein structure preservation and the interactions between protein molecules in the solid state. Human serum albumin (HSA) labeled with MTSSL was used as a model protein. We studied the sucrose content in the 10 Å nearest environment around the spin label by ESEEM and the HSA folding preservation and local concentration changes by DEER at different HSA to sucrose ratios. Additionally, we investigated local protein concentration and microheterogeneity and combined DEER and ESEEM results to a more complete picture of protein molecules in a dry amorphous sugar matrix. Lastly, the potential of EPR as an additional tool in the solid state analysis of dried protein formulations is evaluated and an outlook on future applications is given.

VI.4 Material and Methods

VI.4.1 Materials

Highly purified recombinant human serum albumin (102 g/l) formulated in a 146 mM sodium phosphate buffer pH 6.6 was kindly provided by Albumedix, Nottingham, United Kingdom. Buffer salts were purchased from Merck, Darmstadt, Germany and HPW was prepared by a UF system (Sartorius Arium Pro, Sartorius, Göttingen, Germany). D_2O and slurry Raney Nickel were purchased from Sigma-Aldrich, St. Louis, MO, USA. MTSSL was obtained from Enzo Life Sciences, Lörrach, Germany, and acetonitrile from Carl Roth, Karlsruhe, Germany.

VI.4.2 Protein spin labeling

To detect HSA via EPR, a highly reactive nitroxide spin label radical (MTSSL) was attached via the only free cysteine (Cys^{34}) (Figure VI.1). One spin label per protein molecule renders MTSSL-HSA a highly suitable model.[25,26] MTSSL was diluted in acetonitrile, a 5 times molar excess was mixed with HSA stock in sodium phosphate buffer pH 6.6 and incubated for 18 h at room temperature protected from light. Subsequently, unlabeled MTSSL was removed using Amicon 30 K centrifugal filters (Merck, Darmstadt, Germany). The spin labeling efficiency was confirmed as 1 label/protein from the ratio of the spin concentration measured by an MS300 EPR spectrometer (Magnettech, Berlin, Germany) and the protein concentration measured by UV absorption at 280 nm.

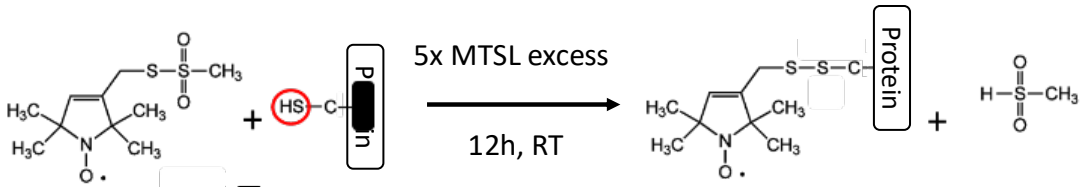

Figure VI.1: Spin-label attachment of MTSSL to a target protein by binding to an accessible cysteine.

VI.4.3 Deuteration of sucrose

Sucrose was deuterated to achieve a detectable cryo- and lyoprotectant by EPR. 60 g slurry Raney Nickel was filtrated, washed 5 times with 20 ml D_2O, and incubated for at least 24 h in 100 ml D_2O. 20 g sucrose was dissolved in 200 ml D_2O followed by D_2O evaporation at 55 °C using a rotary evaporator. Dissolution and evaporation were repeated once. The dried sucrose was mixed with the Raney Nickel slurry in D_2O and refluxed at 55 °C for 10 h. Raney Nickel was filtered and washed three times with 50 ml D_2O, and the resulting deuterated sucrose filtrate was dried at 55 °C using a rotary evaporator. The deuteration efficiency was determined as 6.6 D per sucrose molecule by NMR.

VI.4.4 Lyophilization of EPR samples

2.6 g/l, 8.7 g/l, 20.0 g/l, 42 g/l, and 84.4 g/l MTSSL-HSA in 100 g/l deuterated sucrose containing 1 mM sodium phosphate pH 6.5 were prepared (sucrose to HSA molar ratio: 7469, 2232, 971, 462, and 231). 500 µl of the formulations were lyophilized in 2R vials (Bünder Glas, Bünde, Germany). Vials were semi-stoppered with rubber stoppers (West Pharmaceutical Services, Exton, PA, USA) and freeze-dried in an FTS Lyostar 3 (SP Scientific, Stone Ridge, NY, USA). Samples were equilibrated for 10 min at 20 °C, cooled within 30 min to 5 °C, held for 60 min, frozen to -45 °C at 1 K/min, and held at -45 °C for 30 min. During 48 h of primary drying a vacuum of 0.1 mbar and a shelf temperature of -25 °C were applied. For secondary drying the shelf temperature was increased to 25 °C at 0.5 K/min and held at 25 °C for 5 h. Venting and vial closing was performed in a nitrogen environment at 800 mbar. Samples were crimped sealed using flip-off caps (ChemoLine, Sankt Augustin, Germany) and stored at 4 °C until further use.

VI.4.5 Analysis of residual moisture

The residual moisture of the lyophilizates was analyzed using a headspace Karl Fischer titration system (Aqua 40.00, Analytik Jena, Jena, Germany). Approx. 20 mg were transferred into 2R vials in a glovebox under nitrogen environment (r.h. ≤ 4%). Samples were heated to 120 °C and an Aquastar water standard (Merck, Darmstadt, Germany) was analyzed as a control.

VI.4.6 Glass transition temperature of freeze-dried formulations

The glass transition temperature of the lyophilizates was analyzed by differential scanning calorimetry (DSC 214 *polyma* calorimeter, Netzsch, Selb, Germany). Approx. 10- 20 mg were transferred into aluminum pans under a nitrogen environment and hermetically sealed. An empty pan was used as a reference. Samples were heated from 0 °C to 150 °C at 10 K/min.

VI.4.7 Analysis of monomer content

Size exclusion chromatography was performed on an Agilent 1200 HPLC system equipped with a diode array detector (Agilent Technologies, Santa Clara, California, USA). A TSKgel G3000 SWxl column (Tosoh Bioscience GmbH, Grießheim, Germany) was used as stationary phase, the mobile phase was 150 mM potassium phosphate buffer pH 6.45 and a flowrate of 0.4 ml/min was applied; 10 µl were injected and the chromatograms were evaluated at 280 nm.

VI.4.8 Secondary and tertiary structure analysis

Samples (diluted to a UV absorption at 280 nm of 0.8) were analyzed using a Jasco J-810 spectropolarimeter (JASCO, Pfungstadt, Germany) at 25 °C with a scan rate of 20 nm/min in a quartz cuvette of 10 mm path length. The mean molar ellipticity [θ] was calculated after subtraction of the respective buffer blank.

VI.4.9 Computational simulation of HSA unfolding in sucrose matrix

The HSA structure file (PDB:1AO6) was prepared using the BioLuminate (Schrödinger Release 2022-4, Schrödinger LLC New York, NY, USA) protein preparation tool, and a restrained minimization using the OPLS3e force field was performed. Molecular dynamics simulations were performed using GROMACS (2022.3) with the OPLS-AA forcefield.[27] The LIgParGen Server was used to generate the topology of the sucrose molecule. One molecule of HSA and 1617 molecules of sucrose were placed in a 5 nm x 5 nm x 5 nm box as the starting configuration. The initial configuration was minimized using the steepest descent algorithm. The minimized structures were equilibrated in an NVT ensemble at 300 K and τ_T=0.1 for 100 ps and in a NPT ensemble at 1 bar and τ_P=2.0 for another 100 ps.[28,29] Production runs were simulated at 350 K for 20 ns using the leap frog integrator and a timestep of 2 fs. Long-range electrostatics were handled by the Particle Mesh Ewald method, short-range electrostatics cutoffs were set to 1.0 nm.[30]

VI.4.10 Preparation of glassy solutions to calibrate local spin label concentration

ESEEM and DEER require reference measurements to enable the extraction of parameters like protein concentration and folding, sucrose content, and phase separation. Highly concentrated sucrose solutions provide a glassy state upon freezing in liquid nitrogen without phase separation or ice crystallization and can be used for calibration.[22,31] A calibration curve of the spin labeled HSA (HSA_{lbl}) and the deuterated sucrose (suc_{deu}) in liquid was generated with reference solutions containing a fixed non-deuterated sucrose concentration with varying HSA_{lbl} concentration (HSA_{lbl} reference) as well as with solutions containing a fixed HSA_{lbl} concentration and varying suc/suc_{deu} ratio (suc_{deu} reference). For this purpose, 100 mg suc or 200 mg suc_{deu}/suc (1+4, 2+3, 4+1, and 5+0) lyophilizates were reconstituted with a 100 g/l HSA_{lbl} stock solution to 65 wt% total solid (VI.8.2). For the suc_{deu} reference, suc_{deu}/suc lyophilizates were reconstituted with 1 g/l HSA_{lbl} to 0.46 g/l HSA_{lbl} and 65 wt% sucrose. For the HSA_{lbl} reference, sucrose lyophilizates were reconstituted with solutions of different HSA_{lbl} concentration to 0.86 g/l and 2.6 g/l HSA_{lbl}.

VI.4.11 ESEEM and DEER calibration in glassy water/sucrose matrices

DEER calibration was performed at 0.86 g/l and 2.6 g/l HSA_{lbl} in sucrose solutions. DEER data were fitted to excluded volumes by treating HSA molecules as spheres with a diameter of 11 nm.[32] This DEER calibration in liquid was used to interpret DEER results obtained in solid. The DEER calibration curves in liquid showed 30% reversible HSA dimer formation as previously observed in water/glycerol mixtures and in water.[33,34]

ESEEM calibration was performed with 65%wt solutions consisting of composition of 20%, 40%, 80%, and 100% suc_{deu} (VI.8.6).[35] The height of the ESEEM amplitude is proportional to the sucrose concentration around the spin label and structural changes near the spin label will affect the signal amplitude

VI.4.12 EPR measurement parameters

An Elexsys E580 spectrometer (Bruker Biospin, Rheinstetten, Germany) was used for the EPR measurements. Q-band measurements were performed using a Bruker QT-II resonator and a 150 W pulse Q-band TWT amplifier, X-band measurements using a Bruker MS-3 resonator and a 1kW X-band TWT amplifier. Glassy calibration solutions (VI.4.10) were transferred into quartz capillaries with an outer diameter of 3 mm (Aachener Quarzglas Technologie Heinrich, Aachen, Germany) using a 25 µl Hamilton syringe with PTFE luer lock and PTFE tubing assembly (Hamilton, Bonaduz, Switzerland). Lyophilized samples were transferred into the same capillaries in a glovebox under a nitrogen environment with a relative humidity of ≤ 4%. All capillaries were sealed by melting. Samples were cooled to 50 K using an ESR900 cryostat controlled by an ITC 503S temperature unit (Oxford Instruments, Abingdon, United Kingdom).

ESEEM experiments were performed in X-band with a three-pulse sequence, π/2-τ-π/2-T- π/2-τ-echo, a π/2 pulse length of 16 ns and a τ interval of 208 ns. The time delay T was scanned starting from 280 ns to 12280 ns using 375 steps of 32 ns. The ESEEM spectrum was obtained by a normalization of the experimental trace V(T) with a biexponential fit V(T)fit, as V(T)norm = V(T)/V(T)fit − 1, followed by a Fourier transformation.[36] The absolute value of the Fourier transform was analyzed.

DEER experiments were executed in Q-band using the 4-pulse sequence. The pump π pulse was 20 ns and was set to the dip center, the observer π/2 and π pulses´ lengths were 24 ns and 48 ns, respectively. The pump frequency corresponded to the nitroxide spectrum maximum, and the observer frequency had an offset of 50 MHz. A general introduction to DEER and ESEEM spectroscopy can be found in VI.8.1.

VI.5 Results and Discussion

Our goal was to investigate and better understand the stability, structural integrity, and molecular interactions of lyophilized HSA within a sucrose matrix. To this end we compared the protein structure in the liquid and the solid state at different sucrose to protein ratios and probed the molecular environment of the protein molecules both by using advanced EPR techniques such as DEER and ESEEM.

VI.5.1 Physical properties of the lyophilizates and protein stability

At first, we checked the HSA stability upon lyophilization and reconstitution in liquid. All lyophilizates showed an elegant cake structure without any signs of collapse, with residual moisture of 0.1%. High T_g values resulted in 65.1 °C and 78.6 °C for a sucrose to protein molar ratio of 7469 and 971 respectively. At higher protein content, a T_g could not be determined but can be expected to be even higher, due to the T_g value of pure protein.[37] The monomer content only decreased by 1% from approx. 95% to approx. 94% after lyophilization without a systematic impact of the sugar to protein ratio. Near and far UV spectra showed the characteristic HSA profile without differences in the secondary and tertiary structure after lyophilization and reconstitution compared with the starting solutions (Figure VI.2).[38,39] Thus, no significant instability of HSA upon lyophilization and reconstitution could be detected.

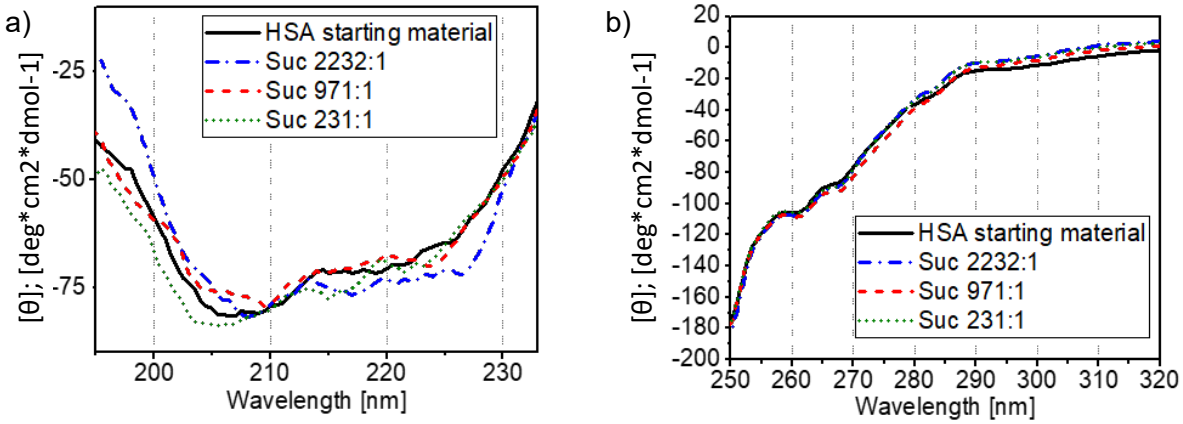

Figure VI.2: Exemplary far UV (a) and near UV (b) spectra of reconstituted samples and before lyophilization (black line).

VI.5.2 Computational simulation of HSA unfolding, excluded volume, and environment in sucrose matrices

DEER provides information on all electron interspinous interactions and can reveal protein concentration, protein excluded volume, and protein dimers or double spin labeled proteins in solids.[22] Excluded volume refers to the phenomenon where proteins cannot come into infinitely proximity due to their large molecular size. Figure VI.3 provides a model from a simulation with one protein per box, serving as a general visualization of excluded volume. Due to steric restrictions, certain distances between two spin labels located on two different proteins are less probable (Figure VI.3a). Upon unfolding, labels buried within the initial native protein can come in closer vicinity to neighbor protein labels as visualized in Figure VI.3b.

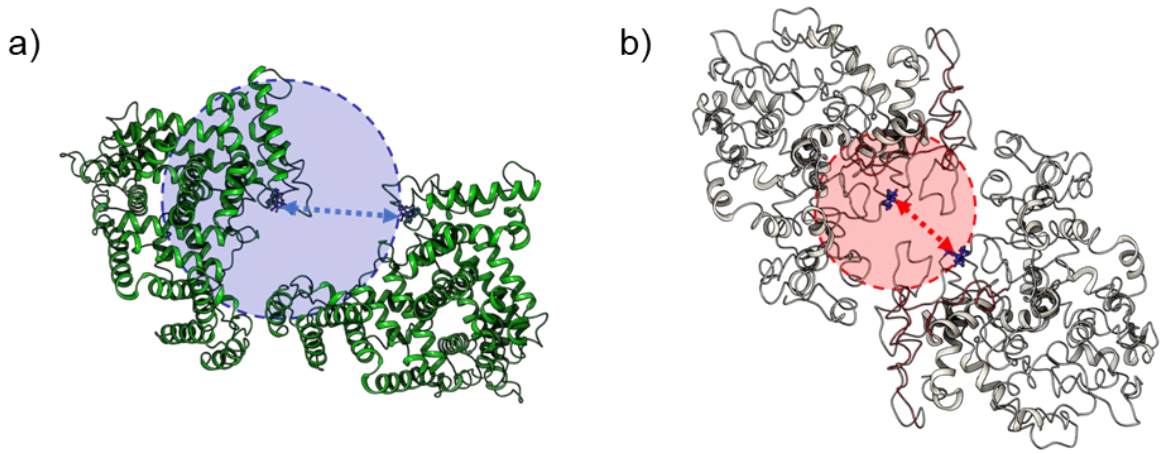

Figure VI.3: Computer model of excluded volume and steric restrictions of (a) native and (b) partially unfolded HSA. (a) shows a snapshot at the start of the MD simulation, while (b) represents the protein after 200 ns of simulation.

Figure VI.4 illustrates the unfolding of HSA within the sugar matrix throughout the MD simulation. The increase in Root Mean Square Deviation (RMSD) between Tyr^{30} and Val^{40}, located around the spin label (Figure VI.4a), indicates significant structural changes before and after the simulation. Additionally, the solvent accessible surface area (SASA) for this sequence section expands during the simulation, reflecting increased exposure within the sucrose matrix and therefore also suggesting unfolding (Figure VI.4b). This comes with an increase in the number of sugar molecules within a 10 Å radius around Cys^{34} from 4 molecules in the condensed native structure to 6 molecules in the last frame representing partially unfolded HSA.

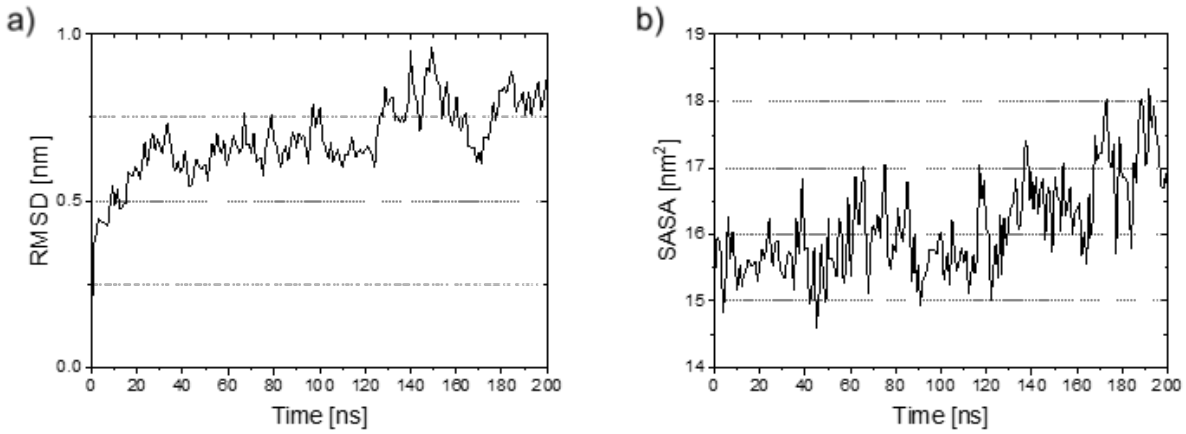

Figure VI.4: a) RMSD evolution of HSA upon unfolding and (b) corresponding SASA of the sequence section between Tyr^{30} and Val^{40} in a sucrose matrix.

VI.5.3 Protein structure preservation and protein vicinity in the solid state using DEER

Conventional protein DEER experimental data reflects the combined effect of two interactions: the intra-protein impact, which arises from interactions between two spin labels within a double-labeled protein (or between single-labeled proteins in a dimer), and the inter-protein impact, which results from interactions with multiple randomly distributed neighboring proteins. The excluded volume effect is generally not considered in protein DEER data processing and is typically regarded as small. However, for a large 11 nm protein, neglecting the protein size (and assuming a dimensionless molecule) introduces a distortion of approx. 20-25% of the inter-protein impact (VI.8.11). Therefore, 11 nm HSA shows a significant change in DEER signal upon unfolding, especially emphasized by the high protein concentrations (by structural biology standards) typically used in lyophilization.

DEER concentrations can be used to calculate the vicinity between proteins simplified as model spheres containing a spin label on their surface (VI.8.4). Larger molecules (>3 nm) show detectable changes in the inter-protein DEER signal, with these changes increasing cubically as the size increases (SI Figure VI.4). In contrast, molecules smaller than 3 nm are indistinguishable from zero-size particles. Unfolding around the spin label leads to less excluded volume and closer possible distances between the spin labels on two different molecules (Figure VI.3). On a semi-log scale, the (partially) unfolded HSA shows a linear signal decay, as seen for 84 g/L. In contrast, the presence of native HSA is indicated by a negative second derivative dependence between 500 and 2000 ns. On the other hand, HSA dimerization leads to a positive second derivative fast decay in the 0–500 ns range, as reported by Chubarov et al.[33] A mixture of partially unfolded molecules, non-perturbed molecules, and dimerization produces a complex decay pattern. Thus, a three-component fitting model was developed that considers those DEER influencing factors to interpret the DEER curves.

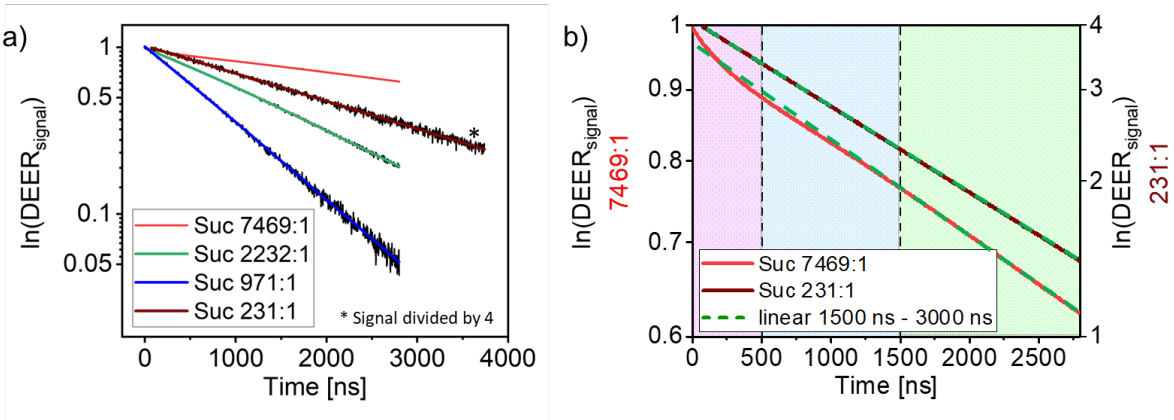

Figure VI.5: (a) Overview of measured DEER signals at different molar ratios, illustrating differences in curve shape and decay characteristics. (b) Close-up of the 7469:1 and 231:1 DEER signals, highlighting a complex exponential-like decay attributed to dimerization (purple area), and native folding (blue area). Partially unfolded protein would lead to an exponential decay throughout all areas.

In this model, five parameters are varied: the fraction and concentration of partially unfolded protein, the fraction and concentration of folded protein, and the fraction of dimers within the folded protein (VI.8.5). The sum of the folded and unfolded fractions consistently equaled 1. The fraction of folded (or non-perturbed) HSA determined by DEER is shown in Figure VI.6, while the local concentrations of the folded and unfolded states are discussed in V.8.9 and illustrated in SI Figure VI.13. In the lyophilized samples, the proportion of dimers within the folded HSA fraction was 0.29 ± 0.02 and 0.11 ± 0.05 for molar ratios of 7469 and 2232, respectively, and zero for lower ratios. Changes in the DEER signal shape and decay were investigated depending on the sucrose-to-protein molar ratios in the lyophilizates (Figure VI.5). In a semi-log scale, low sucrose-to-protein molar ratios (231 to 971) show linear behavior in the resulting DEER curves (Figure VI.5a). This indicates that excluded volume sizes smaller than 3 nm and significant unfolding near the Cys^{34} region are present in these highly concentrated formulations. As a result, two labels on separate HSA molecules can reach close vicinity in a 3D space. Interestingly, high sucrose-to-protein molar ratios (2232 and 7469) show a combination of a fast positive, slow negative exponent-like decay and a linear decay (Figure VI.5b).

At high molar ratios of 7496 approx. 50% of the HSA molecules show partial unfolding. This percentage increases with lower sucrose-to-protein molar ratios leading to almost no excluded volume of the protein and 97% of partially unfolded HSA molecules at a molar ratio of 231. Nevertheless, CD measurements show an intact protein native structure after reconstitution and SEC demonstrates that the monomeric state is preserved. Additionally, corresponding glassy calibration samples show a decay consisting of an excluded volume effect (slow negative

exponential-like decay) and a dimerization effect (fast positive exponential-like increase), which was also shown by Chubarov et al. (VI.8.3).[33] Thus, lyophilized samples show structural perturbation compared to non-perturbated samples in the liquid state. Additionally, the observed changes in the HSA structure in the solid state seem reversible.

The HSA structure in the lyophilized state was previously investigated by FTIR.[40,41] Griebenow et al. observed reversible global changes in the α- helices of HSA. Such α- helices exit near Cys^{34} and shield the introduced spin label.[40] The structural loss in the label region leads to an increased exposition of the label to the matrix as seen in the computational simulation. Although reversible upon promptly reconstitution, the changes in protein structure in the solid state may impact the long term protein stability.

Additionally, the HSA size and local concentration information obtained by DEER was used to stereometric estimate the average protein vicinity, respectively, the sugar layer thickness between two protein centers (VI.8.7). A high molar ratio of 7469 shows an average protein vicinity of 21 nm, whereas at a low molar ratio of 231 the protein molecules reach an average vicinity of 2 nm (Figure VI.6). Less vicinity and partial unfolding leading to exposure of hydrophobic parts could favor protein interactions and aggregation in the long term.[6]

We assume that the HSA dimers observed in the lyophilized samples are similar in nature to those present in the liquid state, as demonstrated by Chubarov et al., suggesting that they were likely carried over from the liquid during lyophilization and are not directly related to the lyophilization process itself.[33] Nevertheless, we would like to note the potential of DEER in studying the oligomerization of biologics resulting from lyophilization.

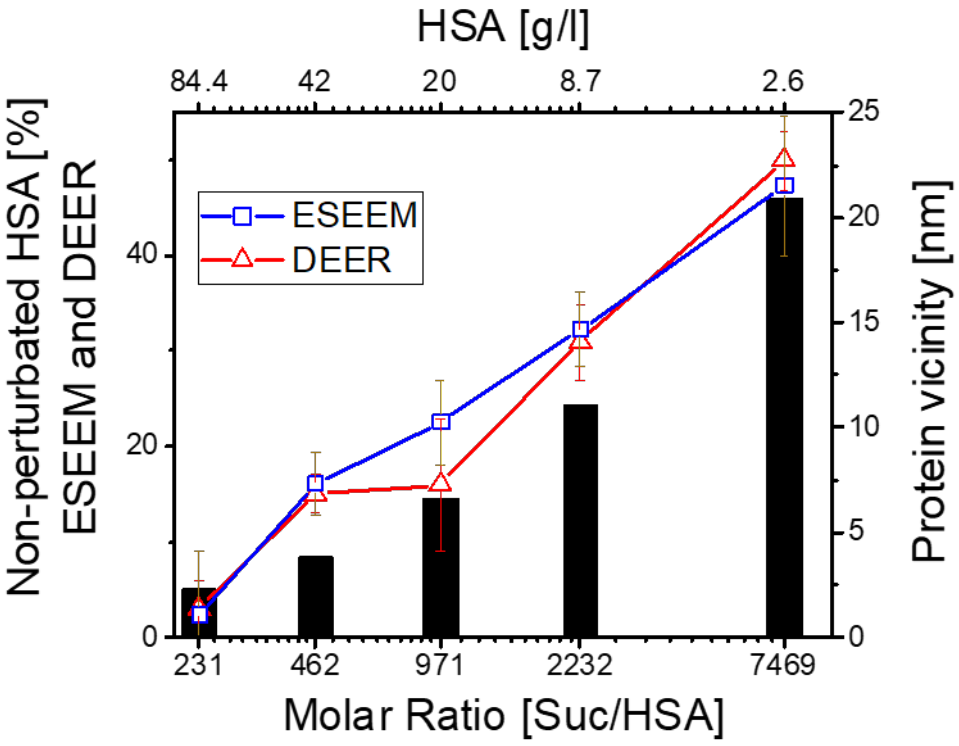

Figure VI.6: Non-perturbed HSA content as determined by DEER (Δ) and ESEEM (□) data at different molar Suc/HSA ratios. Black bars represent protein vicinity at varying Suc/HSA ratios.

VI.5.4 Composition of proteins nearest shell in the lyophilizate using ESEEM

Whereas DEER provides information on protein structure and average protein vicinity, ESEEM analyzes the nearest environment around the label. In the glassy calibration samples, all HSA molecules show non-perturbed structure at all concentrations investigated. Extrapolating this data set leads to a theoretical ESEEM signal amplitude of 52 ns for a non-perturbed HSA in a pure sucrose solid matrix (Figure VI.7).

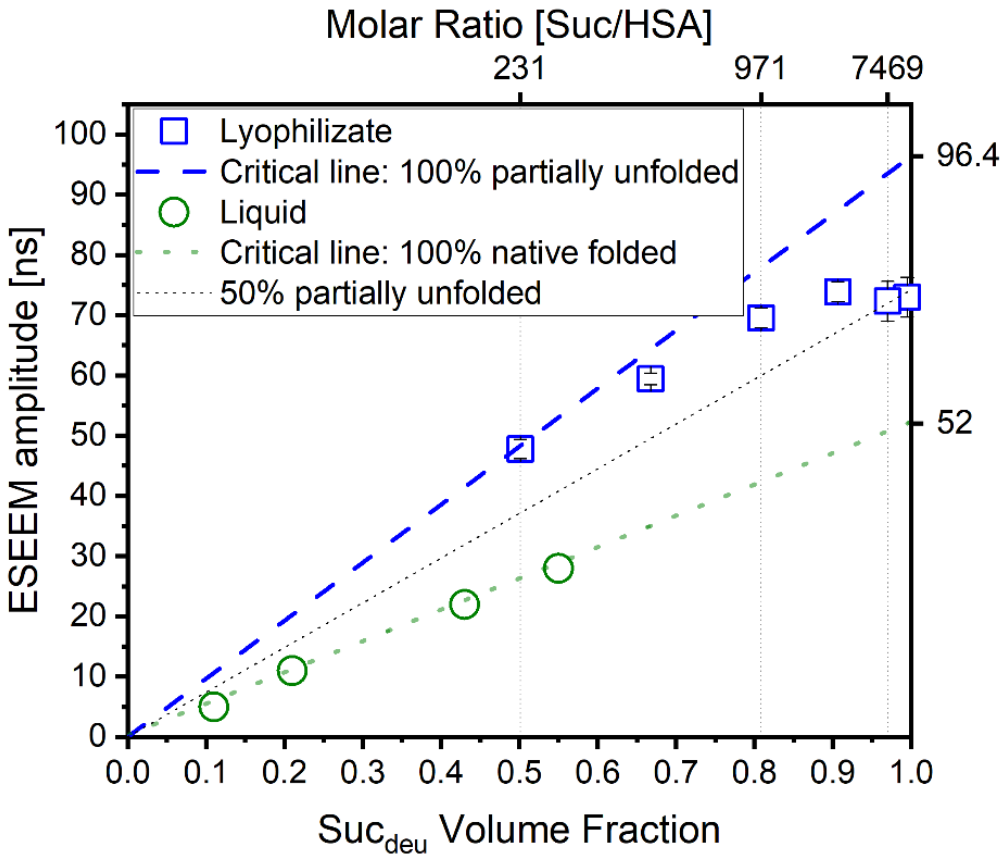

Figure VI.7: ESEEM amplitudes at different deuterated sucrose volume fractions. Glassy calibration liquids (○) show a linear increase in ESEEM amplitude with increasing suc_{deu} volume fractions indicating native structure preservation. Lyophilizates (□) show overall higher ESEEM amplitudes indicating more sugar around the spin label due to structural changes in the protein.

Interestingly, lyophilized samples show higher ESEEM amplitudes with 72 ns at the highest sucrose to HSA molar ratio of 7496. Thus, sucrose is substantially enriched in the proximity of the protein in the lyophilizate. While this observation could correspond to the water replacement theory, the absence of investigation into molecular mobilities and dynamics, such as β relaxations, prevents a definitive interpretation.[19,42,43]

As shown by DEER, a substantial fraction of the HSA molecules is partially unfolded in the lyophilizates. Protein folding can influence the ESEEM signal since a more exposed spin label detects more sucrose in its near environment. We can correlate the ESEEM amplitudes measured for the lyophilizates with the expected ESEEM amplitudes for 100% non-perturbated HSA molecules and 100% partially unfolded HSA molecules (Figure VI.6). The amount of non-perturbated HSA molecules calculated based on the ESEEM results are comparable to the DEER results. Thus, the two independent EPR methods provide similar information on the change of the protein molecules in the lyophilizates (VI.8.8).

To further investigate the influence of protein folding on the ESEEM signal changes, the ESEEM signal of the spin probe TEMPOL was investigated, which acts as a completely accessible spin label (Figure VI.8). Free TEMPOL in solution at a Suc_{deu} volume fraction of 0.55 shows an ESEEM amplitude of approx. 74 ns, compared to 28 ns for the labeled native HSA in solution and 55 ns for the partially unfolded HSA lyophilizate. Thus, the spin label is substantially shielded by the HSA protein structure detecting 2.5 times fewer sucrose molecules. The spin label of partially unfolded HSA molecules could detect approx. 2 times more sucrose than that of native molecules. This is substantiated by the computational simulation indicating an increase in sucrose molecules within 10 nm radius around the spin label by 50% from 4 to 6 upon unfolding. To further understand the local stabilization and to approve or disapprove the water replacement and vitrification theories, $H_2{}^{17}O$ could potentially be introduced into lyophilizates and analyzed by EPR.

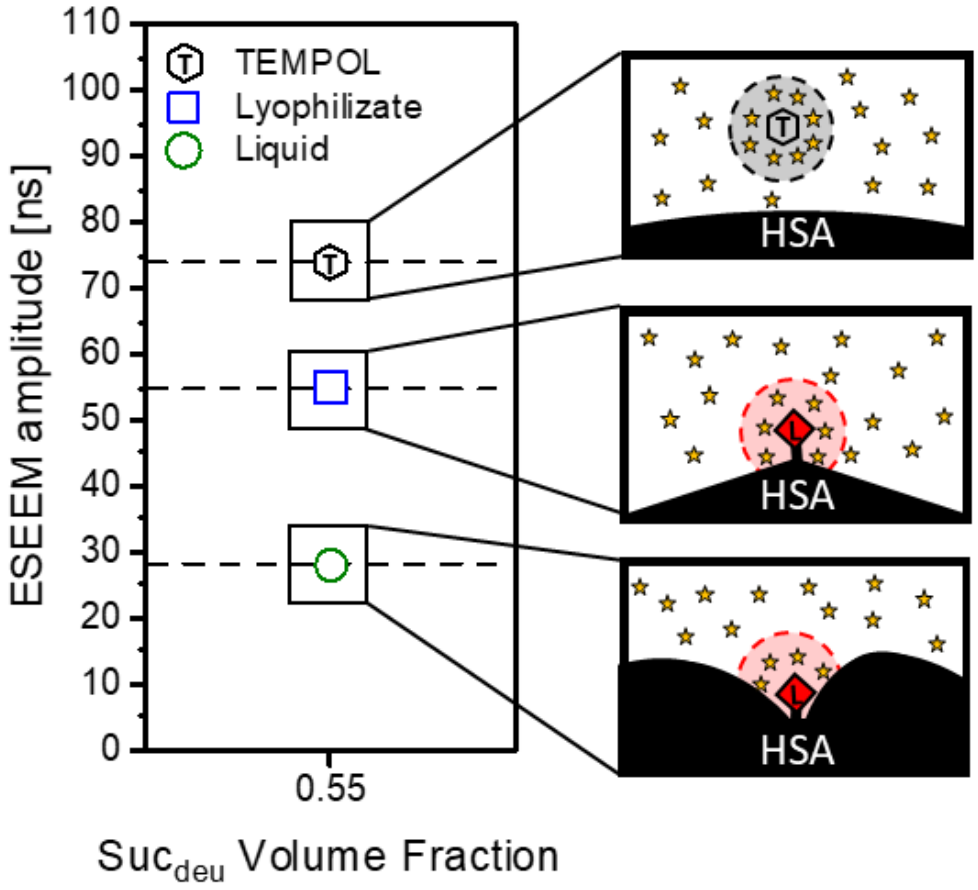

Figure VI.8: ESEEM amplitudes at a deuterated sucrose volume fraction of 0.55. The glassy calibration liquid (○) shows an amplitude of 28 ns, while the lyophilizate (□) reaches 55 ns. The free spin label TEMPOL (Ⓣ) reaches 74 ns. Liquid HSA features a buried label (◈), while lyophilized HSA exposes the spin label (◈) on the surface. TEMPOL experiences no steric hindrance.

VI.6 Conclusion and Outlook

The aim of this study was to establish EPR as a method for solid state analysis of freeze-dried biologics and to gain novel information on the local environment and the folding state of proteins in a sugar matrix as well as ultimately protein stabilization mechanisms. To this end, we used DEER and ESEEM modes in EPR to analyze lyophilized HSA tagged with the spin label MTSSL to investigate molar ratios of deuterated sucrose to HSA at 7469, 2232, 971, 462, and 231 to gain insights into the protein structure preservation and the molecular environment surrounding the spin label. DEER measurements revealed that approximately 50% of HSA molecules exhibited structural perturbation even at a high sucrose to HSA molar ratio of 7469. At lower molar ratios, such as 231, up to 97% of the HSA molecules displayed partial unfolding in the solid state. Interestingly, changes in protein structure were not detectable after reconstitution, underscoring the importance of investigating the solid state itself. Additionally, the vicinity of the protein to its surrounding proteins decreased with lower sucrose content, from 21 nm at a ratio of 7469 to just 2 nm at a ratio of 231. ESEEM analysis showed an increased sucrose concentration near the protein in lyophilized samples compared to liquid ones, likely due to unfolding around the spin label. We showed that EPR can measure protein distances, the composition of the protein environment, and quantify the percentage of unfolded molecules using both ESEEM and DEER techniques. The demonstrated ability to see oligomerization in the lyophilizate is tempting for further studies of lyophilization-induced biologics oligomerization. Thus, EPR provides novel detailed information about protein stabilization in the solid which could not be gained by analytics in liquid. However, our findings are limited to the specific labeling position and the immediate surrounding region. Future studies could benefit from using double-labeled proteins to measure intramolecular distance changes, offering deeper insights into the unfolded state. Additional information regarding the water replacement hypothesis and the influence of additional excipients could be gained using other deuterated excipients or ^{17}O water. Ultimately, whether the protein unfolding and the molecular environment in the solid state correspond with long-term stability parameters like aggregation, deamidation, and oxidation needs to be studied.

VI.7 Acknowledgments and Disclosures

The authors thank Dr. Johann Klare from the University of Osnabrueck for providing the EPR systems used in this study. The authors thank the Group of Prof. Dr. Franz Bracher and especially Karl Sauvageot-Witzku from the chair of Pharmaceutical and Medicinal Chemistry from the Ludwig-Maximilians-Universität München who helped to generate deuterated sucrose and Dr. Lars Allmendinger from the Department of Pharmacy from the Ludwig-Maximilians-Universität München who evaluated deuteration efficiencies by NMR. The authors thank Jonas Binder from the group of Prof. Dr. Wolfgang Frieß who performed the computational simulation of protein unfolding. The authors thank Albumedix, Nottingham, United Kingdom for kindly providing the HSA used in this work. This work was supported, in part, by the Humboldt Research Fellowship. Nikolay Isaev acknowledges the core funding from the Russian Federal Ministry of Science and Higher Education (FWGF-2021-0003).

VI.8 Supporting information

Theoretical background on DEER and ESEEM spectroscopy measurements. Method of creation of glassy references. Details in DEER data interpretation. Preparation and fitting of lyophilized samples. Fitting of DEER curves. Calibration of ESEEM data. Calculations on inter-protein vicinity. Correlation of ESEEM and DEER signals. Evaluation of microheterogeneity in the solid state. 84g/l DEER curves. The magnitude of intra-protein distortion.

VI.8.1 Introduction to DEER and ESEEM spectroscopy

Below, we will briefly outline the basics of the DEER method, which measures the concentration and distances between electron spins, such as spin labels bound to biomolecules or dissolved spin probes.

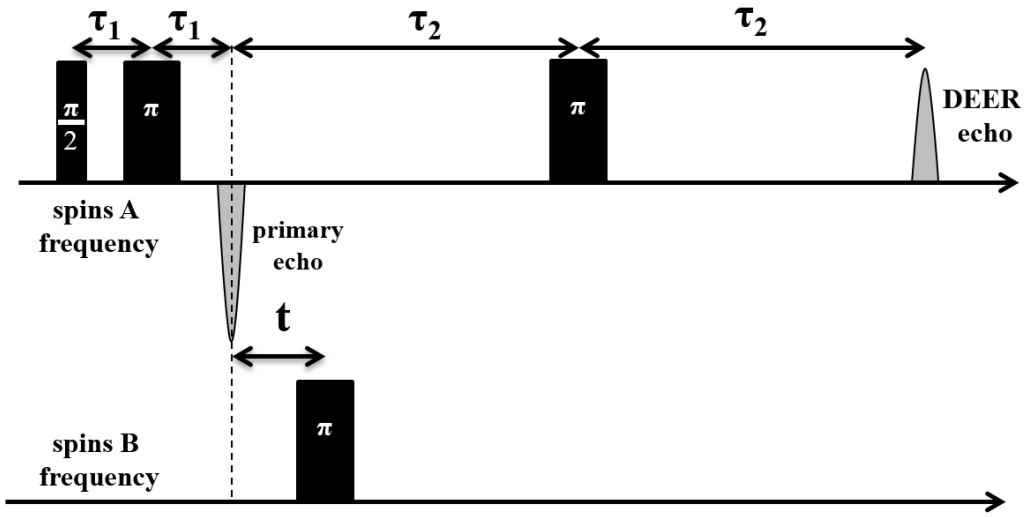

SI Figure VI.1: The figure shows the DEER pulse sequence. The experimental dependence of the DEER echo integral is measured as a function of t.

The main interaction between two electron spins at distances greater than 1.6 nm is referred to the dipole-dipole interaction. Its energy splitting can be written as:

$$E_{dd} = \hbar\Delta\omega_{dd} = \pm\frac{\gamma_e^2\hbar^2}{r^3}(1 - 3\cos^2\theta),\ \Delta\omega_{dd} = \frac{52MHz}{r(nm)^3}(1 - 3\cos^2\theta),$$

where is the frequency of dipole-dipole interaction, is the electron spin gyromagnetic ratio, is an interspin distance and denotes the angle between the direction of the external magnetic field and the interspin vector.

In pulsed EPR methods, discrepancy in frequencies leads to a phase difference in the time domain, which manifests as a modulation of an echo signal. In the DEER experiments performed here, a sequence of four microwave (MW) pulses with two frequencies is used to reveal (SI Figure VI.1). The echo amplitude is then determined by:

$$Echo(t) = \langle 1 - P_B(1 - \cos(\Delta\omega_{dd}t)) \rangle_{r,\theta},$$ **SI Eq. VI.1**

where P_B indicates the fraction of spins flipped by a π-pulse of frequency B, and T represents the time interval between the primary echo and the π-pulse of frequency B.[44]

In the scenario of a low-concentrated powder of biradicals featuring an isotropic orientation distribution of the interspin vectors, we can neglect the interaction between the biradicals and only focus on the intra-biradical interaction. Consequently, the DEER echo will show an oscillatory pattern with depth , and the quantity of observed oscillations will depend on the ratio between the mean distance and the width of the distance distribution (SI Figure VI.2a).

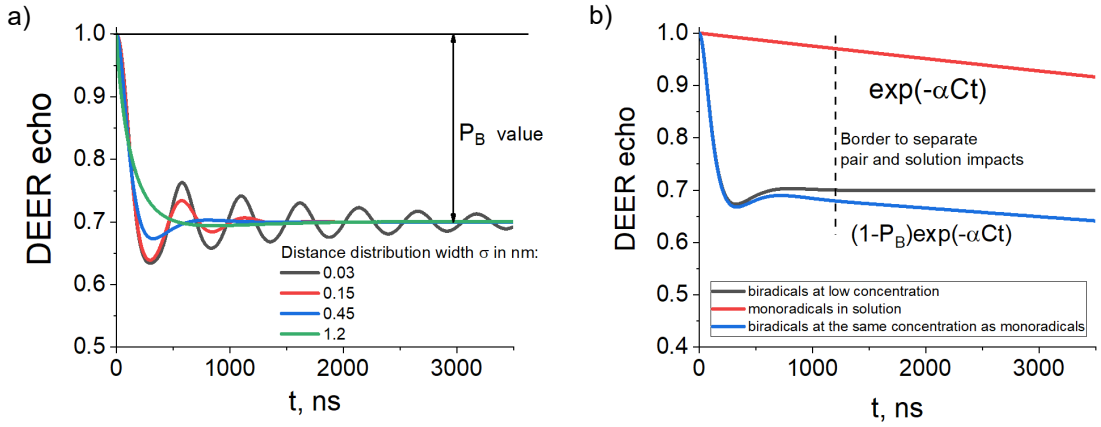

SI Figure VI.2: (a) The dependence of the DEER echo intensity calculated using Eq. (1) for biradicals (or dimers) with a distance of 3 nm between electron spins and a Gaussian distribution of distances with varying widths. More pronounced modulation reflects narrower distribution widths. (b) DEER echo behavior for monoradicals in solution (Eq. 2), diradicals at low concentrations (Eq. 1), and diradicals at the same spin concentration as monoradicals (Eq. 3). The dotted line indicates the lower limit on the curve, beyond which the DEER echo can be considered to decay exponentially.

In the scenario where point size effects are taken into account for uniform distributed spins in a solution in SI Eq. VI.1 should be averaged over all possible pairs, distances, and orientations, including simultaneous flips of several spins in the vicinity of the considered one.[45] This consideration results in an exponential decay:

$$Echo(t) = exp(-\alpha Ct) \qquad \textbf{SI Eq. VI.2}$$

where C represents the local concentration (*see next section*) and α is a spectroscopic parameter proportional to P_B.

When dealing with double-labeled molecules at relatively high concentrations, we will simultaneously observe both contributions, the intra- and inter-molecular interactions, as a product:

$$Echo(t) = exp(-\alpha Ct)\langle 1 - P_B(1 - \cos(\Delta\omega_{dd}t))\rangle_{r,\theta} \qquad \textbf{SI Eq. VI.3}$$

The typical approach to distinguish these contributions is by recording DEER traces for a duration sufficient for the intra-molecular modulation to fade out. This enables the approximation of the remaining trace with an exponential decay (SI Figure VI.2b).

The DEER echo decays exponentially when considering uniform distributions of sizeless or relatively small molecules like TEMPOL. However, solutions containing larger molecules like proteins introduce excluded volumes, altering the probability distribution of inter-molecular distances compared to sizeless particles. This deviation in distance distributions results in non-exponential DEER decay.[23] The shapes of these decays were calculated for various label locations on a protein, including both surface-exposed and buried positions.[24] We calculated DEER traces for spherical proteins with spin labels located on the surface (SI Figure VI.3, SI Figure VI.4).

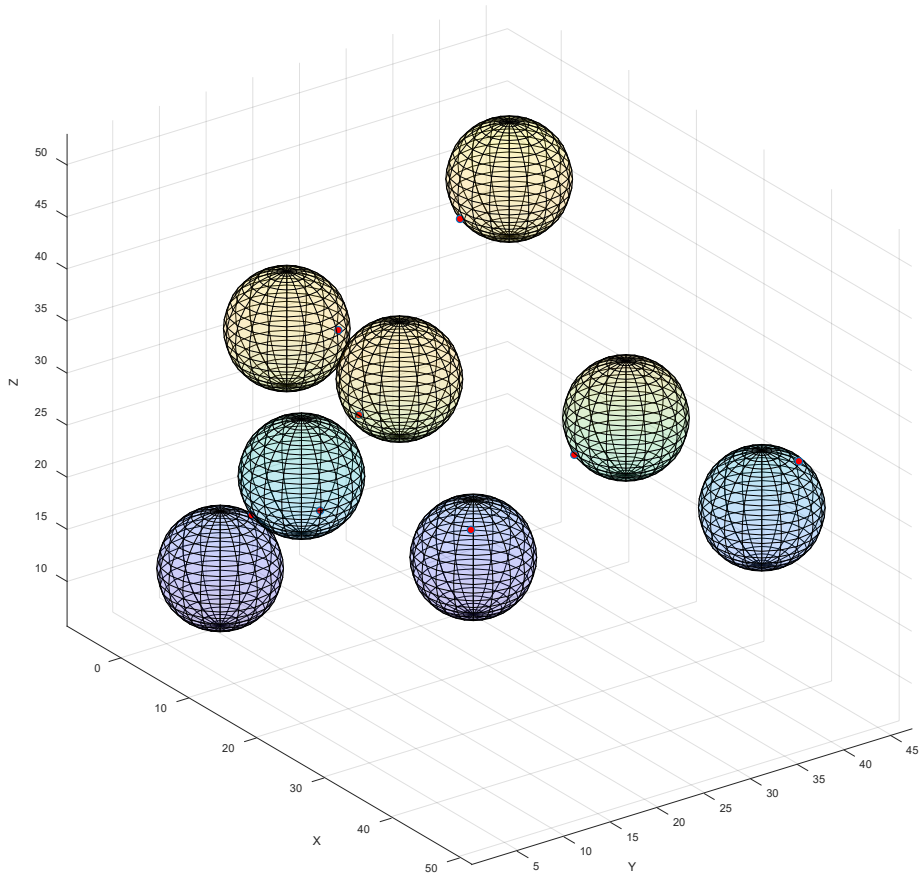

SI Figure VI.3: Illustration of spheres containing a surface spin label (highlighted in red) with a radius of 5.5 nm at a concentration of 0.1 mM within a 50 nm cube.

These calculations involved randomly placing a specific quantity (sufficient to attain a desired concentration of 0.3 mM) of spheres of a predetermined radius into a cube measuring 130 nm in size, ensuring no intersections occurred.

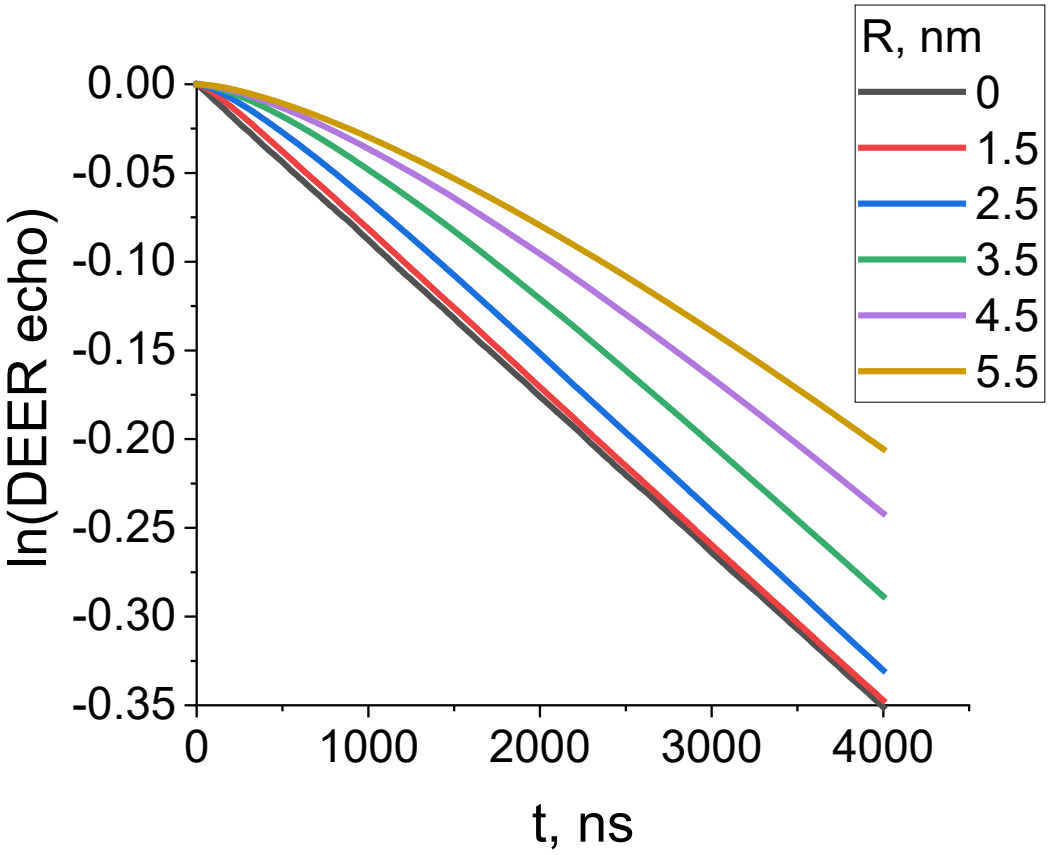

SI Figure VI.4: The influence of the excluded volume on the shape of DEER traces. Calculated DEER traces are shown for a random distribution of spherical molecules with different radii (R), each carrying a single spin label on the surface. These traces are compared with a theoretical molecule with R = 0. It can be seen that for a sphere R < 1.5 nm the excluded volume effect will be difficult to detect due to the insignificant difference with R=0. The concentration was held constant at 0.3 mM.

When dealing with a double-labeled proteins or dimers, we observe additional modulation, which conforms to the equation in SI Eq. VI.3 but involves a corresponding function instead of an exponential decay (SI Eq. VI.4).

$$Echo(t) = Echo_{spheres}(t, R) \cdot \langle 1 - P_B(1 - \cos(\Delta\omega_{dd} t)) \rangle_{r,\theta} \qquad \textbf{SI Eq. VI.4}$$

ESEEM is a 3-pulse single-frequency method, enabling the detection of nuclear spins situated 10 Å away from unpaired electrons by applying microwave pulses to electron spins only (SI Figure VI.5).[46]

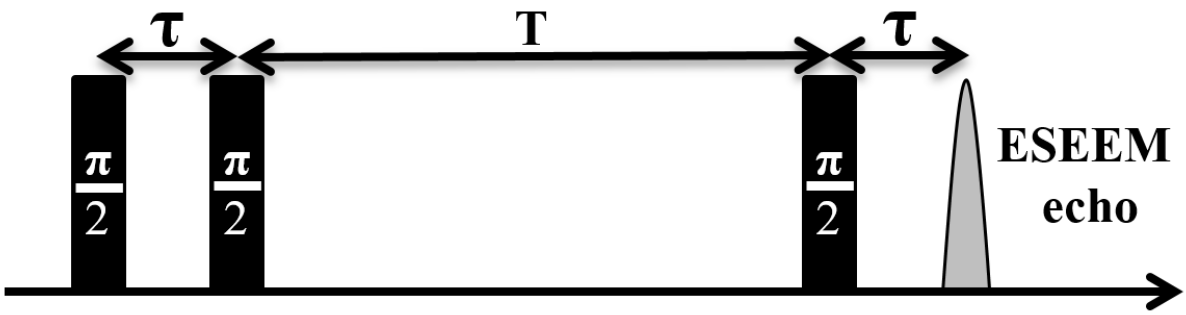

SI Figure VI.5: The figure shows the ESEEM pulse sequence. The experimental dependence of the ESEEM echo integral is measured as a function of T.

Like DEER, spectral characteristics in the time domain are assessed by analyzing the time dependence of the spin echo. Since nuclear and electron spins are coupled by anisotropic hyperfine interaction, electron spins manipulations via microwave pulses can also flip nearby nuclear spins. These nuclear spin flips induce a modulation of the echo amplitude, reflecting the nuclear Larmor frequencies, as shown over time in the ESEEM echo amplitude by varying t (SI Figure VI.6a).

To analyze the spectral shape and its intensity we normalize the echo signal, Echo(t), by a biexponential fit, Fit_{biexp}, (SI Figure V.6b):

$$Echo_{norm}(t) = Echo(t)/Fit_{biexp} - 1 \qquad \textbf{SI Eq. VI.5}$$

The following Fourier transformation produces the ESEEM spectral density in units of nanoseconds, since we employed an experimental time step of 4 ns as dt; we consider an absolute value (SI Figure VI.6c).

$$ESEEM\ spectral\ density(f) = \left| \int_{t_1}^{t_2} Echo_{norm}(t) e^{-2\pi i f(\tau + t)} dt \right| \qquad \textbf{SI Eq. VI.6}$$

This normalization method enables the comparison of ESEEM spectra regardless of signal intensity and the specific spectrometer used.[36].

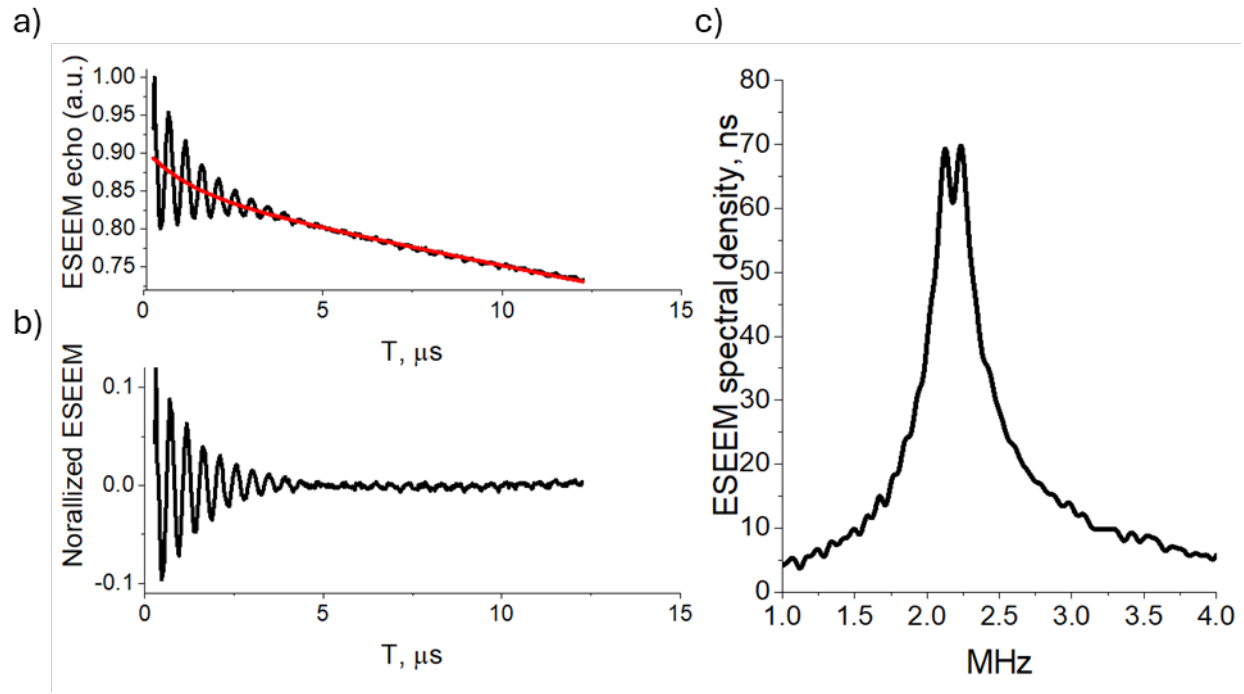

SI Figure VI.6: (a) Experimental ESEEM echo modulation and its biexponential fit of a lyophilizate containing 20 g/l HSA and 100 g/l deuterated sucrose. (b) Normalized ESEEM echo modulation calculated by SI Eq. VI.5. (c) Absolute Fourier transformation derived from the normalized ESEEM curve shown in (b) using SI Eq. VI.6.

VI.8.2 Creation of glassy reference solutions from freeze-dried sugar placebos

For sucdeu calibration, 200 mg of lyophilized sucdeu/suc mixtures were reconstituted with a 1 g/l HSAlbl stock solution in HPW. Considering the density changes of the resulting highly concentrated sucrose solution and given a 65:35 mass-based mix of lyophilizate and protein stock solution, the final volume and protein concentration in the reference solution can be calculated according to SI Eq. VI.7-SI Eq. VI.9.

$$m_{protein\ stock} * \rho_{protein\ stock} = V_{added\ protein\ stock} \quad \textbf{SI Eq. VI.7}$$

$$c_{protein\ stock} * V_{added\ protein\ stock} = m_{protein} \quad \textbf{SI Eq. VI.8}$$

$$V_{final} = {}^{m_{final}}/_{\rho_{65\ wt\%\ sucrose}} \rightarrow {}^{m_{protein}}/_{V_{final}} = c_{final\ protein} \quad \textbf{SI Eq. VI.9}$$

For HSA_{lbl} calibration, 100 mg non-deuterated sucrose lyophilizates were reconstituted with protein stock solutions of different concentrations based on SI Eq. VI.7-SI Eq. VI.9.

VI.8.3 Interpretation of HSA DEER data for glassy HSA/sucrose samples

We hypothesized that HSA remains folded in water/sucrose glass and should exhibit an excluded volume effect. We observe non-exponential DEER decays for 0.86 g/l and 2.6 g/l HSA (SI Figure VI.7a-c). This indicates the presence of excluded volumes (SI Figure VI.4). The dipolar modulation observed suggests the presence of HSA dimers, consistent with previous findings by EPR of HSA in water/glycerol mixtures (SI Figure VI.2).[33] Approximately 30% dimers were detected at 3 g/l HSA.

To differentiate between the impacts of HSA dimers and excluded volume background on DEER data, we followed the standard procedure outlined in SI Figure VI.2b. We estimated that after 1600 ns, the influence of dimers would remain constant and used the curve from 1600 to 3300 ns to fit the size of the sphere representing excluded volume. The best fit was achieved for a sphere radius of 5.5 nm. The resulting fit curves and residuals are illustrated in SI Figure VI.7d-f.

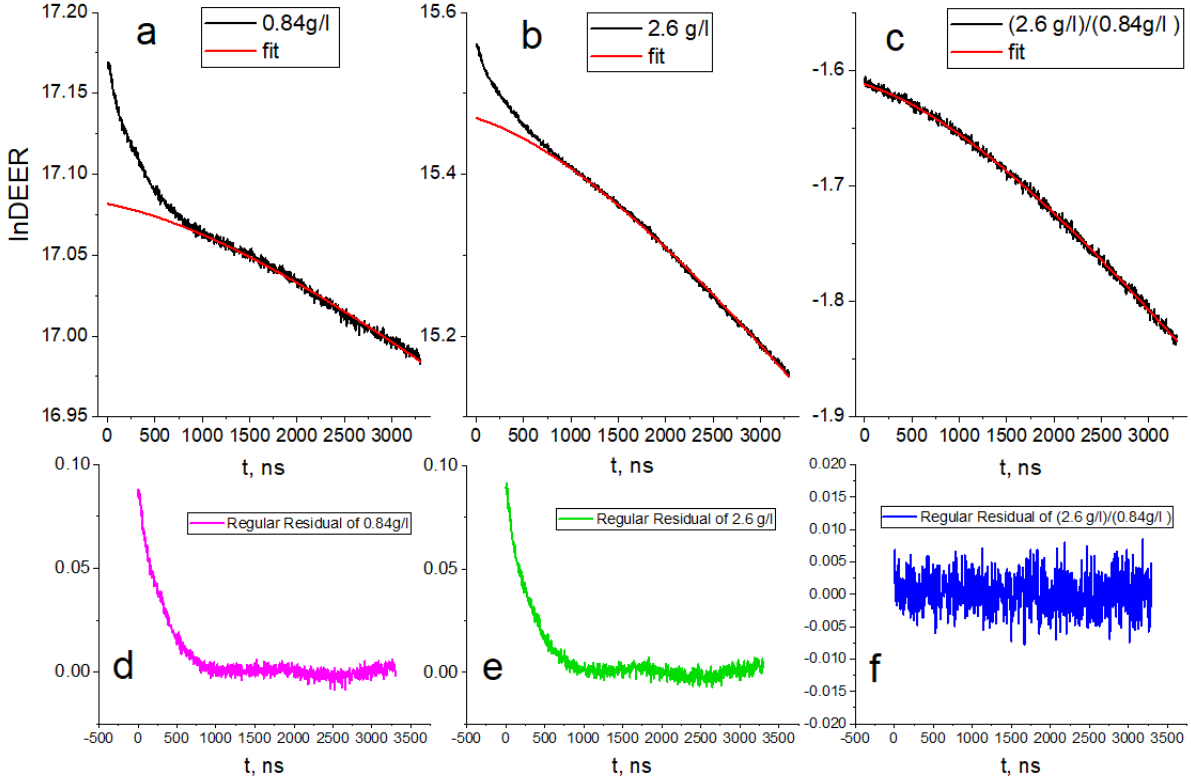

SI Figure VI.7: DEER curves in a semi-log plot for glassy HSA/sucrose solutions for 0.86 g/l and 2.6 g/l HSA, an excluded volume fit for a sphere with R=5.5 nm (a,b,c) and corresponding residuals (d,e,f).

Similar residuals after fitting indicate that the structure and fraction of dimers are consistent for both concentrations. In this scenario, we can extract a pure background contribution by dividing the curve for 2.6 g/l by the curve for 0.86 g/l (SI Eq VI.4).[47]

We were able to analyze the resulting curve over a wider range of 0–3300 ns, enabling us to refine the fit using an excluded volume model where the label is immersed 10% of the radius in a sphere with R = 5.5 nm. This correlates with the shape of HSA and the location of the Cys^{34} label on its dip side (SI Figure VI.8).

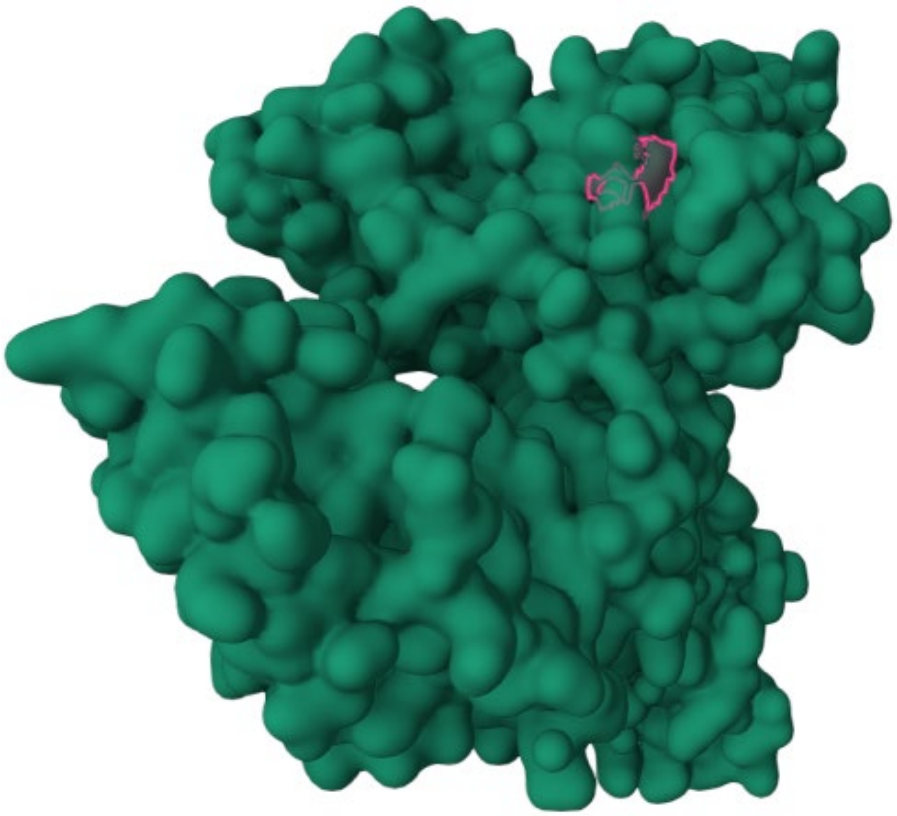

SI Figure VI.8: The shape of HSA and Cys^{34} location according to the 6M4R PDB structure.

VI.8.4 Preparation and fitting of lyophilized HSA samples

The lyo samples exhibited a more complex DEER behavior due to additional impacts like partially unfolded HSA. To make multi-component fitting easier on DEER curves of different lengths and time steps, we used analytical functions obtained from experimental data fitting instead of the raw experimental data.

The impact of dimers on DEER (SI Figure VI.7a-c) was modeled by an exponential decay y0+A*exp(t/t0) (SI Fig. 10). The fitting parameters are presented in SI Table VI.1. However, the resulting residual 0.5% DEER modulation (SI Figure VI.7d-f) was not fitted for glassy samples and lyo cakes with low HSA content (SI Figure VI.12a). We decided not to use a more detailed fit

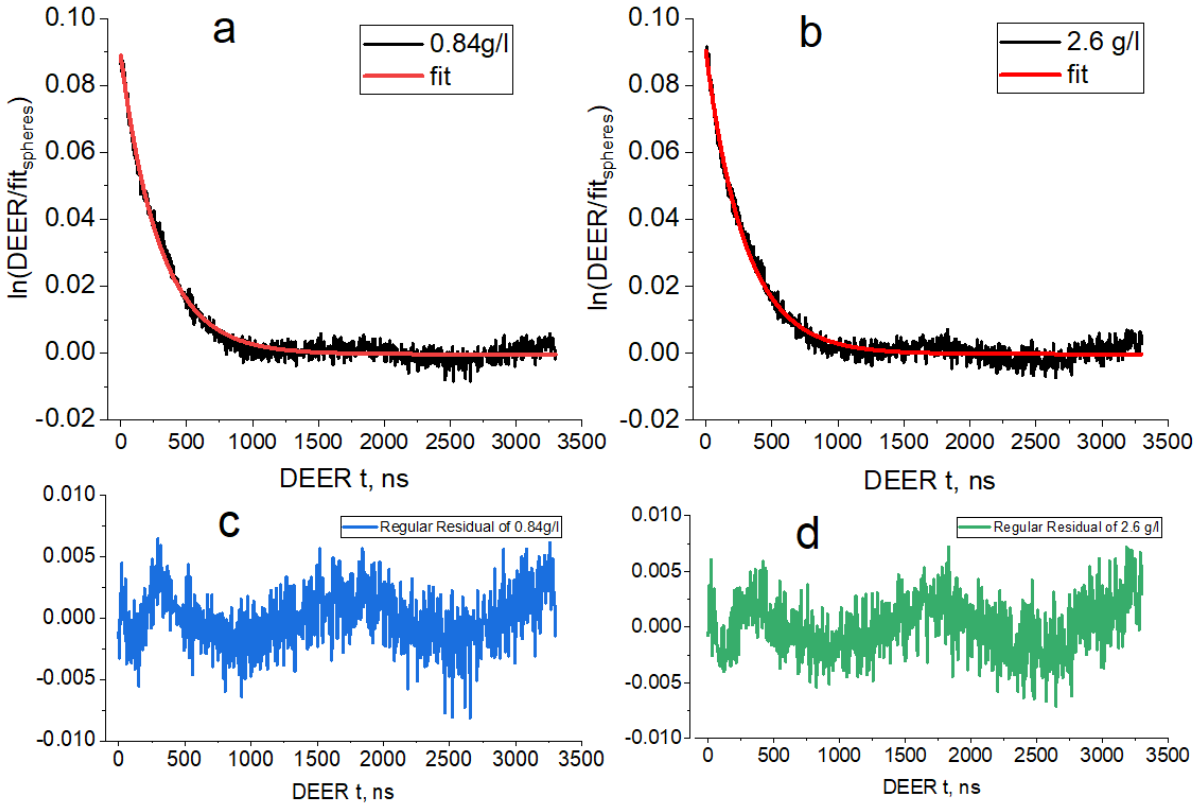

SI Figure VI.9: Exponential decay fitting of the dimer impact for 0.84g/l and 2.6 g/l in glassy samples (a,b) and their fir residual (c,d).

SI Table VI.1: Fitting parameters of the exponential decay of SI Figure V.10.

c	y0	A	t0
0.84 g/l	-0.00035	0.089	295
2.6 g/l	-0.00031	0.091	297

The excluded volume impact of spheres was fitted using a combination of linear and power functions called Shah functions in OriginLab, represented as

$$\text{Shah}(x) = a+b*x+c*d^{x/1000}.$$

The fit for the case of a label on the sphere's surface is depicted in SI Figure VI.11, and the fitting parameters are shown in SI Table VI.2. We decided to provide the surface spin label parameters in this publication so that other researchers can use them as a more general reference, instead of specifically for spin labels buried at a depth of 10%. This allows for easier comparison and application of the results.

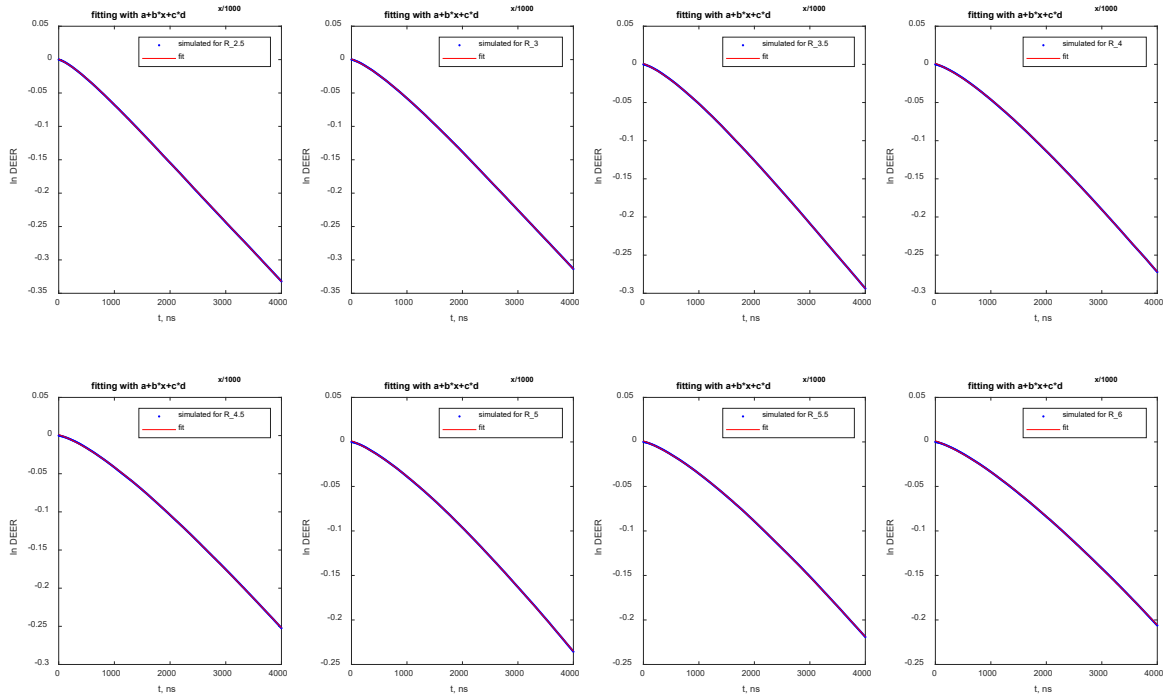

SI Figure VI.10: Shah function fitting of the logarithmically simulated DEER signal for spheres with an excluded volume of a specific size.

SI Table VI.2: Parameters obtained from fitting the logarithmically simulated DEER signal for spheres with an excluded volume of a specific size.

R, nm	a	b	c	d
0	-	-8.785E-05	-	-
2.5	0.0236	-8.90E-05	-0.0231	0.101
3	0.0423	-8.89E-05	-0.0413	0.269
3.5	0.0539	-8.67E-05	-0.0527	0.355
4	0.0719	-8.51E-05	-0.0705	0.466
4.5	0.0720	-8.01E-05	-0.0706	0.472
5	0.0830	-7.78E-05	-0.0817	0.537
5.5	0.0782	-7.27E-05	-0.0770	0.534
6	0.0820	-6.98E-05	-0.0807	0.570

VI.8.5 Fitting DEER curves using a model for folded and partially unfolded HSA

Lyophilized HSA samples showed different DEER curves, for instance, a straightforward exponential decay for HSA at 84 g/l. In contrast, the DEER curve at 2.6 g/l displayed a more complex mixture of exponential decay, non-exponential decay due to excluded volume effects, and modulation caused by dimers.

To model all these features, we used a universal fitting function based on the dimer impact (SI Table VI.1) and the Shah function (SI Table VI.2), with parameterization provided in VI.8.4:

DEER fitting function (R,t) = $\text{fraction}_{\text{unfold}}$ * exp(t*C_{unfold}*Shah(R=0,t)) + $\text{fraction}_{\text{folded}}$ * exp(t*C_{unfold}*Shah(R=5.5nm,t)*exp($\text{fraction}_{\text{birad}}$ * 0.27*(exp(-t/296)-1))

This function includes the sum of folded and partially unfolded HSA molecules at different concentrations, along with the effect caused by dimers on the folded fraction. With P_b=0.27 from the DEER setup, we normalized $\text{fraction}_{\text{birad}}$ by 0.27. The resulting approximation showed the same quality across all samples (SI Figure VI.11).

With this universal fit, we can separately determine the local concentration of folded and partially unfolded HSA, allowing us to observe the behavior of micro heterogeneities. Similar protein heterogeneities were previously observed at the ice/freeze-concentrate interface.[48]

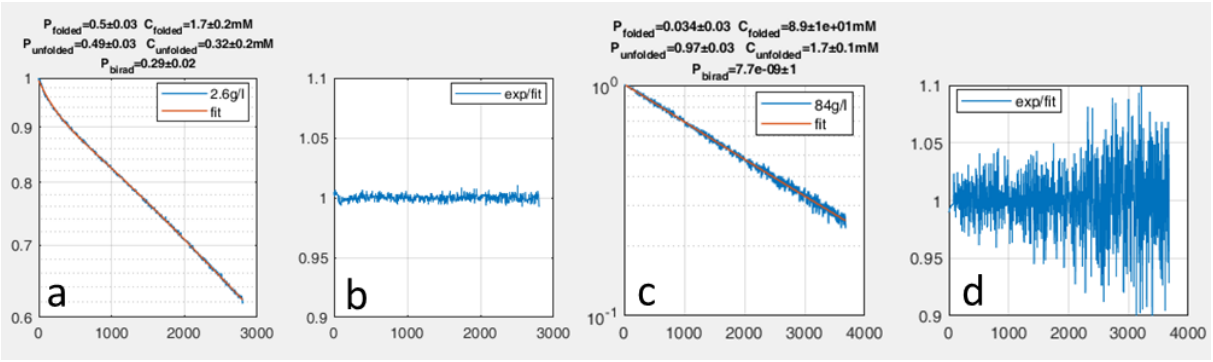

SI Figure VI.11: Exemplary logarithmic DEER signal for lyophilizates containing 2.6 g/l and 84 g/l HSA, with corresponding fitting curves (a, c) and residual curves (b, d).

VI.8.6 Calibration line of ESEEM

ESEEM calibration was conducted using mixtures of HSA and sucrose in a glassy liquid. Ratios of 20%, 40%, 80%, and 100% deuterated to non-deuterated sucrose were employed to detect various ESEEM amplitude heights (SI Figure VI.12). The intensity of the ^{2}H ESEEM peak varied proportionally with the deuterated sucrose fraction in the total sucrose content.

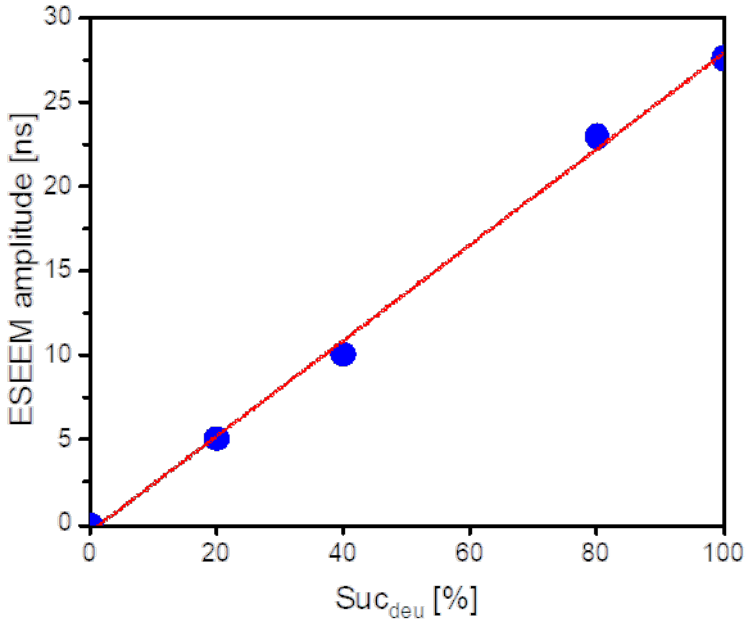

SI Figure VI.12. Calibration line of ESEEM signal. The resulting ESEEM amplitudes of HSA_{lbl} are plotted against the different Suc_{deu} [%] (blue). The calibration line is shown in red.

VI.8.7 Inter-protein vicinity calculation

We estimated average inter-protein vicinities (IPV) via DEER by simplifying the maximal volume occupied by one protein molecule within the freeze-dried matrix (V_{max}) (SI Eq. VI.10)

$$V_{max} = {V_{protein}}/{Volume\ Fraction_{protein}} \approx {(Size_{protein})^3}/{Volume\ Fraction_{protein}} \quad \textbf{SI Eq. VI.10}$$

For example, in a sample with a Volume Fraction$_{protein}$ of 0.1 (equivalent to 10%) and a $V_{protein}$ of 1 nm^3, the resulting V_{max} would be 10 nm^3, indicating that, on average, one protein can be found within every 10 nm^3. The size of this V_{max} can be described as outlined in SI Eq. VI.11 and represents the average distance between the centers of two proteins:

$$Size_{V_{max}} = {V_{max}}^{1/3} \approx {Size_{protein}}/{Volume\ Fraction_{protein}}^{1/3} \quad \textbf{SI Eq. VI.11}$$

The average distance between two protein surfaces can then be estimated as in SI Eq. VI.12:

$$IPV = Size_{V_{max}} - Size_{protein} = Size_{protein}({Volume\ Fraction_{protein}}^{-\frac{1}{3}} - 1) \quad \textbf{SI Eq. VI.12}$$

In the case of the highest HSA content of 84 g/l, the distance between the surfaces of the proteins will be:

$$IPV = 11nm\left(0.5^{-\frac{1}{3}} - 1\right) = 2.5nm$$

SI Table VI.3: Calculated distances of HSA molecules at different volume fractions.

g/l	protein vol.frac.	distance by formula
2.6	0.02971	23.27053
8.7	0.09294	12.52187
20	0.19065	7.556694
42	0.33095	4.468819
84	0.49732	2.523494

VI.8.8 Correlation of ESEEM and DEER signals

By correlating the DEER and ESEEM signals, it was possible to extract folded HSA % from the ESEEM data. We proposed that the measured ESEEM amplitude, h, is a sum of folded and unfolded HSA ESEEM signals normalized by the deuterated sucrose fraction.

$$h = Suc_{Volume\ Fraction} * \left(52ns * \%_{folded}DEER + 96.4\ ns * \%_{unfolded}DEER\right) \qquad \textbf{SI Eq.VI.13}$$

$h_{folded\ HSA}$= 52 ns was obtained by extrapolating ESEEM values of HSA in glassy liquid (see Figure VI.6 lower line). The value of $h_{partiallyunfolded\ HSA}$= 96.4 ns was obtained for the 87 g/l sample using Eq. 1 to match its experimental ESEEM amplitude and 3% non-perturbated HSA fraction obtained by DEER. All other ESEEM values were calculated by the following formula obtained from SI Eq. VI.13.

$$\%_{folded} = (96.4 - \frac{h}{Suc_{Volume\ Fraction}})/44.4 \qquad \textbf{SI Eq. VI.14}$$

VI.8.9 Local concentration microheterogeneity in the solid state

DEER can not only be used to analyze protein distance and folding but also to investigate deviations in the local HSA concentration (VI.8.5). For a comprehensive explanation of local concentration measurements using DEER, please refer to a previous study.[22] HSA can reach at maximum 20.5 mM in the dried state (=pure HSA concentration), which equals 1.35 g/ml.[49] Extrapolating the measured local protein concentrations of partially unfolded HSA molecules and their sucrose volume fractions, a concentration of 20.5 mM is reached for pure HSA indicating an equal distribution throughout the whole cake and their local concentration equals the global concentration (SI Figure VI.13). Extrapolating the measured local protein concentration of non-perturbated HSA molecules leads to an extrapolated line that suggests a 3x higher pure HSA concentration. This suggests an enriched concentration and accumulation of non-perturbated HSA within the lyophilized cake. A freezing induced protein microheterogeneity was also observed by others.[48]

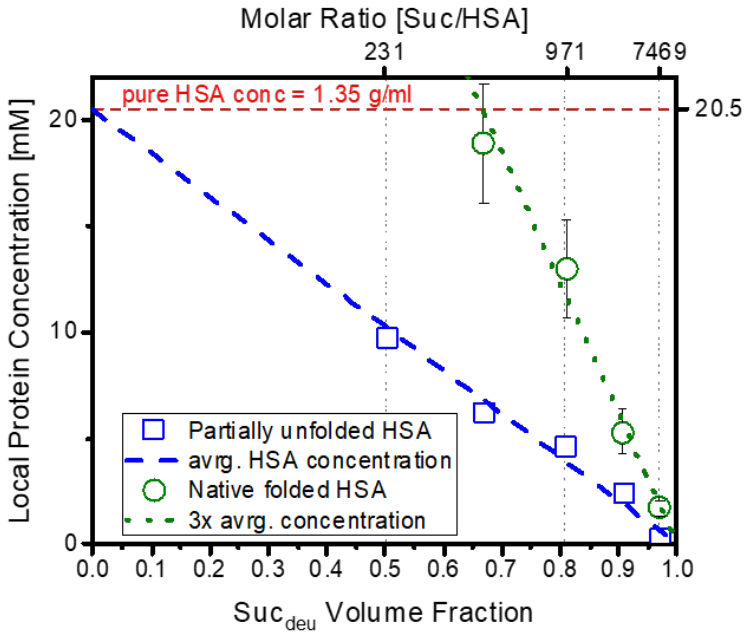

SI Figure VI.13: Local protein concentration in lyophilizates for both partially unfolded and native HSA. When extrapolated, the local concentration of partially unfolded HSA (□) corresponds to 20.5 mM in pure sucrose. In contrast, extrapolating the local concentration of native folded HSA (○) results in approximately 61.5 mM in pure sucrose, indicating a threefold higher local concentration.

VI.8.10 84g/l sample DEER curve reconstitution

Two curves were measured for the highest protein concentration of 84 g/l HSA. Different durations of pump pulses were used (20 ns and 100 ns) to slow down the echo decay. The slightly disturbed beginning of the 100 ns pulse curve was reconstituted using a 20 ns curve at the power of 0.176 to avoid disturbing the DEER curve at low T values.

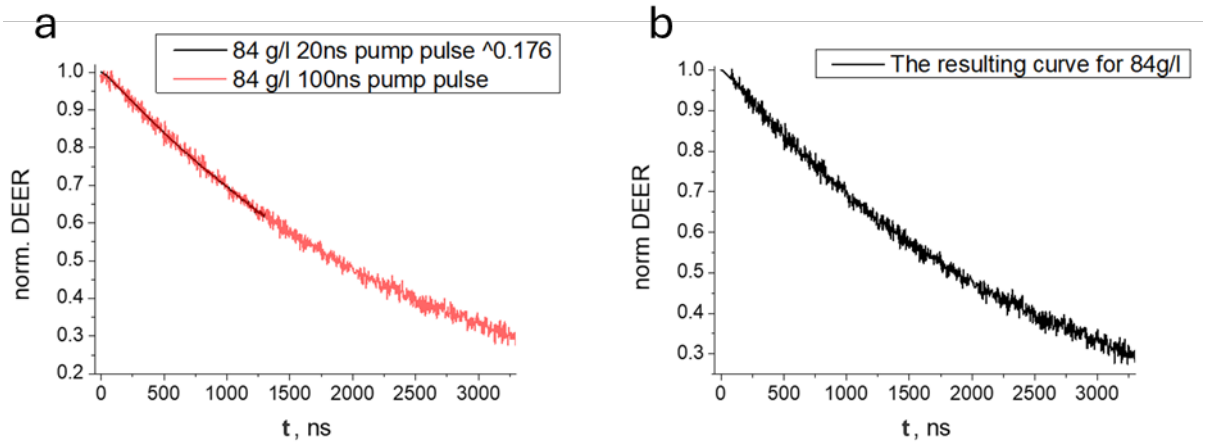

SI Figure VI.14: Superposition of two DEER curves with a 20 ns and a 100 ns pump pulse for the highest HSA concentration of 84 g/l (a) and the curve correction (b).

VI.8.11 Estimating the magnitude of intra-protein impact distortion by neglecting the excluded volume effect in inter-protein impact

SI Figure VI.10 demonstrates the fitting quality for different excluded volumes, which gives us confidence that the 11 nm sphere model works well for HSA. To illustrate the discrepancy between different types of inter-protein impact fitting, we used the 11 nm sphere size (SI Figure VI.7) and applied an exponential decay fitting to the 1000-3300 ns and 1750-3300 ns regions. The DEER curve length of 3300 ns is typical for this experiment. The 1000 ns and 1750 ns positions represent the boundaries of the intra-protein impact decay, after which the inter-protein impact should be approximated using the standard procedure outlined in SI Figure VI.2. The exponential fits differ from the original curve by 0.02 to 0.025 (SI Figure VI.15).

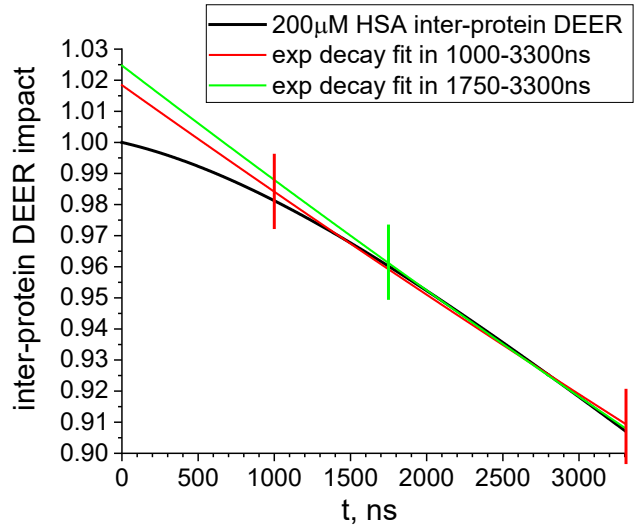

SI Figure VI.15: 11 nm HSA inter-protein DEER impact for single Cys34 labeling at 200 μM in a glassy water/sucrose matrix (black). The exponential fits (red and green) represent the DEER data processing without considering the protein size.

Since obtaining the intra-protein impact requires dividing the experimental DEER curve by the inter-protein impact, $V_{intra}=V_{DEER}/V_{inter,}$ the exponential approximation of the inter-protein impact will result in a distortion of the intra-protein impact. This distortion manifests as a ∩-shaped (negative second derivative) curve with an amplitude of 2–2.5% in the case of 200 μM single-labeled HSA, which corresponds to a concentration of 100 μM double-labeled protein and P_b= 0.26.

To estimate the distortion of intra-protein impact for other concentrations and P_b values, the following relationship can be used:

∩-shape curve amplitude = 2%*(P_b/0.26)(double labeled protein concentration in uM/100)

The magnitude of this contribution for proteins of different sizes can be determined by plotting the corresponding curves using the parameters provided in SI Table VI.2.

VI.9 References

[1] W. Wang, Lyophilization and development of solid protein pharmaceuticals, International Journal of Pharmaceutics 203 (2000) 1–60.

[2] J.F. Carpenter, M.J. Pikal, Chang, Byeong, S, T.W. Randolph, Rational Design of Stable Lyophilized Protein Formulations: Some Practical Advice, Pharmaceutical Research 14 (1997) 969–975.

[3] E. Trenkenschuh, W. Friess, Freeze-drying of nanoparticles: How to overcome colloidal instability by formulation and process optimization, European Journal of Pharmaceutics and Biopharmaceutics 165 (2021) 345–360.

[4] J.J. Hill, E.Y. Shalaev, G. Zografi, Thermodynamic and dynamic factors involved in the stability of native protein structure in amorphous solids in relation to levels of hydration, Journal of Pharmaceutical Sciences 94 (2005) 1636–1667.

[5] Y. Xu, J.F. Carpenter, M.T. Cicerone, T.W. Randolph, Contributions of local mobility and degree of retention of native secondary structure to the stability of recombinant human growth hormone (rhGH) in glassy lyophilized formulations, Soft Matter 9 (2013) 7855.

[6] M.T. Cicerone, J.F. Douglas, β-Relaxation governs protein stability in sugar-glass matrices, Soft Matter 8 (2012) 2983.

[7] S.D. Allison, B. Chang, T.W. Randolph, J.F. Carpenter, Hydrogen bonding between sugar and protein is responsible for inhibition of dehydration-induced protein unfolding, Archives of Biochemistry and Biophysics 365 (1999) 289–298.

[8] L.L. Chang, D. Shepherd, J. Sun, D. Ouellette, K.L. Grant, X.C. Tang, M.J. Pikal, Mechanism of protein stabilization by sugars during freeze-drying and storage: native structure preservation, specific interaction, and/or immobilization in a glassy matrix?, Journal of Pharmaceutical Sciences 94 (2005) 1427–1444.

[9] J.L. Cleland, X. Lam, B. Kendrick, J. Yang, T.-H. Yang, D. Overcashier, D. Brooks, C. Hsu, J.F. Carpenter, A specific molar ratio of stabilizer to protein is required for storage stability of a lyophilized monoclonal antibody, Journal of Pharmaceutical Sciences 90 (2001) 310–321.

[10] K. Dauer, C. Werner, D. Lindenblatt, K.G. Wagner, Impact of process stress on protein stability in highly-loaded solid protein/PEG formulations from small-scale melt extrusion, International journal of pharmaceutics: X 5 (2023) 100154.

[11] R. Fang, W. Obeidat, M.J. Pikal, R.H. Bogner, Evaluation of Predictors of Protein Relative Stability Obtained by Solid-State Hydrogen/Deuterium Exchange Monitored by FTIR, Pharmaceutical Research 37 (2020) 168.

[12] S. Sinha, Y. Li, T.D. Williams, E.M. Topp, Protein conformation in amorphous solids by FTIR and by hydrogen/deuterium exchange with mass spectrometry, Biophysical Journal 95 (2008) 5951–5961.

[13] N.E. Wilson, T.T. Mutukuri, D.Y. Zemlyanov, L.S. Taylor, E.M. Topp, Q.T. Zhou, Surface Composition and Formulation Heterogeneity of Protein Solids Produced by Spray Drying, Pharmaceutical Research 37 (2019) 14.

[14] C.J. Crilly, J.A. Brom, M.E. Kowalewski, S. Piszkiewicz, G.J. Pielak, Dried Protein Structure Revealed at the Residue Level by Liquid-Observed Vapor Exchange NMR, Biochemistry 60 (2021) 152–159.

[15] B.S. Moorthy, I.E. Zarraga, L. Kumar, B.T. Walters, P. Goldbach, E.M. Topp, A. Allmendinger, Solid-State Hydrogen-Deuterium Exchange Mass Spectrometry: Correlation of Deuterium Uptake and Long-Term Stability of Lyophilized Monoclonal Antibody Formulations, Molecular Pharmaceutics 15 (2018) 1–11.

[16] Y. Li, T.D. Williams, R.L. Schowen, E.M. Topp, Characterizing protein structure in amorphous solids using hydrogen/deuterium exchange with mass spectrometry, Analytical Biochemistry 366 (2007) 18–28.

[17] M.M. Castellanos, A. McAuley, J.E. Curtis, Investigating Structure and Dynamics of Proteins in Amorphous Phases Using Neutron Scattering, Computational and Structural Biotechnology Journal 15 (2017) 117–130.

[18] J.E. Curtis, A. McAuley, H. Nanda, S. Krueger, Protein structure and interactions in the solid state studied by small-angle neutron scattering, Faraday Discussions 158 (2012) 285-99; 351-70.

[19] J.E. Curtis, H. Nanda, S. Khodadadi, M. Cicerone, H.J. Lee, A. McAuley, S. Krueger, Small-angle neutron scattering study of protein crowding in liquid and solid phases: lysozyme in aqueous solution, frozen solution, and carbohydrate powders, The Journal of Physical Chemistry B 116 (2012) 9653–9667.

[20] J. Eisermann, M. Hoffmann, F.A. Schöffmann, M. Das, C. Vargas, S. Keller, D. Hinderberger, Molecular-Level Interactions of Nanodisc-Forming Copolymers Dissected by EPR Spectroscopy, Macromolecular Chemistry and Physics 222 (2021) 2100051.

[21] W. Lubitz, M. Chrysina, N. Cox, Water oxidation in photosystem II, Photosynthesis Research 142 (2019) 105–125.

[22] N. Isaev, H.-J. Steinhoff, Protein and solutes freeze-concentration in water/glycerol mixtures revealed by pulse EPR, European Journal of Pharmaceutics and Biopharmaceutics 169 (2021) 44–51.

[23] S. Brandon, A.H. Beth, E.J. Hustedt, The global analysis of DEER data, Journal of Magnetic Resonance 218 (2012) 93–104.

[24] D.R. Kattnig, J. Reichenwallner, D. Hinderberger, Modeling excluded volume effects for the faithful description of the background signal in double electron-electron resonance, The Journal of Physical Chemistry B 117 (2013) 16542–16557.

[25] W.E. Funk, H. Li, A.T. Iavarone, E.R. Williams, J. Riby, S.M. Rappaport, Enrichment of cysteinyl adducts of human serum albumin, Analytical Biochemistry 400 (2010) 61–68.

[26] L. Turell, H. Botti, L. Bonilla, M.J. Torres, F. Schopfer, B.A. Freeman, L. Armas, A. Ricciardi, B. Alvarez, R. Radi, HPLC separation of human serum albumin isoforms based on their isoelectric points, Journal of Chromatography B 944 (2014) 144–151.

[27] M.J. Robertson, J. Tirado-Rives, W.L. Jorgensen, Improved Peptide and Protein Torsional Energetics with the OPLSAA Force Field, Journal of Chemical Theory and Computation 11 (2015) 3499–3509.

[28] G. Bussi, D. Donadio, M. Parrinello, Canonical sampling through velocity rescaling, The Journal of Chemical Physics 126 (2007) 14101.

[29] M. Parrinello, A. Rahman, Polymorphic transitions in single crystals: A new molecular dynamics method, Journal of Applied Physics 52 (1981) 7182–7190.

[30] T. Darden, D. York, L. Pedersen, Particle mesh Ewald: An N ·log(N) method for Ewald sums in large systems, The Journal of Chemical Physics 98 (1993) 10089−10092.

[31] K.B. Konov, D.V. Leonov, N.P. Isaev, K.Y. Fedotov, V.K. Voronkova, S.A. Dzuba, Membrane-Sugar Interactions Probed by Pulsed Electron Paramagnetic Resonance of Spin Labels, The Journal of Physical Chemistry B 119 (2015) 10261–10266.

[32] G. Bisker, J. Ahn, S. Kruss, Z.W. Ulissi, D.P. Salem, M.S. Strano, A Mathematical Formulation and Solution of the CoPhMoRe Inverse Problem for Helically Wrapping Polymer Corona Phases on Cylindrical Substrates, The Journal of Physical Chemistry C 119 (2015) 13876–13886.

[33] A. Chubarov, A. Spitsyna, O. Krumkacheva, D. Mitin, D. Suvorov, V. Tormyshev, M. Fedin, M.K. Bowman, E. Bagryanskaya, Reversible Dimerization of Human Serum Albumin, Molecules 26 (2021) 108.

[34] A. Bhattacharya, R. Prajapati, S. Chatterjee, T.K. Mukherjee, Concentration-dependent reversible self-oligomerization of serum albumins through intermolecular β-sheet formation, Langmuir 30 (2014) 14894–14904.

[35] L. Urban, H.-J. Steinhoff, Hydrogen bonding to the nitroxide of protein bound spin labels, Molecular Physics 111 (2013) 2873–2881.

[36] A.D. Milov, R.I. Samoilova, A.A. Shubin, Y.A. Grishin, S.A. Dzuba, ESEEM Measurements of Local Water Concentration in D2O-Containing Spin-Labeled Systems, Applied Magnetic Resonance 35 (2008) 73–94.

[37] M.J. Pikal, D.R. Rigsbee, M.L. Roy, Solid state chemistry of proteins: I. glass transition behavior in freeze dried disaccharide formulations of human growth hormone (hGH), Journal of Pharmaceutical Sciences 96 (2007) 2765–2776.

[38] F. Zsila, Circular dichroism spectroscopic detection of ligand binding induced subdomain IB specific structural adjustment of human serum albumin, The Journal of Physical Chemistry B 117 (2013) 10798–10806.

[39] B. Ahmad, S. Parveen, R.H. Khan, Effect of albumin conformation on the binding of ciprofloxacin to human serum albumin: a novel approach directly assigning binding site, Biomacromolecules 7 (2006) 1350–1356.

[40] K. Griebenow, A.M. Klibanov, Lyophilization-induced reversible changes in the secondary structure of proteins, Proceedings of the National Academy of Sciences of the United States of America 92 (1995) 10969–10976.

[41] J.-J. Lin, J.D. Meyer, J.F. Carpenter, M.C. Manning, Stability of Human Serum Albumin During Bioprocessing: Denaturation and Aggregation During Processing of Albumin Paste, Pharmaceutical Research 17 (2000) 391–396.

[42] M.T. Cicerone, A. Tellington, L. Trost, A. Sokolov, Substantially Improved Stability of Biological Agents in Dried Form: The Role of Glassy Dynamics in Preservation of Biopharmaceuticals, BioProcess International (2003) 36–47.

[43] R.T. Berendt, D.M. Sperger, E.J. Munson, P.K. Isbester, Solid-state NMR spectroscopy in pharmaceutical research and analysis, TrAC Trends in Analytical Chemistry 25 (2006) 977–984.

[44] G. Jeschke, DEER distance measurements on proteins, Annual Review of Physical Chemistry 63 (2012) 419–446.

[45] A.M. Raitsimring, K.M. Salikhov, Electron spin echo method as used to analyze the spatial distribution of paramagnetic centers, Bulletin of Magnetic Resonance 7 (1985) 185–217.

[46] S. van Doorslaer, Hyperfine Spectroscopy: ESEEM, EMagRes (2017) 51–70.

[47] A.D. Milov, Y.D. Tsvetkov, F. Formaggio, S. Oancea, C. Toniolo, J. Raap, Aggregation of Spin Labeled Trichogin GA IV Dimers: Distance Distribution between Spin Labels in Frozen Solutions by PELDOR Data, The Journal of Physical Chemistry B 107 (2003) 13719–13727.

[48] J. Dong, A. Hubel, J.C. Bischof, A. Aksan, Freezing-induced phase separation and spatial microheterogeneity in protein solutions, The Journal of Physical Chemistry B 113 (2009) 10081–10087.

[49] H. Fischer, I. Polikarpov, A.F. Craievich, Average protein density is a molecular-weight-dependent function, Protein Science 13 (2004) 2825–2828.

Chapter VII Summary

Protein stabilization in lyophilized drug products is primarily based on water replacement by hydrogen bond formation between protein and excipient molecules, as well as on vitrification of the proteins in a rigid amorphous excipient matrix. Yet, the fundamental details of both mechanisms are not fully understood. To this end, protein stability was studied as a function of sugar size and concentration. In addition, novel analytical methods capable of examining protein structure, accessibility, and molecular environment in the solid state were developed and used for lyophilizate characterization. Another important focus of this thesis was to elucidate whether products being as dry as possible also yield the best stability or if and how overdrying disturbs stability.

Residual moisture significantly impacts protein stability, and controlled generation of different, well-defined moisture levels in lyophilizates is challenging. Therefore, at first, a moisture-spiking method for precise post-lyophilization adjustments was developed (**Chapter III**). Using microliter Hamilton syringes, volumes of less than 1 µl of water can be introduced into the product by puncturing the stoppered vial and allowing the droplet to evaporate on the needle tip. The vapor evenly distributes throughout the lyocake, as confirmed by measuring the moisture content in different segments of dissected cakes. Spiking is an accurate, fast, and reproducible approach for targeted residual moisture adjustment without altering the lyophilization process for vials sizes of 2R to 20R and cake masses up to 2 g. This technique makes it possible to adjust defined moisture levels of vial obtained in the very same freeze-drying run for stability tests, which allow to assess the residual moisture level impact and justify specifications. Additionally, spiking D_2O enables ssHDX experiments at controlled, low and thus relevant D_2O moisture levels and even combined H_2O and D_2O moisture mixtures.

The “more is better” approach in formulation development proposes that increasing the ratio of amorphous sugar to protein improves protein stability. Previous studies suggest optimal stability at sucrose to mAb ratios of 360:1 or higher and did not explore lower ratios. We therefore systematically tested low ratios and analyzed mAb monomer retention upon storage (**Chapter IV**). Our findings indicate that sucrose stabilizes mAbs already well at ratios significantly below 360:1, being relevant for highly concentrated mAb products. We observed an exponential relationship between a lower sucrose to protein ratio and increasing aggregation. Amorphous mannitol offers similar stabilization as sucrose at equivalent ratios; the high protein content prevents mannitol crystallization. Arginine, despite its pronounced glass-forming

properties, was less potent than sucrose and mannitol at the low ratios, potentially due to a difference in hydrogen bond formation. While buffer concentration and surfactants also affect protein stability, the excipient-to-protein ratio remains a critical factor in the different formulations. Thus, low excipient concentrations significantly stabilize the protein. The exponential relationship between monomer content preservation and excipient to protein ratio yields high potential to improve formulation design. It warrants further investigation whether it could enable stability forecasts for optimal ratios based on degradation rates of less stable formulations.

Additionally, besides the influence of the molar ratio of excipient to protein, sugar size, and residual moisture are critical (**Chapter V**). A series of glucose-based mono- to tetrasaccharides, glucose, maltose, maltotriose, and maltotetraose, as well as mixtures thereof, were investigated for their capacity to stabilize protein lyophilizates. An ssHDX MS could be successfully established by adapting the spiking technique developed in **Chapter III**, employing D_2O and D_2O/H_2O mixtures. Lyophilizates based on larger sugars are less capable of protein stabilization, and increased deuterium incorporation indicates enhanced protein accessibility. This effect is attributed to the rigidity of larger sugars, which are less effective at filling voids and forming hydrogen bonds, although they can form less mobile glasses. Increased residual moisture content, adjusted post-lyophilization using the spiking approach, improved the monomer retention in the glucose-free formulations, highlighting the importance of residual moisture and the risk of overdrying a lyophilized product. Larger sugars benefit more from additional water due to their limited capability to replace water. ssHDX MS showed that increasing D_2O content from 1% to 2% does not change deuterium incorporation, likely due to a balance between moisture content and deuterium uptake. Spiking samples with 1% D_2O + 1% H_2O reduces deuterium uptake, supporting the stability improvement hypothesis with higher residual moisture. Besides some limitations based on decreasing T_g with increasing moisture content, a combination of small and large sugars can provide good stabilization through water replacement and vitrification. Our findings show that smaller sugars and an adequate residual moisture level are important means for protein stabilization in lyophilizates. Additionally, ssHDX MS with headspace spiking is a valuable tool for assessing the stability of lyophilized drug products, complementing long-term stability studies.

To better understand protein stabilization mechanisms even at molar ratios below 360:1, EPR was employed as a novel approach to provide direct insights into protein structure and molecular environment in the solid state (**Chapter VI)**. Spin labeled HSA was freeze dried with deuterated sucrose ratios ranging from 7469:1 to 231:1. While CD and SEC after reconstitution

did indicate the absence of structural changes and aggregates, EPR flags changes in the protein structure in the solid state. The structure of about 50% of the HSA molecules is perturbed at the high molar ratio of 7469, and unfolding is even more pronounced at lower ratios. Additionally, EPR indicates a higher sucrose content in the immediate proximity of the protein in the solid state compared to in solution. Thus, EPR offers highly valuable insights into protein structure in the solid state without the need for reconstitution and demonstrates structural changes that are reversible upon reconstitution with water. In addition, the results support the findings of improved stabilization with increasing sugar to protein ratio. Overall, the EPR study highlights the importance of investigating the protein molecular structure and environment es in the solid state.

In summary, this thesis provides a deeper understanding of the stabilization mechanism and protein structure preservation in freeze dried products, which is crucial for rational and effective formulation development. Key factors include excipient to protein molar ratio, residual moisture content, and sugar size. Advanced analytical techniques such as ssHDX MS and EPR are valuable tools for assessing protein structure, environment, and accessibility in the solid state. Correlating structural parameters such as sucrose enrichment around the protein and deuterium incorporation, with storage stability data, can help to judge long term protein stability early in development.

Appendix 1: Publications and submissions associated with this thesis

Lo Presti, K.; Frieß, W. Adjustment of specific residual moisture levels in completely freeze-dried protein formulations by controlled spiking of small water volumes. *European Journal of Pharmaceutics and Biopharmaceutics* 169 (2021) 292-296:
https://doi.org/10.1016/j.ejpb.2021.10.011.

Lo Presti, K.; Jègo, M.; Frieß, W. "The more, the better?" - The impact of sugar-to-protein molar ratio in freeze-dried monoclonal antibody formulations on protein stability. *Molecular Pharmaceutics* 21 (2024) 6484-6490.
https://doi.org/10.1021/acs.molpharmaceut.4c01174.

Lo Presti, K.; Frieß, W. Lo Presti, K.; Frieß, W. "Bigger, the Better?" – The Influence of Sugar Size and Residual Moisture on Protein Stability and Accessibility in Lyophilizates. *Molecular Pharmaceutics 22 (2025) 5952–5958.*
https://doi.org/10.1021/acs.molpharmaceut.5c00596.

Isaev[§], N.; Lo Presti[§], K.; Frieß, W. Insights into folding and molecular environment of lyophilized proteins using pulsed electron paramagnetic resonance spectroscopy. *Molecular Pharmaceutics* 22 (2025) 424-432.
[§]These authors contributed equally to this work
https://doi.org/10.1021/acs.molpharmaceut.4c01008.

Appendix 2: Presentations and Grants associated with this thesis

Poster presentations:

Lo Presti, K.; Frieß, W. Assessing Protein Accessibility in Lyophilizates by UPLC-HDX-MS.
Annual DPhG – Meeting 2021, Virtual Meeting, September 29th – October 1st, 2021

Lo Presti, K.; Frieß, W. Adjustment of specific residual moisture levels in completely freeze-dried protein formulations by controlled spiking of small water volumes.
13th World Meeting on Pharmaceutics, Biopharmaceutics and Pharmaceutical Technology, March 28 – 31, 2022, Rotterdam

Lo Presti, K.; Isaev, N.; Frieß, W. Insights into folding and molecular environment of lyophilized proteins using pulsed electron paramagnetic resonance spectroscopy.
2022 Colorado Protein Stability Conference, August 8th – 11th, 2022, Breckenridge

Awarded with the student poster competition prize as 2nd runner up.

Lo Presti, K.; Isaev, N.; Frieß, W. Insights into folding and molecular environment of lyophilized proteins using pulsed electron paramagnetic resonance spectroscopy.
Annual DPhG Student & Postdoc Meeting 2023, March 1st – 3rd, 2023, Bonn

Awarded with the oral presentation prize

Lo Presti, K.; Jégo, M.; Frieß, W. The More the Better? Impact of the Molar Ratio of Sucrose to mAb in Lyophilizates on Protein Stability.
Freeze-drying of Pharmaceuticals and Biologicals- Short Course and Conference, August 1^{st} – 4^{th}, 2023, Breckenridge

Grants:

Lo Presti, K.; Frieß, W. Using Hamilton syringes for specific spiking of small water volumes in freeze-dried protein formulations.

"Hamilton Syringe Grant" Winner September 2022